Protection Challenges in Future Converter-Dominated Power Systems: Investigation and Quantification using a Novel Flexible Modelling and Hardware Testing Platform

Ruiqi Li

A thesis submitted for the degree of Doctor of Philosophy to

Department of Electronic and Electrical Engineering

University of Strathclyde

July 2022

This thesis is the result of the author's original research. It has been composed by the author and has not been previously submitted for examination which has led to the award of a degree.

Abstract

The research work presented in this thesis addresses anticipated (and documented) protection challenges that will be introduced by the domination of power electronics interfaces in future power systems. A flexible and programmable voltage source converter (VSC) model with controllable fault response has been developed and this is tested using realistic network data (including transmission lines and the corresponding power flow/fault level data) from the GB transmission network, provided by National Grid ESO (the research project sponsor).

The results of tests, where a range of variations to the converter controllers' fault-responses have been implemented (e.g. to reflect different detection and initial converter response delays, output current ramp rates and magnitudes), are presented and analysed. The simulated voltage and current waveforms are injected into actual protection relays using secondary injection amplifiers. The responses of the relays are recorded and a number of issues are highlighted, particularly with respect to the response of distance protection.

It is shown that, when the system is dominated by converter-interfaced sources (especially where the sources are modelled as being unable to provide "fast" and "high" fault currents, which is typically the case for actual converter systems), the responses of traditional distance protection systems (and other systems relying on measurement of current magnitude) could be delayed, lose discrimination, e.g. by tripping with a zone

2 delay for a zone 1 fault, or may be completely unable to detect faults at certain locations within the system.

Based on the test results, potential solutions are then presented relating to changes to relay algorithms and/or the requirements for converters in terms of behaviour during faults. The outcomes of the work will be of interest to grid code developers (publications arising from this work have already been referred to by ENTSO-E guidance document for national implementation for network codes on grid connection [1]), transmission network operators, other researchers and protection/converter manufacturers.

An overview of future work, relating to comprehensive studies (using injection and the developed system/converter models) of a range of faults/infeeds/converter mixes with a wide range of protection relays including distance and unit-type, and development of a standard commissioning testing method of protection relays under future power system scenarios that are dominated by converters, is included in the concluding section. This will assist in the investigation and resolution of issues associated with protection performance in future converter-dominated power systems.

Acknowledgements

I would like to express my deepest gratitude to my first supervisor Prof Campbell Booth for his continuous dedication throughout my PhD study and the writing of this thesis. I would like to thank him for his great patience, powerful encouragements, and invaluable knowledge. No words can adequately express my appreciation for all his precious inexhaustible support.

I would also like to express my gratitude to my second supervisor Dr Andrew J. Roscoe for providing me with his precious knowledge and technical support. His keen understanding of the emerging technologies regarding power systems and power electronics greatly motivated my PhD study.

My special thanks to Dr Adam Dysko, who has been extremely supportive of my research. I cannot thank him enough for his continuous help in providing me the knowledge, skills and tools through my research.

My gratitude extends to National Grid ESO as the sponsor of my research. I would like to express my great appreciation to Jiebei Zhu and Helge Urdal for their incalculable technical input and tireless assistance to my research.

A big thank you to Dr Qiteng Hong and all my friends and colleagues in the Advanced Electrical Systems group. Your friendly support really helped me throughout my days in Strathclyde.

Finally, the greatest thanks of all go to my parents. Thank you so much for being so patient, thoughtful, and supportive during all these years.

Contents

Figures

Glossary of Terms

AC	Alternating Current
AVR	Automatic Voltage Regulator
CSC	Current Source Converter
CSC-HVDC	Current Source Converter Based HVDC
CT	Current Transformer
DC	Direct Current
DFIG	Double Fed Induction Generator
EU	European Union
ETYS	Electricity Ten Year Statement
FACTS	Flexible Alternating Current Transmission Systems
GB	Great Britain
HVDC	High Voltage Direct Current
HVAC	High Voltage Alternating Current
IDMT	Inverse Defnite Minimum Time
IEEE	The Institute of Electrical and Electronics Engineers

IET	The Institute of Electrical and Technology
IGBT	Insulated Gate Bipolar Transistor
LCC	Line Commutated Converter
LCC-HVDC	Line Commutated Converter Based HVDC
LOM	Loss Of Mains
LPF	Low-Pass Filter
LV	Low Voltage
MMC	Modular Multilevel Converter
MV	Medium Voltage
PCC	Point of Common Coupling
Ph-E	Phase-Earth
Ph-Ph-Ph	Phase-Phase-Phase
PI	Proportional and Integral
PLL	Phase-Locked Loop
POD	Power Oscillation Damping
PSS	Power System Stabiliser
PV	Photovoltaic

PWM	Pulse Width Modulation
RES	Renewable Energy Source
RMS	Root Mean Square
RoCoF	Rate of Change of Frequency
RTDS	Real-Time Digital Simulator
SC	Short Circuit
SG	Synchronous Generator
SI	Standard Inverse
STATCOM	Static Synchronous Compensator
SVC	Static Var Compensators
UK	United Kingdom
VI	Very Inverse
VSC	Voltage Source Converter
VSC-HVDC	Voltage Source Converter Based HVDC
VSM	Virtual Synchronous Machine
VT	Voltage Transformer

Chapter 1

Introduction

1.1 Introduction and objectives of the research

Power electronics converters, which are used to facilitate the integration of renewable energy to AC grids and underpin HVDC transmission networks, will play a growing and critical role in future power systems [2]. National Grid ESO (NGESO), the system operator in Great Britain (GB), has stated that renewable generation may contribute an overall average of 75 % of electricity supply by 2030 according to its UK Future Energy Scenarios publication [3]. The maximum instantaneous renewable energy penetration level could be significantly higher than this value [4]. As stated by NGESO, the UK should be capable of operating a "net zero carbon" power system by 2025 [5].

Converter-interfaced sources behave very differently from traditional directly-connected rotating synchronous generators, particularly under fault conditions, and this will have consequences such as reduced and variable fault levels, and possibly higher levels of distortion in current and voltage waveforms during faults [6]. Converters could also potentially lead to relatively slower responses of power system protection to short circuits due to delays in the delivery of fault current from converter-interfaced sources caused by delayed controller actions and responses. Through the System Operability Framework consultations and associated documentation [7], NGESO has raised concerns relating to the fact that converter-interfaced sources may lead to issues with fault discrimination and detection for traditional network protection methods in the future.

At present, there is no universally-defined or accepted response for converter sources in response to AC system faults. The Network Code published by ENTSO-E [8] has specified how converters should provide "maximum" reactive current and "fast" fault

current, but the terms maximum and fast are not defined explicitly and it is incumbent on national operators to define and quantify specific requirements at the national level. It is, therefore, necessary to investigate when and how protection systems, including both modern numerical systems and legacy electro-mechanical schemes, may be affected by the introduction of converter sources with different types of response to faults.

To address the challenges previously mentioned, the following research objectives are defined for the work reported in this thesis:

- Review elementary power electronic devices, and investigate and compare the relative features of VSC-HVDC and line commutated converter-based HVDC (LCC-HVDC);

- Study of VSC-HVDC system design and operation, specifically in terms of component specifications, converter switching mechanisms and control strategies for various connection and application arrangements;

- Identification of research challenges associated with high penetrations of renewable power, coupled via HVDC on to AC systems, with a particular focus on behaviour and responses during AC fault conditions;

- Develop a method to analyse the impact of converters on transmission system protection through both modelling/simulation and hardware-in-the-loop experiments;

- Quantify the impact of varying levels of converter penetration (and assumed converter fault responses) on transmission system protection, with a particular focus on distance protection;

- Propose potential changes to power system protection (e.g., settings) and/or grid codes to ensure safe and reliable protection systems in future converter-dominated power systems.

1.2 Research contributions

The thesis presents the following primary contributions:

- Development of a novel flexible model that can be used to simulate a range of responses of converter interfaces to AC system faults. With the designing of a fault detection and fault ride through blocks, the model can be configured with variable parameters (sustained fault level, ramp rate, delays in initial response etc.). This model is based upon a dual sequence controller and has been tested and verified.

- Assessment and quantification of the impact of the converter–dominated power system on distance protections are performed both completely in simulation and using actual protection relay devices as hardware-in-the-loop) to assess protection response to a range of different assumed converter behaviours for a wide range of power system faults (different fault types, different location, varying system fault levels and varying assumed converter/synchronous machine ratios).

- The findings provide a contribution to knowledge relating to how protection systems (with a focus on distance protection) will behave, and experience problems, under certain scenarios in converter-dominated systems (this has been reported in a journal publication arising from this work [9]).

- Mitigation methods are proposed from both converters and protection device's aspects including providing testing platforms to allow the coordination between relay and converter manufactures.

The thesis presents the following secondary contributions:

- Investigation and report of the state of the art of HVDC systems, and development of a model capable of producing controllable fault response representing realistic converters.

- Systematic investigation of the challenges associated with future power systems. Identified and quantified a range of particular problems with specific protection types/devices.

- Review of solutions to facilitate higher amounts of converter sources to be connected to grid systems.

1.3 Thesis organisation

Chapter 2 summarises traditional transmission system protection practice and presents a review of how future power systems will evolve to be dominated by power electronics

interfaces. Details of how the new technologies shall change the response of the system during fault conditions will be included.

Chapter 3 presents an introduction to the operating principles of traditional protection systems and how protection relays might be affected by converter-interfaced generation and interconnector sources.

Chapter 4 contains a review of literature related to studies of the impact of converters on protection, identified protection problems and possible solutions and illustrates how this research work aligns with the work of others and addresses identified requirements in the literature.

Chapter 5 presents and describes the design and operation of a comprehensive, flexible and credible converter-interfaced generation/infeed model that is capable of reproducing appropriate voltage and current output waveforms, that can be modified depending on the type of response required by configuring various model parameters, during grid network faults.

Chapter 6 contains a complete and comprehensive overview and description of the testing system and the methodology that allows different converter responses to be emulated and the resultant waveforms to be directly injected into protection relays (or models of relays), with the relay responses monitored and recorded in a “hardware in the loop” experimental arrangement.

In Chapter 7, using the aforementioned model and hardware in the loop laboratory set up, investigations into how protection performance is impacted by different types of converters (and converter responses and “mix” of converter/synchronous sources

supplying fault current) are conducted. The systematic tests of network protection performance are performed under a variety of situations, including different fault locations; different fault types (single-phase, phase to- phase and three-phase faults). Solutions for specific identified challenges are discussed in the concluding section of the thesis, based on the experimental results and findings.

Chapter 8 presents conclusions arising from the work and provides several suggestions for future research.

1.4 Publications

The following publications have been produced during the PhD project:

1.4.1 Journal articles

- R. Li, J. Zhu, Q.Hong, C. D. Booth, A. Dysko, A. J. Roscoe, and H. Urdal, "Impact of low (zero) carbon power systems on power system protection: a new evaluation approach based on a flexible modelling and hardware testing platform," IET Renewable Power Generation, vol. 14, pp. 906-913. https://doi.org/10.1049/iet-rpg.2019.0518

1.4.2 Conference papers

- R. Li, C. D. Booth, A. Dysko, A. J. Roscoe, and J. Zhu, "Development of models to study VSC response to AC system faults and the potential impact on network protection," in *Power Engineering Conference (UPEC), 2014 49th International Universities,* 2014, pp. 1–6
- R. Li, C. D. Booth, A. Dysko, A. J. Roscoe, J. Zhu, and H. Helge, "Protection challenges in future converter dominated power systems," in *Protection, Automation & Control World Conference 2015,* 2015, pp. 1–6.
- R. Li, C. D. Booth, A. Dysko, A. J. Roscoe, H. Urdal, and J. Zhu, "Protection challenges in future converter dominated power systems: demonstration through simulation and hardware tests," in *International conference on Renewable Power Generation 2015,* 2015, pp. 1–6.
- R. Li, C. D. Booth, A. Dysko, A. J. Roscoe, H. Urdal, and J. Zhu, "A systematic evaluation of network protection responses in future converter-dominated power systems," in *13th International Conference on Development in Power System Protection 2016 (DPSP),* 2016, pp. 1–6.

Chapter 2

Power Systems with High Penetrations of Converter-Interfaced Generation/Infeed Sources

2.1 Introduction

This chapter reviews the fundamentals of power systems dominated by power electronics converter interfaces, with a particular focus on the behaviour of "traditional" power systems (dominated by synchronous generation sources) during faults, and the fault behaviour of future power systems that have a high proportion of converter-interfaced sources and infeeds. The following content will be presented in detail:

- A review of the driving forces behind the changes that are presently being witnessed in electrical power systems and how they are anticipated to continue to evolve in the future.

- A brief review of traditional generation technologies, focussing on synchronous generation (SG) and the typical response to faults in terms of fault current supplied.

- A review of converter-interfaces used for non-synchronous generation (NSG), including current source converters (CSC) and voltage source converters (VSC). The operating principles of these technologies are outlined, and a comparison, with a particular focus on behaviour during faults (which is not uniform nor easily modelled), is presented between VSC, CSC and the fault behaviour of SGs – this shows the need for a flexible model to investigate performance and potential impact on protection performance during faults.

- An introduction to the specific design and configuration of the VSC converter used in this research project for modelling a range of fault responses, along with

a detailed description of the VSC modelling and control algorithms incorporated in the model.

2.2 Future energy scenarios

The majority of traditional and historic energy generation has been based on fossil fuels and CO_2 and other undesirable emissions [1] [2]. As described in [3], fossil fuel-based energy sources including petroleum, natural gas and coal, will be exhausted in 50, 65 and 200 years respectively if present rates of consumption continue (although exploration and rates of consumption mean that these numbers could change).

NGESO, the system operator in GB, has stated that they aim to be capable of operating a "net zero carbon" power system by 2025 [4]. To meet this ambitious target, a significant increase in renewable energy capacity is required [5]. The future energy scenario document [3] published by NGESO claimed that the future power system requires over 132 GW more renewable generation capacity in the electricity system, with 71% of the demand required to be met by renewable generation by 2030.

As demonstrated in Figure 2-1, the report proposes four different sets of scenarios relating to different rates of decarbonisation. These scenarios include consumer transformation, system transformation, leading the way and steady progression. The predicted electricity generation capacity is demonstrated in Figure 2-2.

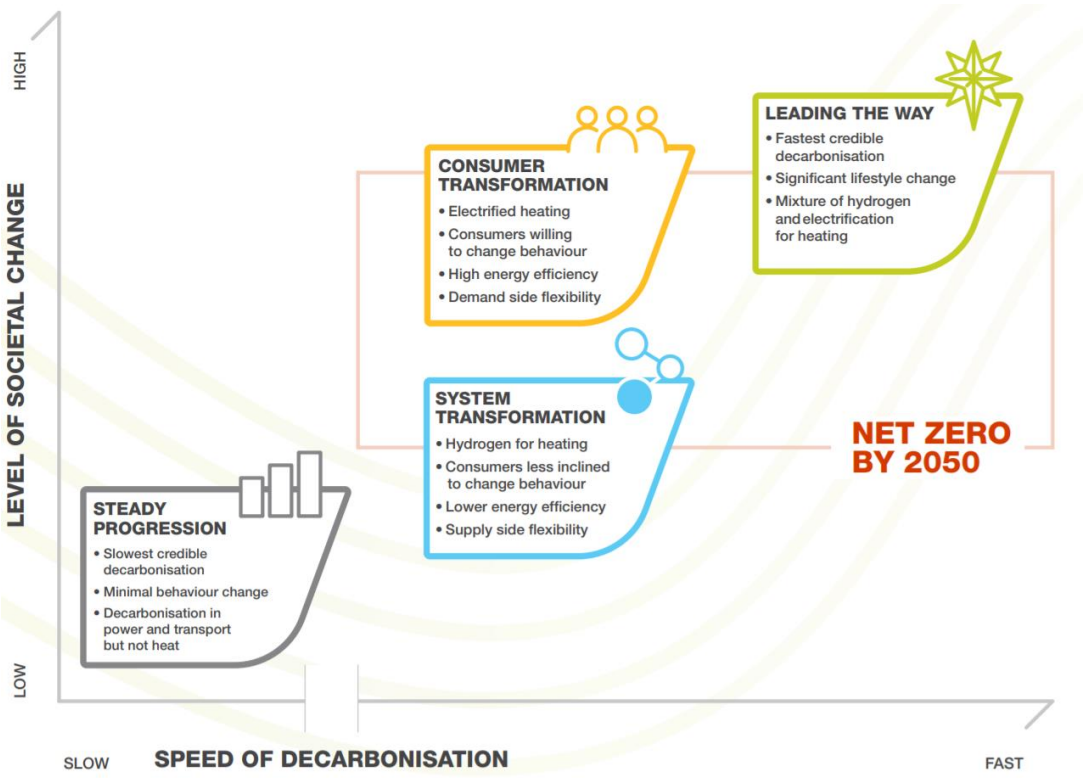

Figure 2-1 Future energy scenarios 2021 [5]

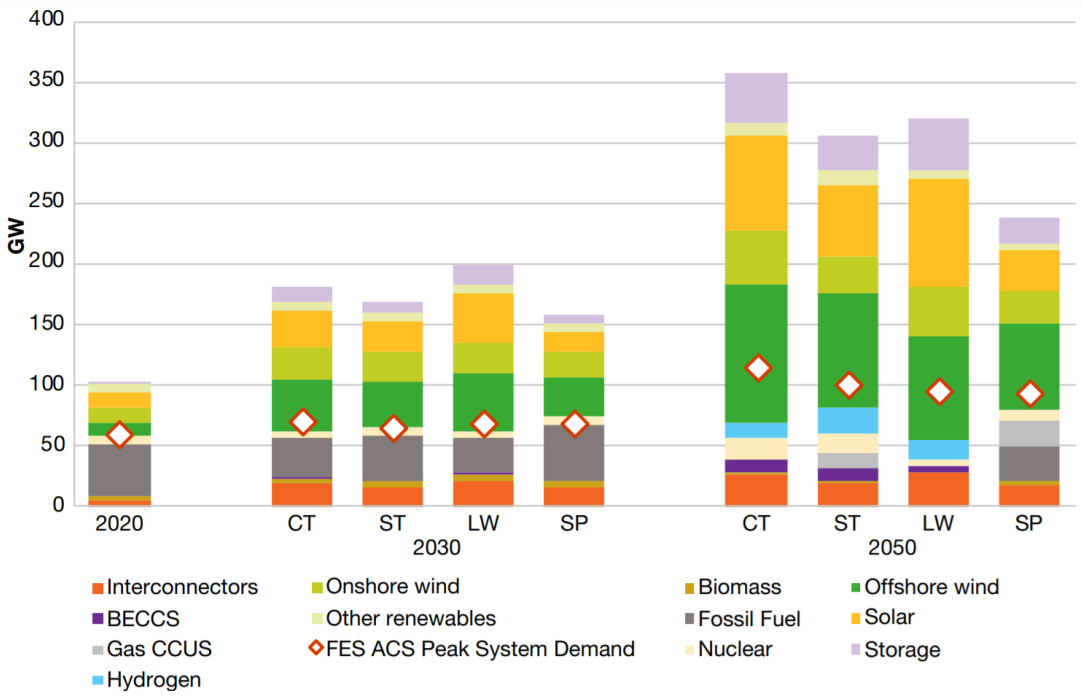

Figure 2-2 Installed electricity generation capacity, storage and interconnection to 2050 (CT: consumer transformation. ST: system transformation, LW: leading the way SP: steady progression) [5]

Converter interfaces employing power electronics are used to facilitate the integration of renewable energy into AC grids and underpin HVDC transmission networks. These play a continuing, growing and critical role in future power systems.

2.3 Traditional synchronous machine-based power systems

Historically, the vast majority of electrical power systems were composed of solely AC electric generation, transmission and distribution systems. Synchronous generators were the predominant sources of electrical power, typically mechanically powered

using steam (generated by fossil fuels, and more latterly nuclear) or gas turbines. Synchronous machines can also be used to control the output and system voltages by providing reactive power compensation and can normally output power at a leading or lagging power factor if required. The operation principle of the synchronous machines is outlined in the following section.

The synchronous machine operates according to Faraday's law of electromagnetic induction. For large synchronous generators, the mechanically-driven rotor is placed with the field winding charged by a DC power source generating the excitation magnetic field. The mechanical force driving the rotor creates a rotation of the magnetic field and therefore induces (typically) three-phase AC currents in the armature windings arranged around the circumference of the stator. The difference between the mechanical force and the induced back electromotive force shall determine the acceleration speed of the rotor, which means that the generated electric power has to be balanced with the mechanical power (with losses accounted for) to ensure that the rotor maintains a steady rotation speed once it has reached its operating speed (this is also influenced by the system "speed" or frequency in a multiple machine system) and the rotor speed is effectively "locked" to the system speed electromagnetically, although this speed will tend to change if there is a change in the overall balance between supply and demand. A typical simplified diagram of a synchronous machine is presented in Figure 2-3 with its equivalent circuit. From the diagram the generator is providing an induced voltage E, transmitting real and reactive power (P&Q) to the grid with a voltage of V with an angle difference of δ referring to E at its connection point, through an equivalent generator reactance of X. The transmitted power is calculated through the following equations:

$$P = \frac{|E||V|}{X} sin\,\delta \qquad \text{Equation 2-1}$$

$$Q = \frac{|V||E|\,cos\,\delta - |V|^2}{X} \qquad \text{Equation 2-2}$$

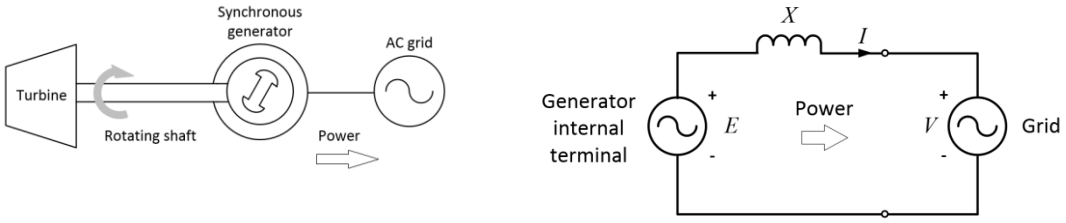

(a) (b)

Figure 2-3 Schematic diagram of a synchronous machine; and (b) its equivalent circuit [10]

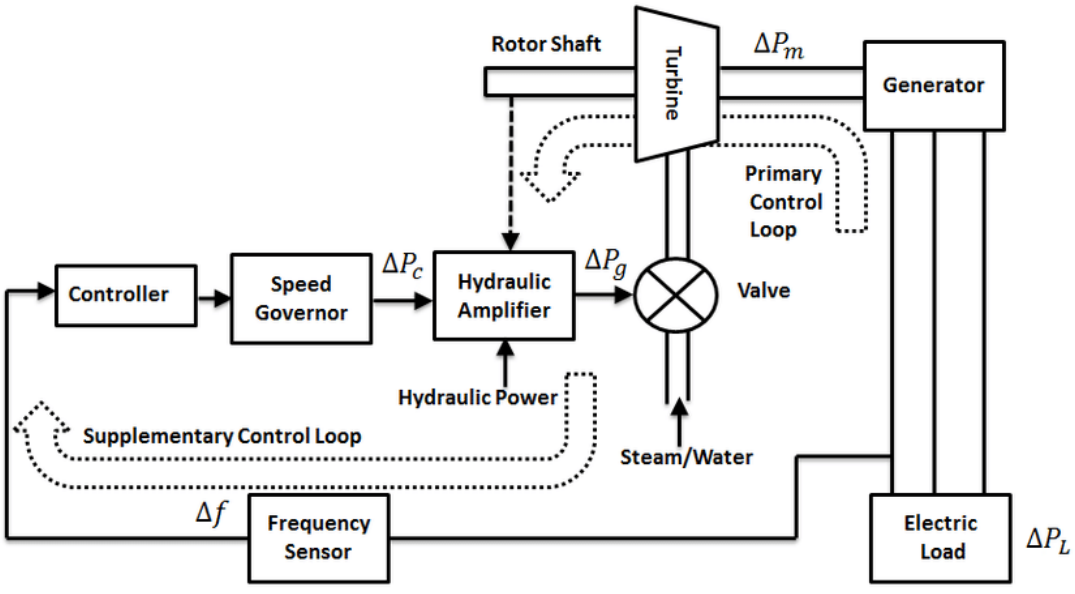

Figure 2-4 A synchronous generator with basic frequency control loops[11]

Figure 2-4 illustrates the frequency control system used in a typical synchronous machine/turbine arrangement. The rotation frequency output is measured by the

frequency sensor, and any corresponding frequency deviation Δf (between desired and actual frequency) will result in a change of the output mechanic power ΔP_m from the prime mover (capable of doing so), leading to an attempt to change the generator's rotational frequency which will affect the electrical frequency. The rate of the change of the frequency (*RoCoF*) of a system in response to an imbalance/change in load/generation is determined by the change of the power deviation ΔP, the total rated power of all SGs S_{rated}, the current frequency f_0 and the inertia H through the following equation:

$$\text{RoCoF} = \frac{\Delta P}{S_{rated}} \frac{f_0}{2H} \qquad \text{Equation 2-3}$$

Droop characteristics are almost universally utilised when multiple synchronous generating units are connected to the same synchronous system [12]. By applying this function, the phenomenon of generators acting against each other and "hunting" as they strive to control their individual outputs and effectively the system frequency can be mitigated. For a speed governor with droop characteristic, the ratio of the frequency deviation Δf changes with the value of the power output ΔP with an overall range specific by a percentage *R*, as described in the following equation:

$$Percent\ R = \frac{percent\ frequency\ deviation}{percent\ power\ output\ \ change} \times 100 \qquad \text{Equation 2-4}$$

When R is specified, a change of frequency *R%,* or Δf, shall result in a 100% change of the output power ΔP. The relationship between frequency deviation and power output is presented in Figure 2-5.

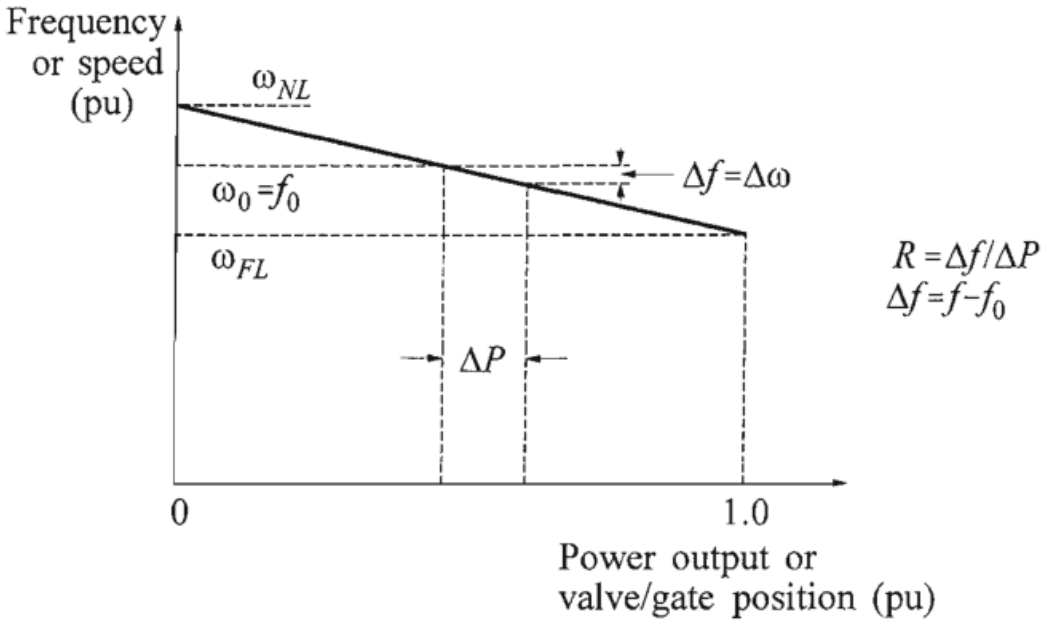

Figure 2-5 Ideal steady-state characteristics of a governor with speed droop [12]

During a system fault the energy stored within a synchronous machine, due to its rotating masses (and the masses of the often directly-couple turbine driving the generator) acts to inject a large current immediately into the grid, and therefore, protection systems can easily detect such situations through observing the marked difference in current magnitudes (and in some cases the marked reduction in system voltages around the fault location) and act to isolate the faulted component(s). These fault currents provided by the traditional generators are around 5~10pu [4]. Figure 2-6 demonstrates a typical response of a traditional power system with synchronous machines providing generation for a three-phase fault, where the system's equivalent resistance and inductance is *R* and *L*, with earth return path resistance R_e and inductance L_e. The transient current in each phase $i_{ryb}(t)$ can be expressed as a summation of its transient *ac/dc* components $i_{ryb(ac/dc)}(t)$ using the following equations:

$$i_{ryb}(t) = i_{ryb(ac)}(t) + i_{ryb(dc)}(t) \qquad \text{Equation 2-5}$$

Where:

$$i_{ryb(ac)}(t) = \sqrt{2} i_{rms} sin[\omega t + \varphi_{ryb} - tan^{-1}\left(\frac{\omega(L+L_e)}{R+R_e}\right)] \qquad \text{Equation 2-6}$$

$$i_{ryb(dc)}(t) = -\sqrt{2} i_{rms} sin[\varphi_{ryb} - tan^{-1}\left(\frac{\omega(L+L_e)}{R+R_e}\right)] \times exp[\frac{-t}{\left(\frac{L+L_e}{R+R_e}\right)}] \qquad \text{Equation 2-7}$$

$$I_{rms} = \frac{V_{rms}}{\sqrt{R^2 + (\omega L)^2}} \qquad \text{Equation 2-8}$$

Where V_{rms}/I_{rms} is the rms voltage/current magnitude, φ_{ryb} is the corresponding voltage phase angle in rad in each phase, ω is the voltage angular frequency in rad/s.

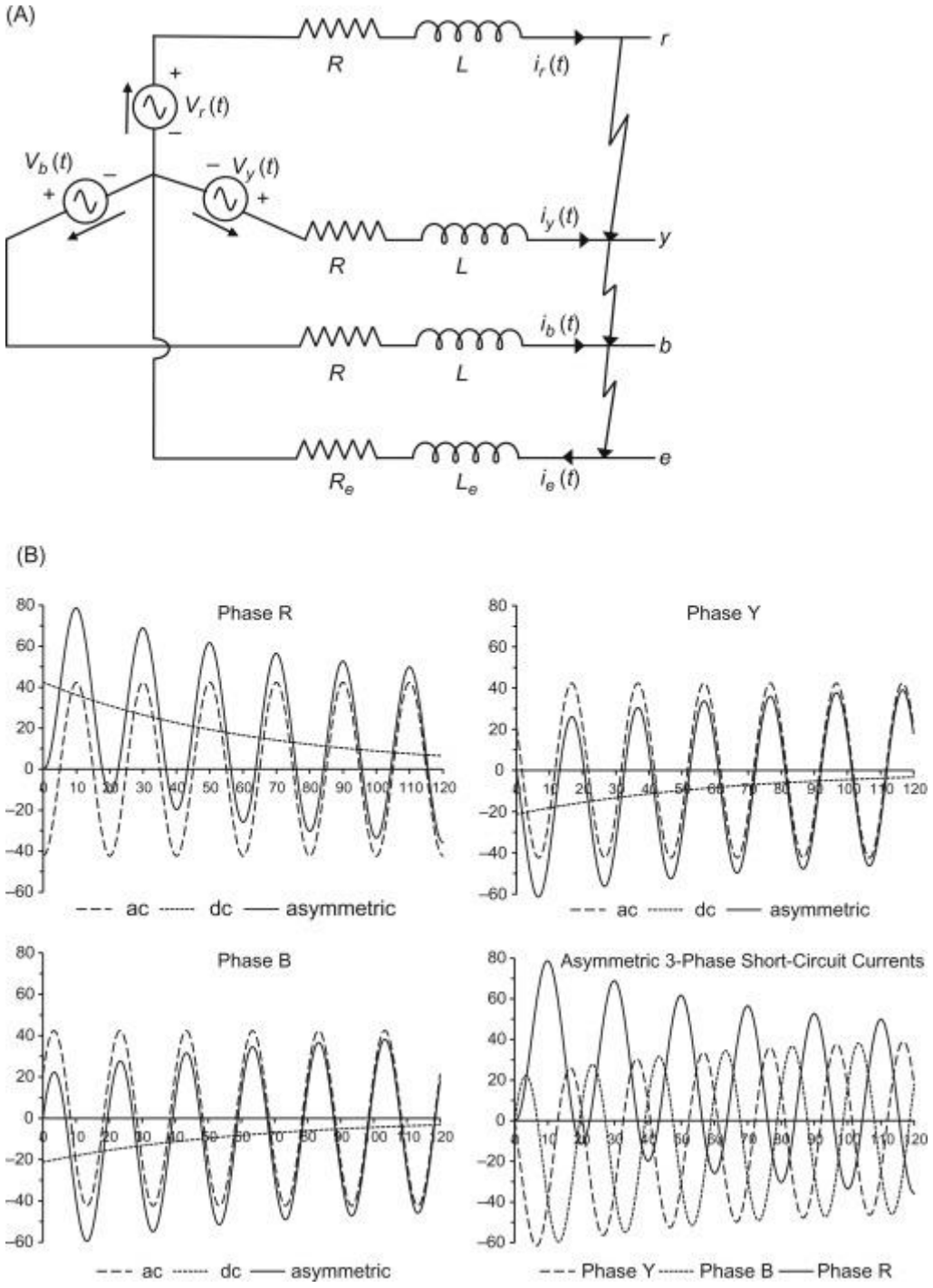

Figure 2-6 (A) Basic balanced three-phase electric circuit with earth return and a solid three-phase short-circuit fault. (B) Three-phase short-circuit current waveforms [13]

2.4 Overview of standards relating to the integration of converter-based systems

A converter's fault response is directly impacted by the nature and performance of its control system. The details of the required converter fault response are typically defined through grid/network codes [8], [14], [15], but in some cases the performance at specific initial periods following a disturbance (e.g. during the first 5-10 ms, the time when protection systems are typically making decisions relating to whether there is a fault and what type of response, if any, is required) is not specified in exact detail, meaning that there may be some potential for different converters to behave differently, even if they are compliant with the grid codes. It should be noted that at the early stages of this research project (which was sponsored by NGESO), the work reported in this thesis influenced and is cross-referenced to by the ENTSO-E guidance document for national implementation of network codes on grid connection [16].

For example, the requirements for fault current provision may be different in a relatively weak power system (e.g., the GB system in future with lots of renewables) and a strong system (e.g., France, dominated by nuclear and therefore large SG). A key challenge is to determine the actual requirements of the grid and of course, the protection systems that are protecting the grid, and design methods to test the performance and compliance of converters, and also the impact on protection, against those requirements and the converter responses. These are not simple tasks. Therefore, to assist with this understanding of converter response and impact on network protection, an adjustable and reliable converter model, capable of generating a range of V/I outputs under grid disturbances has been developed. By adjusting the configuration

of the model, the fault responses can be varied widely from a number of perspectives. Using a secondary injection set in the laboratory, the performance of relays in response to the simulated fault voltages and currents can be (and has been) monitored and evaluated.

2.4.1 Requirements for converters

2.4.1.1 ENTSO-E network code requirements

From the most recently-updated European Network Code on Requirements for Grid Connection Applicable to all Generators [8] and the Network Code on HVDC Connections and DC-connected Power Park Modules [17], published by ENTSO-E, it is stated that generating units shall fulfil the following requirement during network faults:

- The units should be able to provide fast fault currents under symmetrical faults if they are required.
- The characteristics of the voltage deviation and fault current should be specified.
- Under asymmetrical faults, the units should be able to generate asymmetrical currents if they are required.

It should be noted that there is a large suite of documents available from ENTSO-E covering various aspects of performance and requirements, but the above provides a succinct summary of what is relevant to the performance of converters during faults and the associated power system protection considerations. One thing that is notable is

that there is no precise definition nor quantification for what the word “fast” means and that asymmetrical currents shall be produced “if they are required”. This leaves the code open to differing interpretations and in practice means that fault current signatures from converters may vary quite significantly, but still be compliant with the code, which results in the need for studies of protection response under a wide range of possible fault current profiles, as carried out in the research reported in this thesis.

2.4.1.2 GB grid code requirements

The overall requirements from the GB grid code documentation [15] published by NGESO can be summarised as follows:

- Each Generating Unit shall remain transiently stable and connected to the System without tripping, for a close-up solid short circuit fault on the Transmission System.

This is only focussed on the requirement for generators (and converter-interfaced infeeds) to remain connected during faults. With reference to the work reported in this thesis, the only real relevance is that any faults, which invariably involve significant voltage depressions around the area of the fault, must be cleared within a maximum of 140 ms, as the risk of generators (both local and remote) tripping increases if the fault remains on the system for longer than 140 ms; ultimately threatening overall system stability. The part of the code reproduced above does not specify exactly what converter-interfaced sources should actually do in terms of provision of fault current during the voltage depression – but this is covered in the next section.

The detailed requirements for different types of generating units are listed as follows:

2.4.1.2.1 Requirements of Fault Ride through:

(a) Short circuit faults on the Onshore Transmission System (which may include an Interface Point) at Supergrid Voltage up to 140ms in duration：

Generating Unit shall remain transiently stable and connected to the System without tripping, for a close-up solid short circuit fault on the Transmission System.

(b) Supergrid Voltage dips on the Onshore Transmission System greater than 140ms in duration:

Generating Unit shall follow the requirements demonstrated in Figure 2-7.

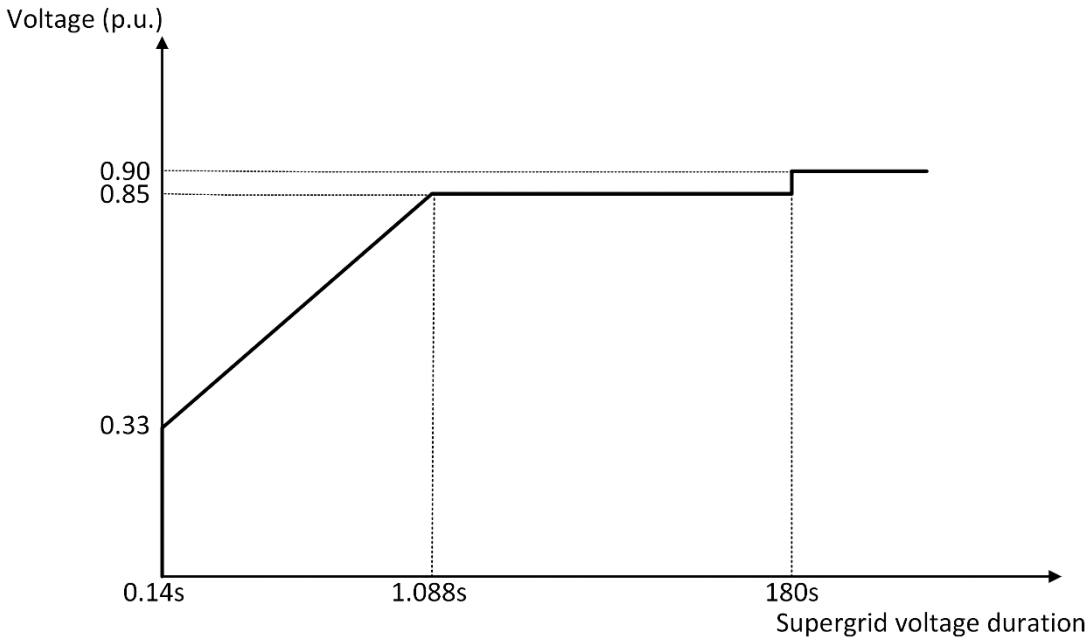

(a)

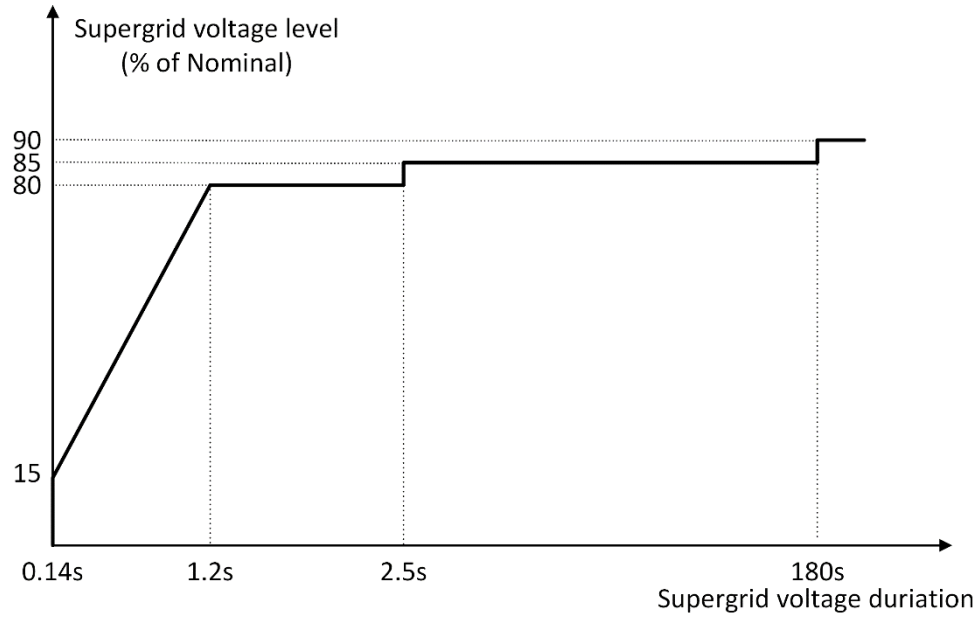

(b)

Figure 2-7 Requirements applicable to (a) Synchronous Generating Units (b) The undertaking of Offshore Transmission System Developer User Works（OTSDUW） Plant and Apparatus and Power Park [15]

2.4.1.2.2 Requirements for reactive current injection

In the GB Grid Code relating to converter-interfaced sources [15], a reactive current of at least 0.65 pu is required to be injected 60 ms after fault inception (and the reactive increase must begin 20 ms or less from the initiating event). These timescales are still relatively slow when one considers that transmission protection will typically complete its decision-making process in 20 ms or less. It is also worthy of note that this is somewhat more specific than the ENTSO-E code – while compliant with the code, it is a national interpretation and is more specific. It is shown in the figure that in the period after 60 ms, the current should continue to increase (above the solid red area shown in the figure). After a further time (the fault should ideally be cleared around 80 ms), then the converter output can either increase still further if the fault is not cleared, but it is also permissible that the converter may "block" in the red shaded area (block means that the converter can cease the output of power and disconnect from the system). This would only happen for faults that have not been cleared correctly and within the stipulated maximum fault clearance time in practice. While these codes have been defined relatively recently, there are still clear concerns (in the author's opinion) that in a converter-dominated power system, with converters fully code-compliant, during the first 20 ms period (when the protection is typically analysing the voltage and current and deciding whether to trip or not), then, according to the prevailing code, converters are not required to output any current at all. This has the potential for protection not operating quickly enough – which is clearly a concern. Accordingly, this further justifies the need for the work reported in this thesis: that is, a detailed investigation of the performance of protection in the presence of converter-interfaced sources.

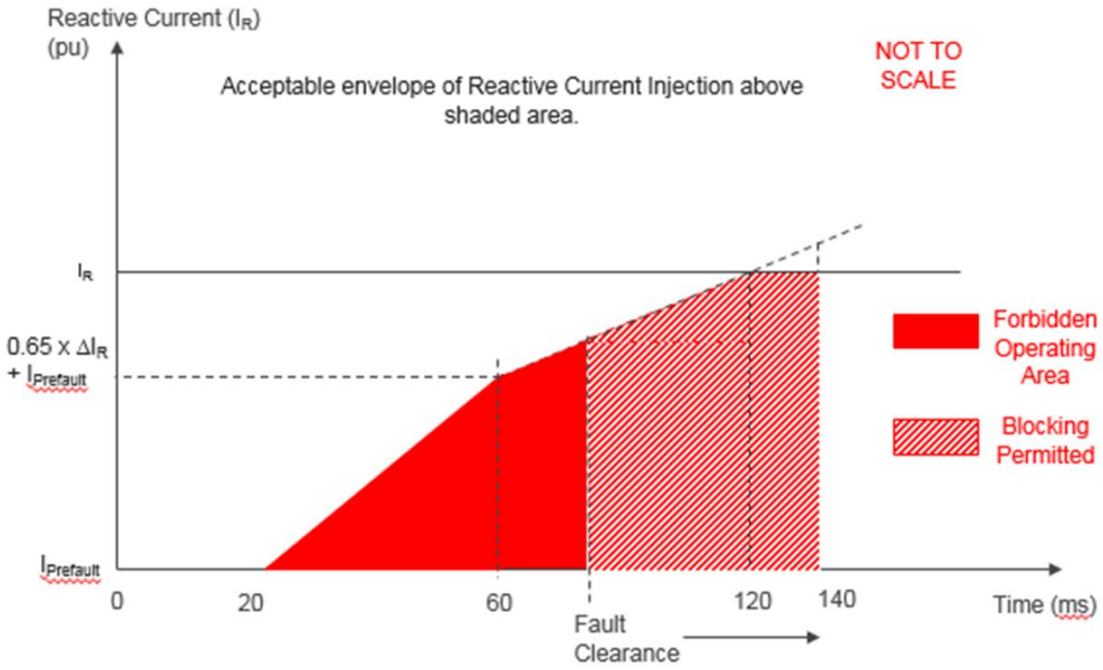

Figure 2-8 Required reactive current injection after faults [15]

As demonstrated in Figure 2-8**,** the reactive current (I_R) produced by the sources should be higher than the shaded area. When the operation mode of the sources is switched between normal mode and FRT mode, the transition is required to be relatively smooth to avoid perturbing the power system, which could lead to instability concerns.

During the first 20ms where the fault occurs, the source is not required to generate additional reactive currents. In the next 40ms, the source has to produce 65% of the required additional reactive current ΔI_R, where is defined as the difference between the required reactive current I_R and the pre-fault current I_{pre}:

$$\Delta I_R = I_R - I_{pre}$$

In the next 60 ms, the source has to gradually ramp up its reactive current output to I_R.

The final output of the required reactive current I_R generated by the sources connected to the grid is dependent on the pre-fault operating condition and the retained voltage of the grid as displayed in Figure 2-9. The lower the retained voltage at the grid connection/interface point, the higher the additional reactive current that will be required from the generating source.

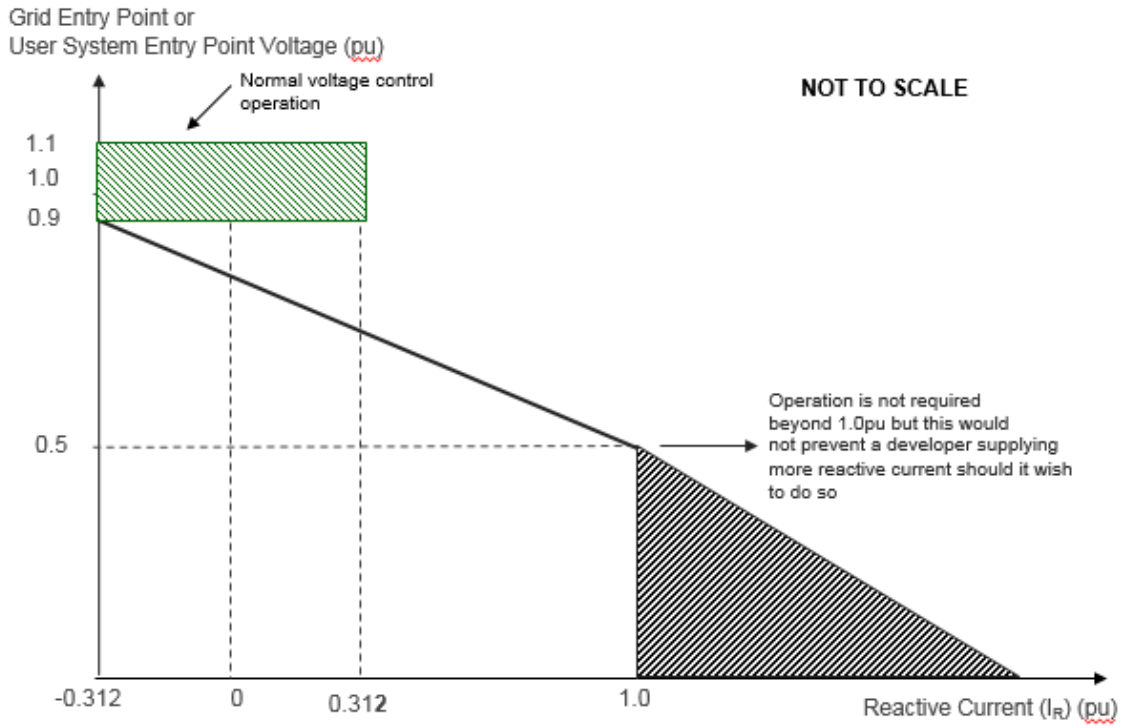

Figure 2-9 required reactive current injection under different voltage levels [15]

2.4.2 Requirements for protection devices

The requirements from the GB grid code documentation code [15] published by NGESO are as follows:

- “The fault clearance time specified in the Bilateral Agreement shall not be shorter than 80 ms at 400 kV.”

With typical circuit breaker operation times of 50 ms [18], faults shall be detected (and a decision made as to whether a tripping command is issued or not) by the protection system in around 30 ms, although many modern protection relays achieve this in 20 ms or less.

While there are requirements in terms of the time of operation of protection, there is still a requirement to understand more completely how future power systems with high penetrations of converters will behave, and how this may impact protection (with a focus on distance protection in this work, as this is deemed more likely by the author and the project sponsor to be at risk compared to differential schemes, which are the other main type of protection used at transmission).

2.5 Power electronic converters

Power electronic converters, which are used to facilitate the integration of renewable energy to AC grids, and underpin HVDC transmission networks, are already playing a critical role in power systems, and this will increase markedly in the future. The development of power electronics has a long history, and the main events in the early phases of this history are summarised in Figure 2-10.

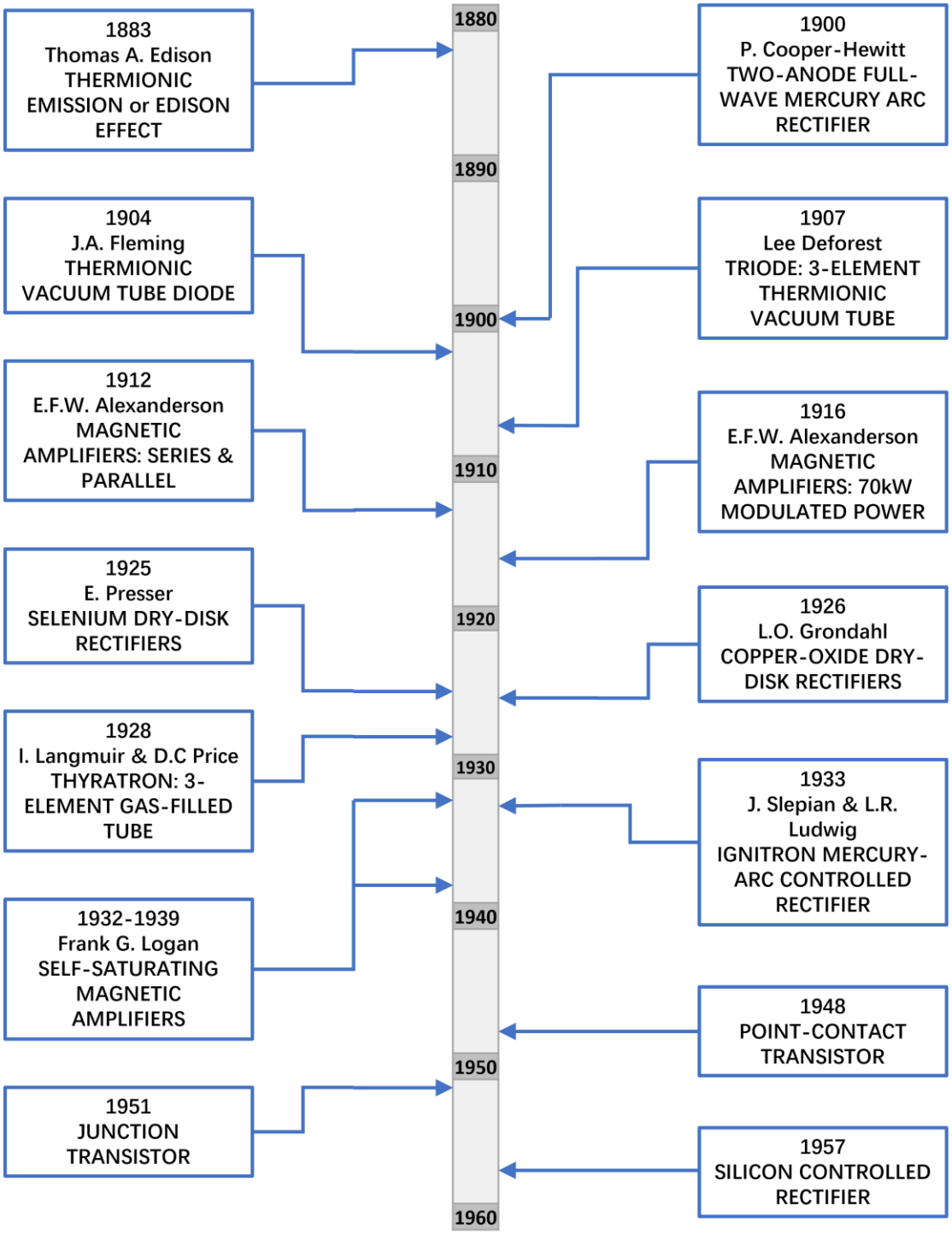

Figure 2-10 Timeline of the early evolution of power electronics [19]

The first power electronic device was the mercury arc rectifier, developed by Peter Cooper Hewitt in 1902 [20]. In 1925 the concept of the field-effect transistor was developed by Julius Edgar Lilienfeld and then in 1948, William Shockley invented the

first bipolar junction transistor (BJT) [21]. In 1957 General Electric introduced the three-terminal p-n-p-n device, also known as the silicon-controlled rectifier (SCR).

Following on from the above relatively early phases of development, the initial research and prototyping in the areas of high-power converters began in the 1970s and 1980s, with the gate turn-off (GTO) thyristor being developed and introduced commercially [22]. Subsequently, the insulated gate bipolar transistor (IGBT) was introduced in 1983 [23]. In the 1990s, the injection-enhanced insulated gate bipolar transistor (IEGT) and the integrated gate-commutated thyristor (IGCT) were invented by Mitsubishi and ABB [24] [25]. Since then, new materials and technologies have resulted in ever-higher ratings and power densities, along with enhancements to reliability, performance and flexibility.

As defined in [26], based on the number of layers, semiconductors can be classified into the following two types :

- Thyristor-based devices: SCR, GTO, and IGCT,
- Transistor-based devices: IGBT and IEGT.

The corresponding voltage and current ratings of these switching devices are illustrated in Figure 2-11. Note that these ratings were correct at the time of publication of the diagram below, and ratings and voltage levels are continually changing and increasing.

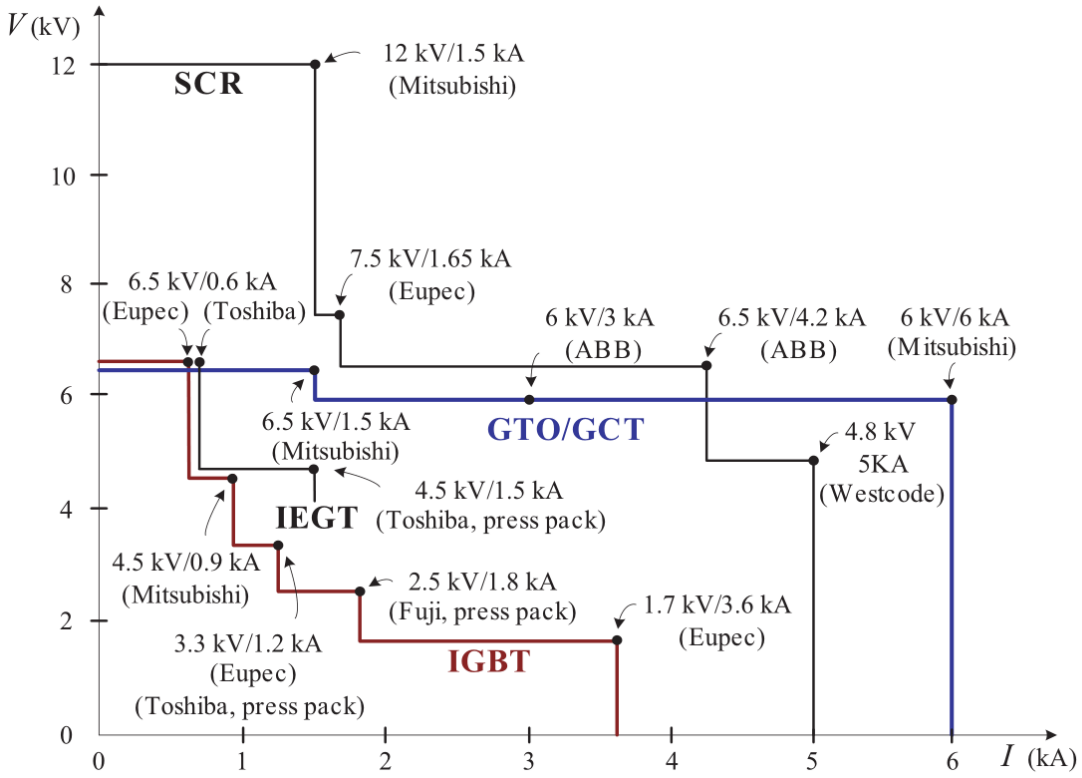

Figure 2-11 Voltage and current ratings of high-power semiconductor devices [26]

2.6 HVDC systems

The utilisation of HVDC interconnectors and infeeds to AC systems is increasing significantly due to the numerous advantages that HVDC offers over traditional HVAC systems, including transmission capacity, reduced losses, the ability to decouple and remove the need for synchronism between individual large AC synchronous systems, the buffering and limiting of the impact of disturbances on one system to the other system connected via the HVDC link, etc. [27]. The commonly utilised HVDC systems can be classified into the following two types: current-source converter (CSC); and voltage-source converter (VSC) based HVDC systems. Details of each type of system will be introduced in the following sections.

2.6.1 CSC HVDC system component and operation principles

CSC HVDC systems, also known as line-commuted converter (LCC) HVDC transmission systems, have a history that can be traced to 1954 when ABB introduced its first commercial HVDC link. Before the 1970s, the HVDC links utilised mercury arc valves to enable the conversion between AC and DC. Subsequently, thyristor valves were used. A typical CSC HVDC system is depicted in Figure 2-12. The system contains the following components: converters, converter transformers, smoothing reactors on the DC side, reactive power compensation, filters, control and communication system.

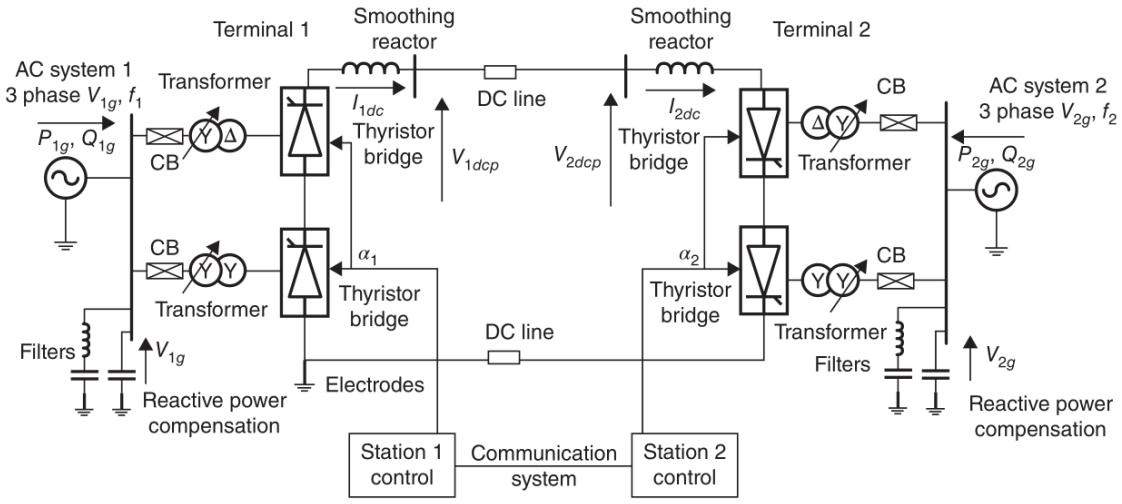

Figure 2-12 A typical CSC HVDC system [28]

Each converter station, i.e. the rectifier station and inverter station, contains at least six valves, which is often referred to as a "six-pulse Graetz Bridge" [29], as shown in Figure 2-13.

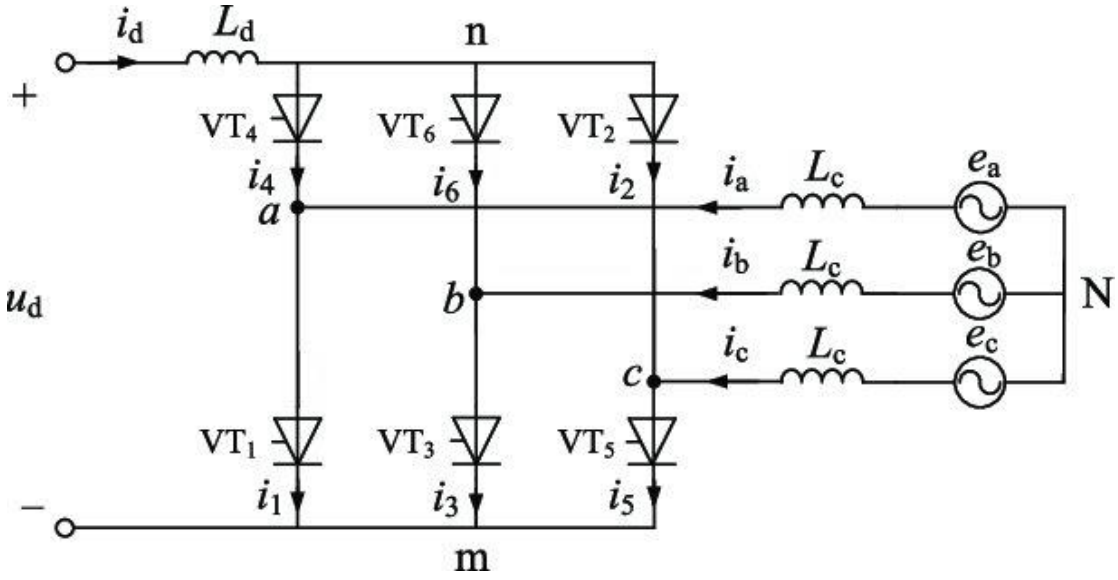

Figure 2-13 Six-pulse bridge with thyristor values [30]

When the line voltage from the AC system reaches the phase known as the firing angle, the thyristor is switched to conduct the current. AC voltage from the grid side is required for the commutating process. The operation of the CSC HVDC station always absorbs reactive power. Reactive power compensation is therefore required in all cases. The direction of the DC current shall remain unidirectional, but the polarity of the DC voltage can be controlled by varying the firing angle. When the firing angle is lower than 90°, the converter is operating as a rectifier. When the firing angle is higher than 90°, the converter is operating as an inverter. The relationship between the DC voltage and the firing angle is demonstrated in Figure 2-14.

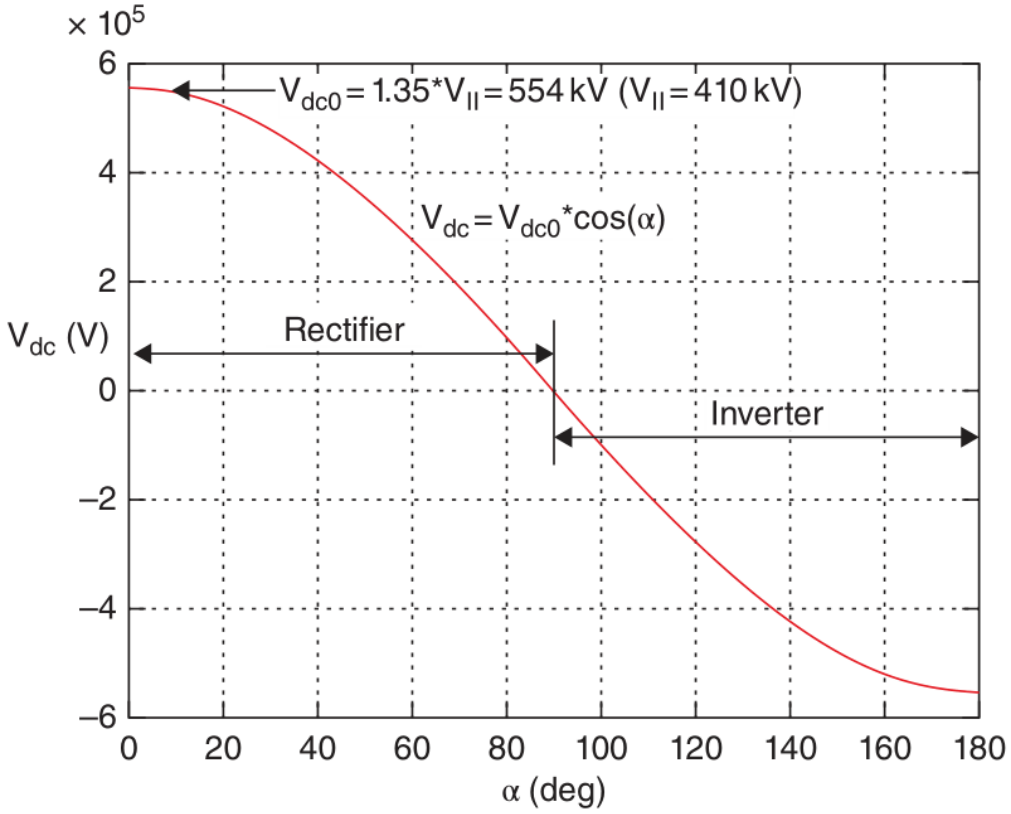

Figure 2-14 Thyristor converter DC voltage as the function of firing angle [28]

To avoid voltage instability during disturbance, the CSC system requires a “strong” AC system and voltage from the grid side (a strong system normally has a high fault level and is relatively robust in terms of voltage stability during and after disturbances) [31]. Large AC and DC filters are essential in the system to mitigate harmonic issues.

Sufficient turnoff time (extinction angle) is required for CSC converters to ensure that the thyristor can regain forward blocking capability. Commutation failure will occur when the requirement is not met since the thyristor cannot get into a blocking state (the device will keep conducting current). Commutation failure is very likely when there is a 5-10% depression at the AC side for CSC inverters [28], meaning that CSC HVDC systems can be extremely vulnerable to network faults in the vicinity of the AC system terminals.

Figure 2-15 shows the typical output waveforms from a CSC converter (operated in inverter mode). The converter aims to generate a sinusoidal waveform at the desired frequency, with the gate opened at the firing angle and closed at the extinction angle – it is clear that the waveforms are very non-sinusoidal and would require a large degree of filtering before connection to the AC system.

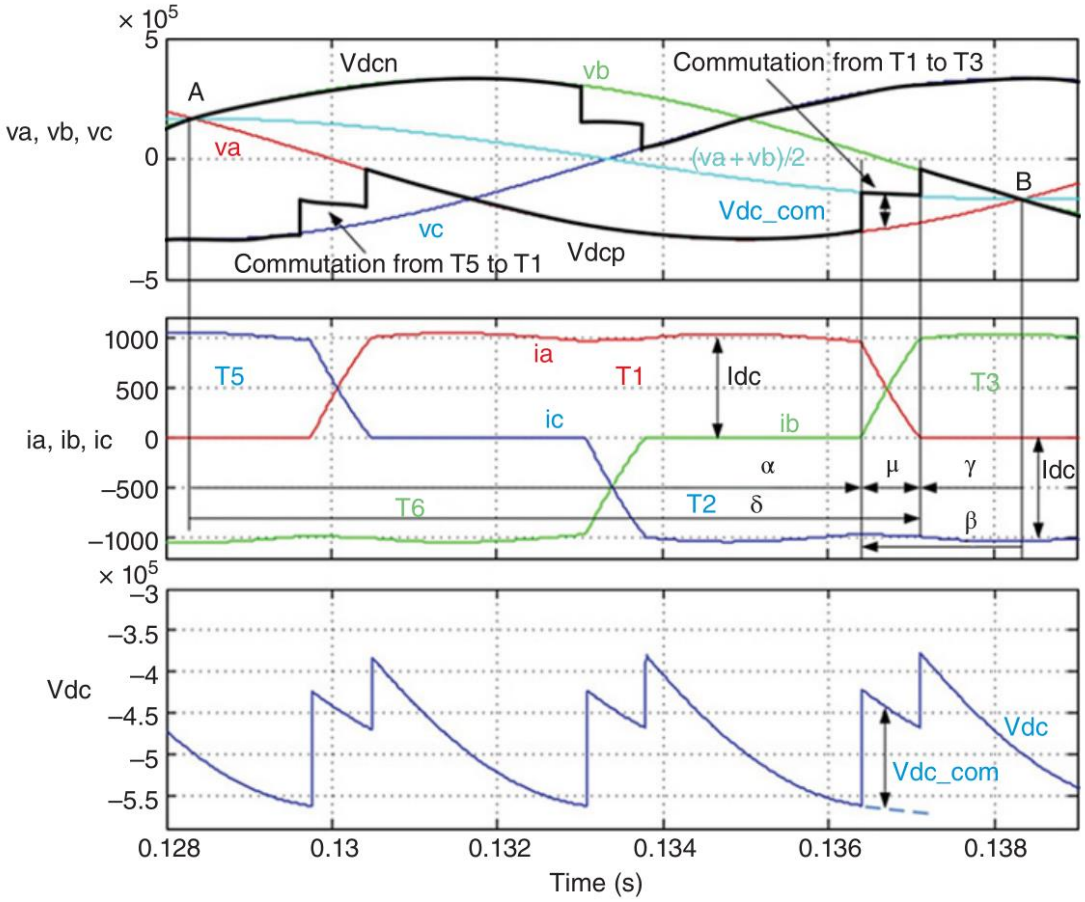

Figure 2-15 Typical output waveforms from a CSC converter (α - firing angle; δ - extinction angle; μ - commutation overlap angle; β - ignition advance angle; γ - extinction advance angle) [28]

As mentioned in this section, LCC HDVC systems have a number of drawbacks, particularly in terms of operation during disturbances and network faults. However, the drawbacks are overcome in the emerging development of VSC technology which will

be explained in detail in the next section. It is presumed that during network faults a CSC-connected infeed will most likely block/trip during the fault, so the thesis is more focussed on the behaviour and modelling of VSC converter-connected sources and infeeds.

2.6.2 VSC HVDC system component and operation principles

Compared with a CSC HVDC system, the VSC HVDC system has multiple technical advantages (controllability, flexibility, etc.) [32]–[36]. Different from the LCC system, the control of the VSC system is achieved by fast switching of the IGBT switches while the operation is independent of the AC voltage. With the help of Pulse Width Modulation (PWM), the converter can provide fast control of its output real and reactive power. As summarised in [32], the comparison of LCC and VSC schemes is demonstrated in Table 2-1.

Table 2-1 Comparison of LCC and VSC systems (modified from [32])

LCC	VSC
Thyristor based technology	IGBT based technology
The semiconductor can withstand voltage in either polarity	Withstand current in either direction
Constant current direction	The current direction changes with power
Turned on by a gate pulse but rely on an external circuit for its turn off	Both turn on and off are carried out without the help of external circuits
Good overload capability	Weak overload capability
Requires stronger AC systems for excellent performance	Operate well in a weak AC system
Requires additional equipment for black start operation	Possesses black start capability
Poor reactive power control	Good reactive power control
Lower station losses	Higher station losses
Reversal of power is done by reversing the voltage polarity	Power is reversed by changing the current direction
Higher voltage capability of over 1000KV	Lower voltage capability of around 600KV
Mostly used to transmit bulk power for a long distance	Used for transmitting power from remote areas with renewable energy
Suffers commutation failures as a result of a sudden drop in the amplitude or phase shift in the AC voltage.	Does not suffer commutation failure.
Commutation failures and the need for change in dc polarity, when the converter wants to change from rectifier to inverter mode, make LCC HVDC more problematic to adopt in a multi-terminal HVDC system.	Suitable for multi-terminal HVDC systems because it does not suffer from commutation failures, has independent, multidirectional power flow, and operates with the same voltage polarity.

Figure 2-16 presents a commonly used three-phase, two-level VSC with switch bridges. By altering the on/off stage of the switches (constructed using an IGBT and a diode), the converter can output voltages with magnitudes of $+\frac{V_{DC}}{2}$ and $-\frac{V_{DC}}{2}$ with a variable, controllable, duration. The PWM technique is the fundamental mechanism by which

VSCs can modulate voltage waveforms to provide different AC voltage phase angles and magnitudes from a DC voltage input (or vice versa in rectification mode). This is achieved using a carrier waveform in conjunction with a reference waveform. Figure 2-17 illustrates the PWM process for a single phase of VSC switches. When the sawtooth modulating signal rises higher than the voltage waveform reference from the VSC control system, then in each bridge, the lower switch is in the on position, with the upper switch in the off position, and a voltage magnitude of $-\frac{V_{DC}}{2}$ is produced. When the sawtooth modulating signal drops lower than the voltage waveform reference, a magnitude of $+\frac{V_{DC}}{2}$is produced with the upper switch on and lower switch off. The upper and lower switches are operated in a complementary mode which means that when one switch is on and the other switch must be off.

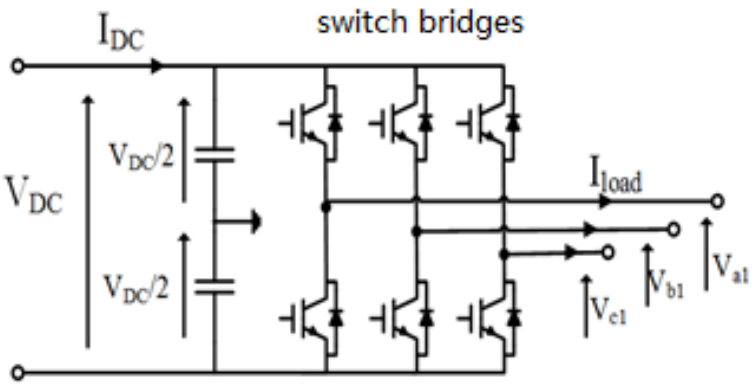

Figure 2-16 Configuration of two-level VSC converter

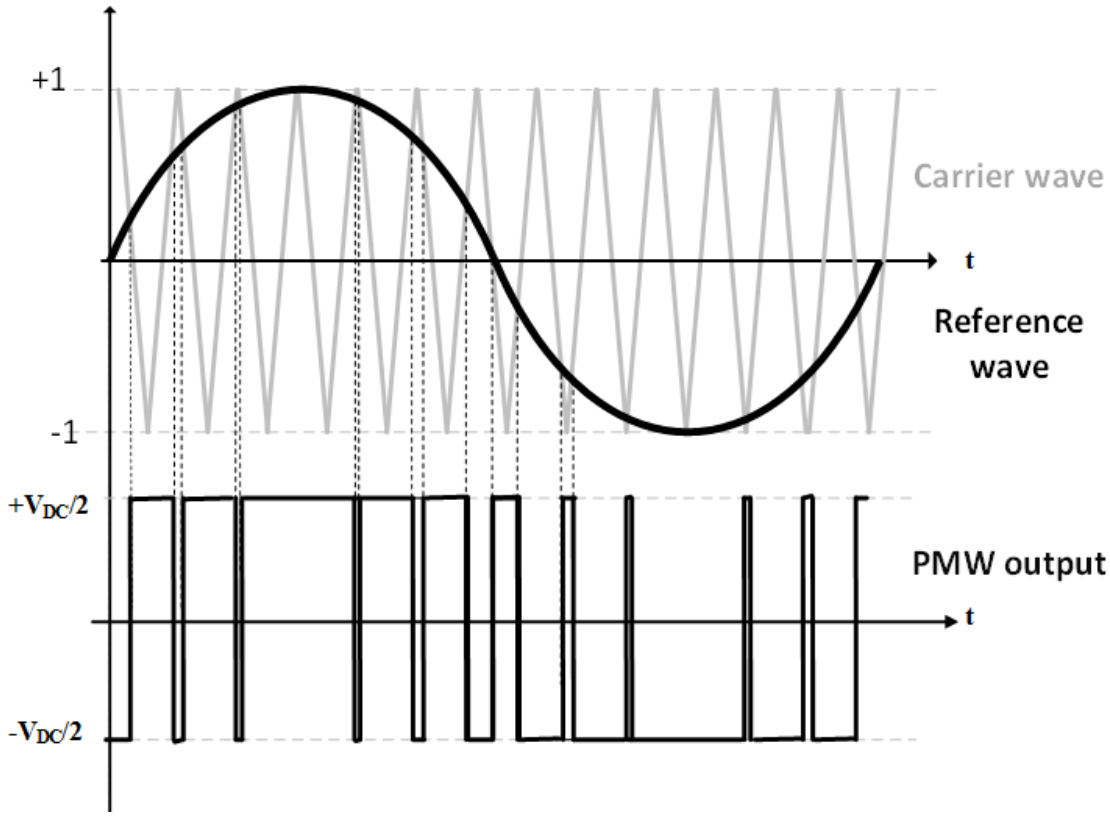

Figure 2-17 Output of a two-level converter using Pulse Width Modulation (PWM) [37]

The frequency of the carrier wave determines the switching frequency of the power electronic devices. High-order harmonics are inevitably produced due to the VSC switching actions and steep-fronted waveform on the PWM output signal and these harmonics can be removed using a low-pass filter to enable a relatively smooth sine-wave VSC voltage output – typical outputs from inverters are shown in Figure 2-15 and Figure 2-19. As the orders of high harmonics are predictable from the VSC switching frequency, a relatively small-sized filter device can be selectively tuned to remove the designated orders of harmonic orders (normally 1st order or 2nd order with respect to the switching frequencies). By increasing the number of the sub-modules in each of the bridge arms, the modulated multilevel VSC converter is introduced to mitigate the

challenges related to the harmonics issues and release the stress of the switching frequency of the converter station. The difference between the topology of two-level VSC and multilevel VSC is displayed in Figure 2-18 and their corresponding output voltage after PWM is demonstrated in Figure 2-19.

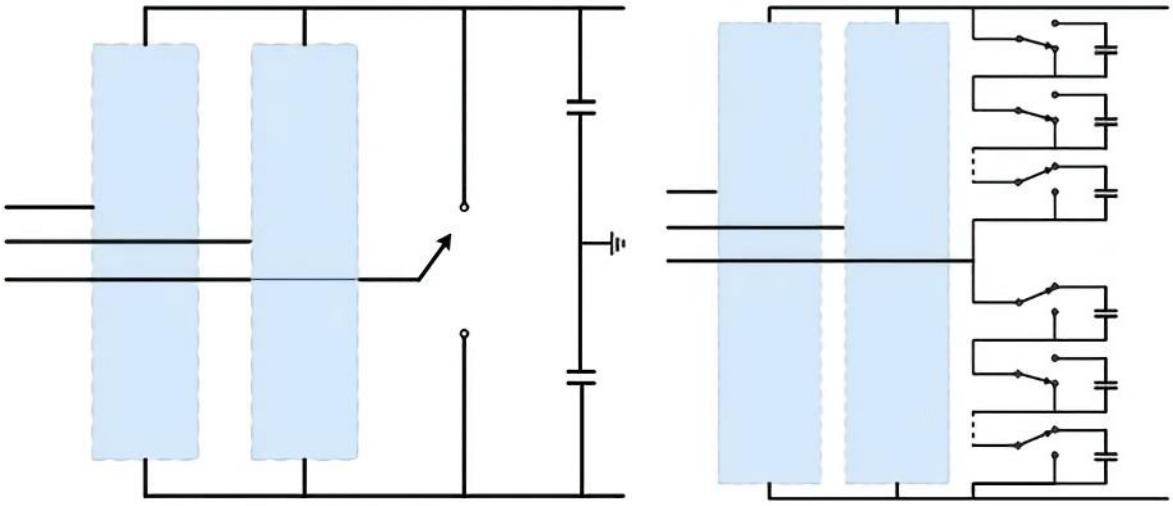

(a) Two-level VSC converter (b) Modulated multilevel VSC converter

Figure 2-18 Different types of VSC converters[37]

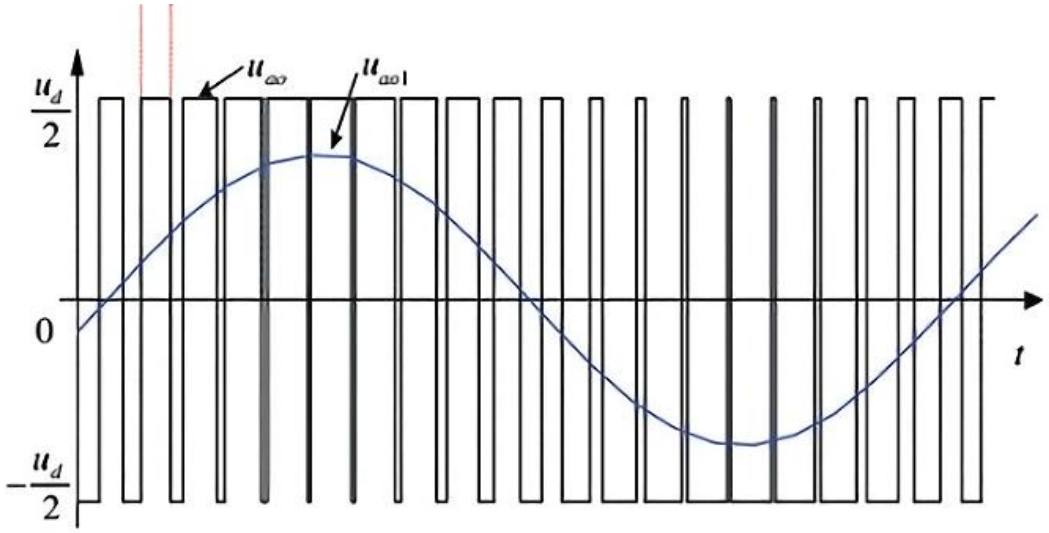

(a) Two-level VSC converter

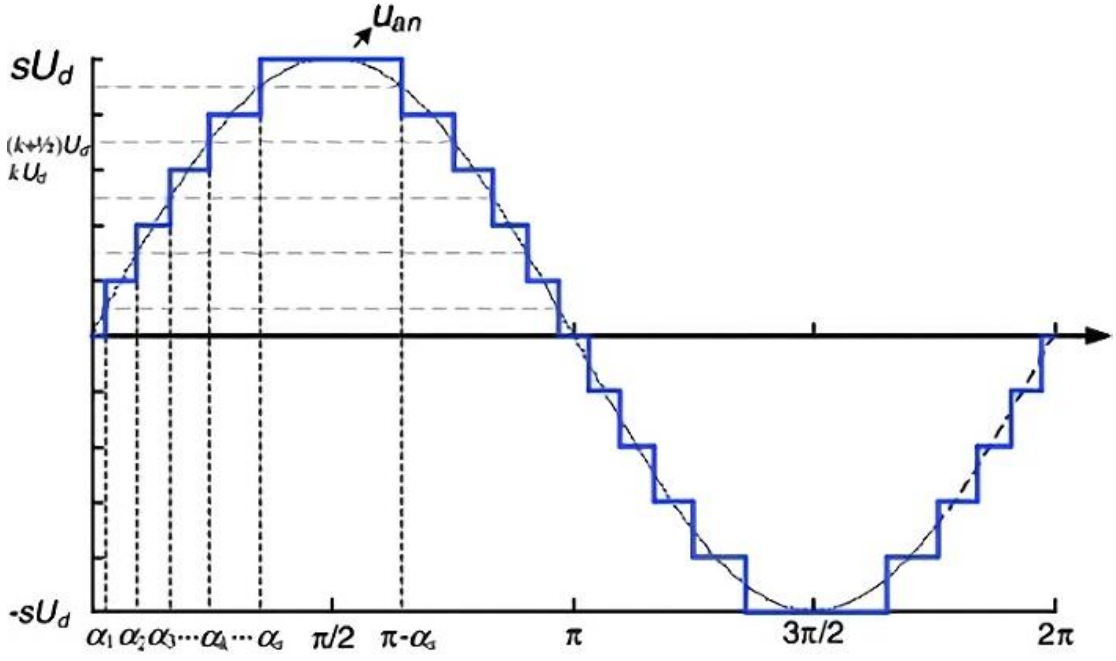

(b) Modulated multilevel VSC converter

Figure 2-19 Output of different types of VSC converters [37]

After the PWM, the output of the system is managed through the following components:

- *Phase Locked Loop (PLL*): this tracks the system's AC voltage phase and frequency continually at the point of connection. The information is used by the Park and Inverse Park transformation processes within the controller.
- *The Park transformation:* this converts *ABC* three-phase voltages and current into *dq* values under a rotating reference frame, as *dq* values can be more efficiently manipulated by the controllers.
- *Inner current control system:* this reacts quickly to regulate the converter's output current to its reference value by manipulating the VSC output voltage.
- *Outer control system:* this provides a reference value for the current controller. The selection of the reference values can be varied by a user or in accordance with the intended role of the converter.

In the inner control loop, the three-phase voltages and currents, as measured at the point of common coupling (PCC), are transformed into *dq* values by one positive sequence rotating reference frame and one negative sequence frame, both of which mutually rotate in opposite direction with the same fundamental frequency.

$$v_{dq} = v_d + \mathrm{j}v_q = \frac{2}{3} j e^{-j\omega t}(v_a + e^{j\frac{2}{3}\pi} v_b + e^{-j\frac{2}{3}\pi} v_c) \qquad \text{Equation 2-9}$$

$$i_{dq} = i_d + \mathrm{j}i_q = \frac{2}{3} j e^{-j\omega t}(i_a + e^{j\frac{2}{3}\pi} i_b + e^{-j\frac{2}{3}\pi} i_c) \qquad \text{Equation 2-10}$$

The magnitudes of i_d and i_q are regulated by the PI controllers with the inner current control according to the reference values. To achieve the control of i_{dq}, the VSC output

voltage references v_d and v_q are computed taking account of the coupling effect of the VSC phase reactor and transformer.

When the current is controlled, the associated output voltage of the converter can then be determined. The following Figure 2-20 demonstrates the equivalent circuit of VSC converters are connected to the grid at the point of common coupling (PCC) through phase reactor and transformers （represented by the equivalent resistance and reactance）:

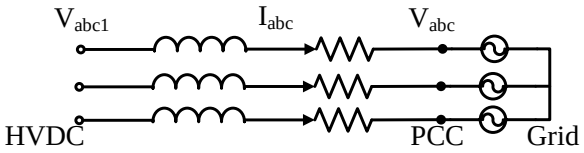

Figure 2-20 Converters connected to the grid.

It is clear that the relationship between the grid voltage v_{abc}, converter output voltage v_{abc1} and current value i_{abc} is as follows:

$$v_{abc1} = L\frac{di_{abc}}{dt} + Ri_{abc} + j\omega Li_{abc} + v_{abc} \quad \text{Equation 2-11}$$

Where *R* and *L* are the equivalent resistance and reactance of the phase reactor and transformer between the converter station and the grid.

Representing the above in the *dq* positive and negative sequence forms:

$$v_{d1} = L\frac{di_d}{dt} + Ri_d - \omega Li_q + v_d$$ Equation 2-12

$$v_{q1} = L\frac{di_q}{dt} + Ri_q + j\omega Li_d + v_d$$ Equation 2-13

Following the inverse transformation of the *dq* voltage components to *abc* voltage components, the PWM produces the required voltage waveforms to complete the final step of VSC control.

In the outer loop, the reference values of i_d and i_q can be computed by controlling various system variables (*P*, *Q*, V_{DC} and V_{AC}) using the equations presented below:

The reference value of i_d can be determined by the desired reference value of AC real power:

$$i_d^* = \frac{2}{3}\frac{P_{AC}^*}{v_d}$$ Equation 2-14

Or by the desired reference value of DC voltage:

$$i_d^* = \frac{2}{3}\frac{V_{DC}^*}{v_d}\left(C\frac{V_{DC}}{\mathrm{dt}} + i_{load}\right)$$ Equation 2-15

The reference value of i_q can be determined by the desired reference value of AC reactive power:

$$i_q^* = \frac{2}{3}\frac{Q_{AC}^*}{v_d}$$ Equation 2-16

Note that the voltage drop between v_{abc} andv_{abc1} is dependent on the current passing through the impedance (resistance is typically negligible compared to the high values of reactance) of the phase reactor and transformer as shown in Figure 2-20. Therefore, in order to regulate the AC voltage amplitude to the reference value (i.e. make the voltage amplitude v_{abc} at the PCC close to its desired reference value v_{abc}^*), the reactive power should be controlled accordingly [7].

The output current references i_{dq}^* are computed by comparing the power/voltage references with the measured values:

$$i_d^* = \frac{2}{3}\frac{P_{AC}^*}{v_d} + \mathrm{PI}(P_{AC}^* - P_{AC})$$ Equation 2-17

$$i_d^* = \mathrm{PI}(V_{DC}^* - V_{DC})$$ Equation 2-18

$$i_q^* = \frac{2}{3}\frac{Q_{AC}^*}{v_d} + \mathrm{PI}(Q_{AC}^* - Q_{AC})$$ Equation 2-19

$$i_q^* = \mathrm{PI}(\,|v_{abc}^*| - \,|v_{abc}|)$$ Equation 2-20

Relatively recently, inverters have been classified as “grid following” or “grid-forming”. The latter category of inverters, as the name suggests, is capable of “starting”

and forming an (islanded) system and can potentially be used for black start applications. More information on these types of inverters can be found here [39].

In terms of their responses to faults, grid-following converters are basically what is considered in this thesis. For grid forming converters, the behaviour during faults is depending on their current limiting strategies [40], including switching to the grid following converter mode, adjusting virtual impedance mode, additional inner current limitation mode and outer power reference adjustment mode.

Figure 2-21 below [41] shows the behaviour of a grid-following converter during the fault. The current limiting strategies applied in this paper are achieved by inner current limitation and outer power reference adjustment. While it behaves well and exhibits strong ride-through behaviour, it is clear that the response is still “delayed” and there is a ramp-up to a sustained, and relatively low, fault current similar to other converters, and this may still cause issues for power system protection.

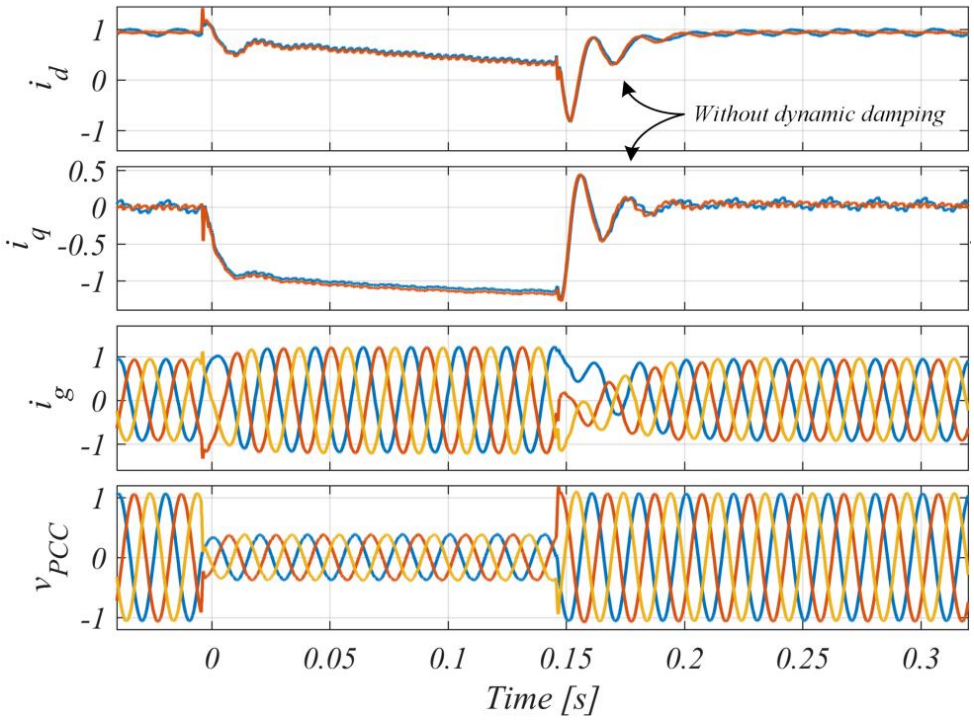

Figure 2-21 Fault response of a grid-following converter [41]

2.6.2 Fault response and behaviour of VSC converters

The fault response of converters is not "standard" in the way that synchronous machines respond (which is effectively governed by the physics and magnetic/mechanical interactions in the machine – certainly for the first several cycles following fault inception). A converter's response to short circuits is effectively dictated by the converter control system (and to an extent the energy source "behind" the converter), and while standards [8], [14], [15] exist relating to the performance of converters, the actual exact and detailed response can vary widely across different converters, and, as highlighted earlier, grid codes are not always precise in defining the exact nature of responses to voltage depressions and short circuits on the AC network being supplied

by the converter. It is clear that these waveforms are not uniform and completely different from a synchronous machine output, which can be easily modelled and well-understood (more examples of the output voltage and current waveforms of a converter for a range of faults, with a range of voltage depressions, based on actual laboratory tests can be found in figures from Chapter 4). This further justifies the research reported here and the need for a model that is flexible and can provide different fault responses to evaluate the potential impact of converter-interfaced sources on power system protection for a range of scenarios and assumed converter responses. In Chapter 4, responses of converters to external faults are covered in more detail and examples of simulated and measured responses are included, which shows the non-standard and non-repeatable nature of converter responses to external short circuits.

Accordingly, a flexible model for a converter providing fault response has been developed. This is described in detail in Chapter 4, but the basic performance of the model can be configured to allow changes to be made to the initial delay in responding, any initial dip or drop in output current immediately after fault inception, the maximum amplitude of the fault current that can be provided, and the ramp rate of the increase in output current to its full value. This is shown in Figure 2-22.

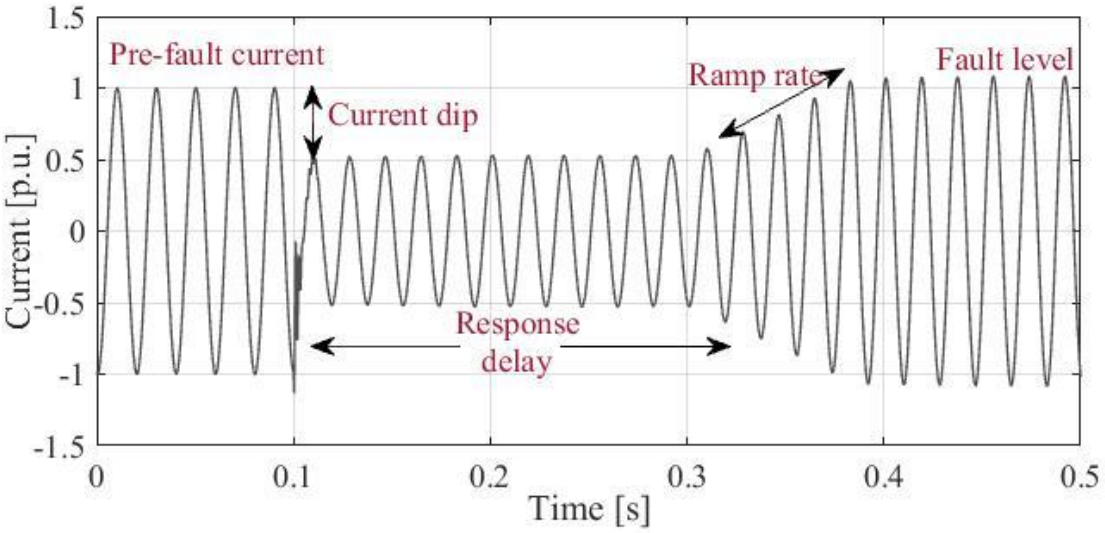

Figure 2-22 Controllable output current provided by converter#

2.7 Summary

Detailed studies have been conducted in this chapter to gain insights into the behaviour of power systems dominated by traditional synchronous machines and converter-based energy sources. The review has highlighted how the increasing introduction of converter-based energy sources has brought changes in system behaviour.

The chapter has begun with an examination of the driving forces behind the ongoing transformations in electrical power systems, highlighting their expected future evolution. The fundamentals of power systems dominated by converter-based energy sources have been explored. Additionally, traditional generation technologies have been reviewed, including their response to faults in terms of fault current supply. Converter interfaces used for NSG, such as CSC and VSC, have also been discussed. A comparison has been presented, focusing on their behaviour during faults, which has

revealed the need for a flexible model to investigate performance and potential impact on protection systems. Furthermore, the chapter has provided an introduction to the specific design and configuration of the VSC converter employed in the research project.

In conclusion, it has been established that the future power system will exhibit significant differences due to the integration of converter-based energy sources, posing considerable challenges to traditional protection systems. The next chapter will provide a review of the fundamentals of protection systems to address these challenges.

Chapter 3

Review of Protection Fundamentals

3.1 Introduction

This chapter reviews power system protection principles and the associated challenges introduced by converter-interfaced sources. The fundamentals of power system faults are explained in section 3.2; while sections 3.3 and 3.4 introduce the detailed operating principles of traditional protection systems and how the power and protection systems might be affected by changes to fault behaviour in future converter-dominated power systems.

3.2 Faults

This section presents an introduction to faults including definitions, typical fault types and examples of voltage and current characteristics in three-phase systems during different types of faults.

3.2.1 Faults definition and classification

Fault can be defined as any abnormal condition of connections between conductors [42]. If faults are not removed quickly from power transmission systems, this could lead to severe damage to the system and may also have significant public safety implications [13].

Faults can be classified into open circuit (OC) faults (due to unwanted breaking of conductors including joint failures, circuit breaker failures where they become in a non-instructed open state, unexpected degradation or melting of fuses, etc) and short circuit

(SC) faults (due to insulation failures, lightning strikes, vegetation encroaching on to conductors, switching transient overvoltage, etc.) [43]. SC faults are the most common type of faults within power systems and are considered to be the potentially most harmful type of fault as the excessive currents involved can result in damage to equipment and has the potential to lead to instability within the power system. As demonstrated in Figure 3-1. In three-phase power systems, SC faults can be divided into the following types: three-phase (Ph-Ph-Ph); phase-to-phase (Ph-Ph); phase-to-phase to-earth (Ph-Ph-E), and single-phase-to-earth (Ph-E) faults.

In a system dominated by VSC, the behaviour of energy sources differs from traditional SG-based systems. In a fault situation within a traditional power system, the voltage at the faulted point collapses while the current simultaneously rises with a high magnitude provided by the SG. However, in future converter-dominated power systems, the fault response is influenced by the control algorithm of the converter. This control algorithm will be discussed in detail in the subsequent section.

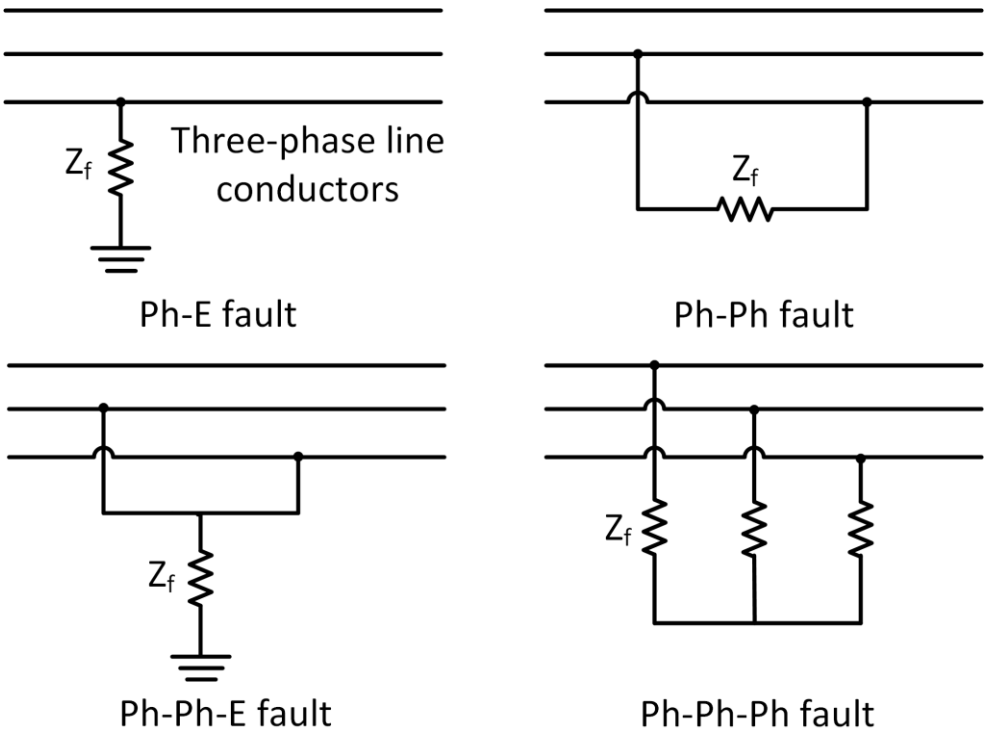

Figure 3-1 Fault types [44]

3.2.2 Overview of typical in-field fault current responses

As the project reported in this thesis was supported by NGESO, the technical specification for the fault current studies all comply with the relevant EYTS documents [45].

A typical fault current waveform (as displayed in Figure 3-2) in a transmission system consists of two parts (as shown in Figure 3-3 and Figure 3-4): an AC component with a moderately slow decay rate and a DC component with a comparatively fast decay rate. The AC component is self-explanatory and arises simply from the sources being presented with a massively reduced impedance; the DC component depends on the point of a wave of fault occurrence, the value of current at the time of the fault, and is

due to the inductance in the system. As is well-known, the current in an inductor cannot change instantaneously due to Lenz's Law, and the DC component is introduced to compensate, and its initial value is equal, but opposite to, the instantaneous value of the AC current at fault inception, but of opposite polarity. As already mentioned, the magnitude of the DC component is dependent on where in the cycle the fault inception takes place. In the worst case, the initial dc offset will be $\sqrt{2}$ times the symmetrical short circuit value (RMS). The decay rate of the fault current is dependent on the *X/R* ratio of the system supplying the fault current. If the *X/R* ratio is higher, the DC component will decay relatively slowly.

It is clear that around 10 ms (although this may vary depending on the point on wave at which the fault occurs and on the impedance to the fault) following the inception of the fault, the fault current shall reach its maximum peak instantaneous value which is named "peak current" since the fault level will continuously decay with time (both AC and DC components). At a point later in time, when the protection has detected the fault and issued a trip – this time is typically (at the fastest) around 10-15 ms, which is then added to by other delays associated with communications and circuit breaker initiation, it is assumed that circuit break contacts may begin to separate at around 50ms, with fault clearance taking another additional variable amount of time, as typically the arc between the breaker contacts will extinguish as the current passes through a zero crossing, and all three phases may extinguish at different points. Accordingly, after this delay of several 10s of milliseconds, the "peak break" duty of the breaker will be carried out. Following fault clearance, many auto-reclose schemes will instruct circuit breakers to close. If the fault on the system is permanent, then the circuit breakers have the duty of being able to close onto the fault, and this is named "peak make" associated with the

circuit breaker. It is also important to note that all electrical equipment in the system close to the fault will also experience peak make currents before faults, and again if circuit breakers are closed onto the faults [45]. The peak break and make currents are the combination of the aforementioned AC and DC components.

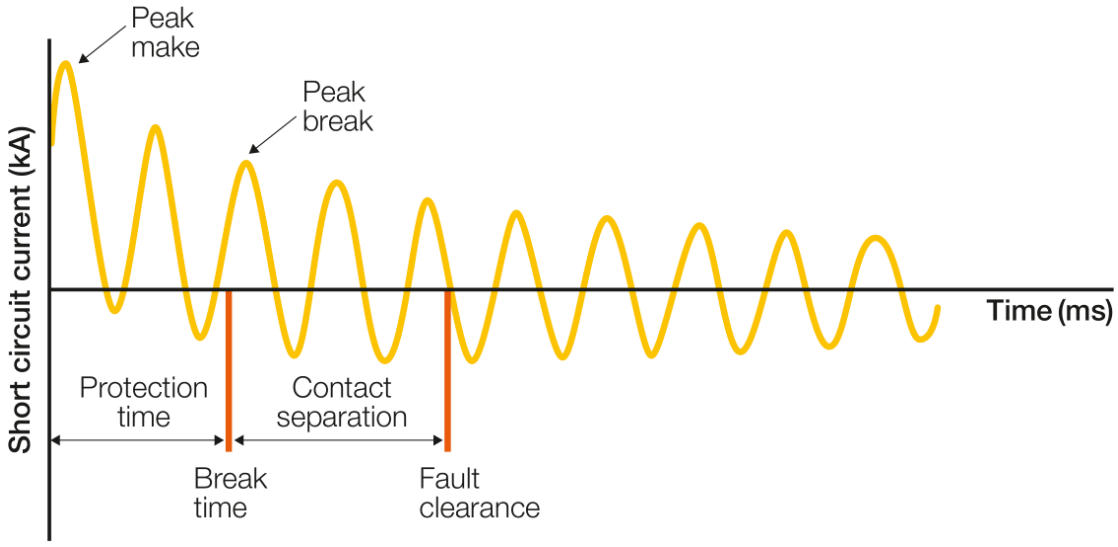

Figure 3-2 A typical fault current with AC and DC components combined [45]

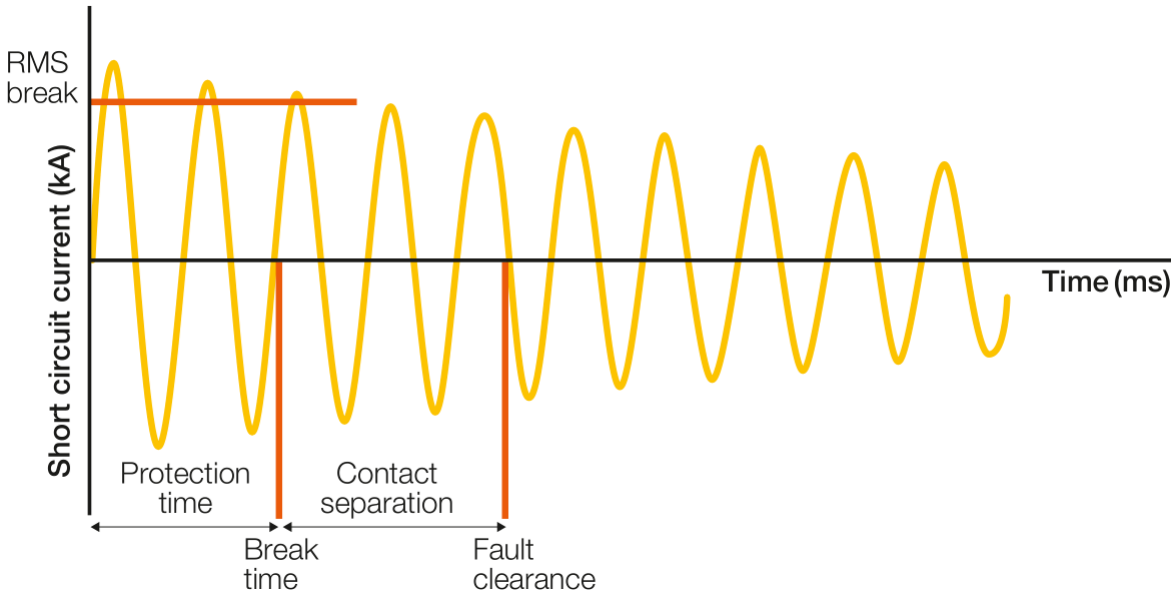

Figure 3-3 AC component of a typical fault current [45]

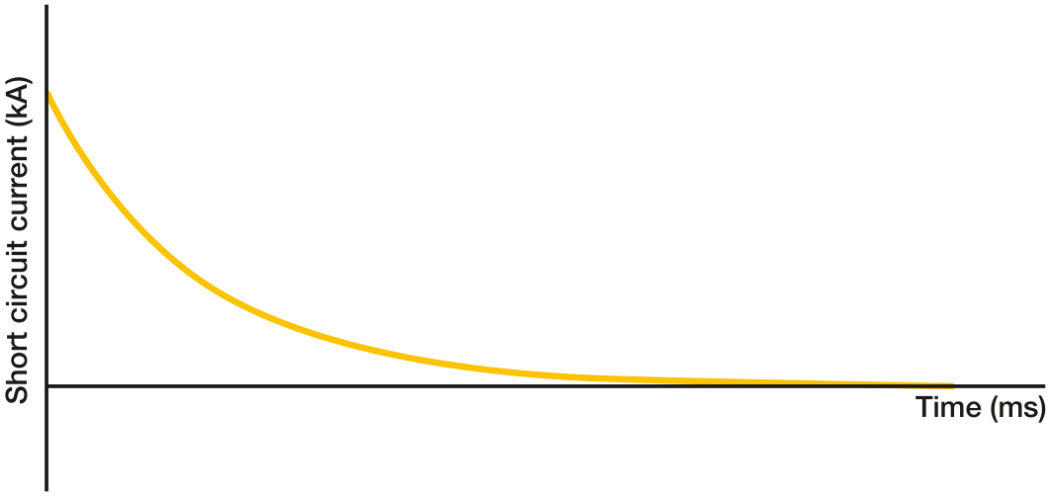

Figure 3-4 DC component of a typical fault current [45]

3.3 Power system protection

This section presents an overview of typical protection systems, definitions and common practices. The main types of protection summarised include differential, distance and overcurrent protection systems.

3.3.1 Definition

From section 3.22, it is clear that faults in power systems are impossible to eliminate due to inevitable mechanical and natural causes, which emphasises the need for and the importance of protection systems. As defined by Blackburn [46], protection engineering, “is the science, skill, and art of applying and setting relays and/or fuses to provide maximum sensitivity to faults and undesirable conditions, but to avoid their operation on all permissible or tolerable conditions”. A typical protection system is

presented in Figure 3-5. The operation of the protection system can be summarised as follows:

Measuring primary system quantities (voltage and/or current) and converting them into appropriate secondary values through transformers including voltage transformer (VT) and current transformer (CT). The selection of VTs and CTs and their characteristics is dependent on the type of protection system and the system being protected.

After receiving inputs from CTs and VTs (outputs of CTs and VTs are subject to standards and should be the same regardless of the manufacturer [43], [47]), relays are required to analyse and make key decisions: whether a fault is detected, and whether the relay should issue trip signals to circuit breakers (or not operate or operate after a time delay in backup mode).

Under certain circumstances (for example, differential protection systems), communication channels are required. Relays are required to exchange data to make decisions [48]. Communications can also be used for signalling – e.g., to instruct remote circuit breakers to trip, to instruct remote protection systems to operate or not, etc [49]–[51].

The following key criteria, many of which are inter-related, can be used to quantify the ability and quality of protection systems:

Discrimination: The ability of the system to identify whether the fault is located within its protected zone/area based on the measured system data. This can also be described as selectivity. A discriminative protection system will only react to faults (by tripping – whether as main or backup) within its defined area of protection.

Stability: the capability of a protection system to remain inoperative during and after faults and disturbances when it is not required to operate. This can also be described as safety. A stable protection system will only operate when it is certain that the fault/disturbance is within its area of protection coverage. Stability is related to discrimination.

Sensitivity is the ability of the protection system to sensitively operate for all faults/disturbances – even though some faults (e.g., highly resistive faults) may present themselves as very similar to non-fault conditions. A highly sensitive protection system will always detect and operate any fault that it should react to, within its protected area.

Operating time: the total reaction time of a protection system from a fault occurring to it generating a tripping signal – the clearance time is greater than this and includes the circuit breaker(s) opening times – which can be significant. The setting of operating time is depending on the purpose of the protection system taking into consideration clearance times required, discrimination, stability and sensitivity.

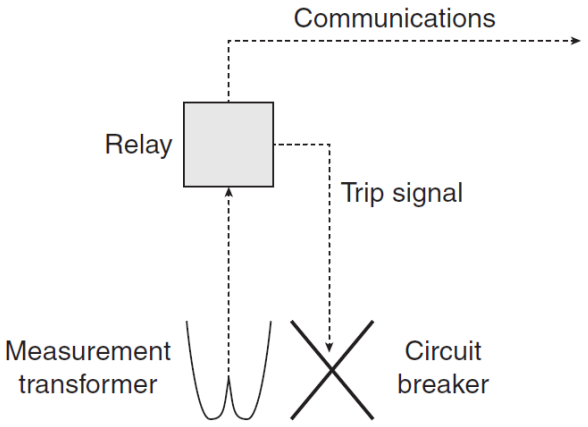

Figure 3-5 Components within a protection system [44]

3.3.2 Protection relaying

As defined in [52]:

Relaying is the branch of electric power engineering concerned with the principles of design and operation of equipment (called 'relays' or 'protective relays') that detects abnormal power system conditions, and initiates corrective action as quickly as possible in order to return the power system to its normal state.

Relays are the key component of the protection system. The history of the utilisation of protection relays can be traced back to the very early part of the 20th Century when electromechanical relays were introduced. Following that the relay technology further developed in the forms of static/electronic relays, digital relays, and numerical relays [53]. This thesis focuses on protection challenges related to modern numerical relays, as they are almost exclusively applied at the transmission level in modern power systems.

3.4 Protection Functions

This section gives a brief review of typical main and backup protection functions used in transmission networks and covers differential, distance and overcurrent protection systems. There then follows a subsection which is dedicated to explaining and analysing the operation of distance protection (including modern numerical/software-based distance protection) in detail, since the focus of the research is on the impact of converter-dominated systems on distance protection specifically.

3.4.1 Differential protection

Differential protection is widely used in GB power networks (and in power transmission systems internationally) as one of the main protection schemes for transmission systems. It is a type of unit protection, which means that it can and will only operate during a fault within its protected area, which is normally bounded by two or more measurement locations. Its operating principle is based on the Merz-Price principle following Kirchhoff's first law [53]. A typical set-up for a differential system (which is a circulating current system – using directly connected CTs to a single relay) is illustrated in Figure 3-6. In this arrangement, the primary current flowing into and out of the protected area ($I_{f1_{pri}}$, $I_{f2_{pri}}$) is measured at left and right end through current transformers which output secondary values (I_{f1_sec}, I_{f2_sec}). When faults are located outside of the protected area, the corresponding differential current I_{diff} is equal to 0 (under ideal situation) since I_{f1_sec} and I_{f2_sec} are in the same direction and magnitude. When a fault occurs inside the protected area, I_{diff} will become the summation of I_{f1_sec} and I_{f2_sec} since they are now anti-phase. The relay shall be triggered by comparing I_{diff} to the setting of the threshold current I_d. When I_{diff} is higher than I_d, the tripping signal will be sent to the circuit breakers.

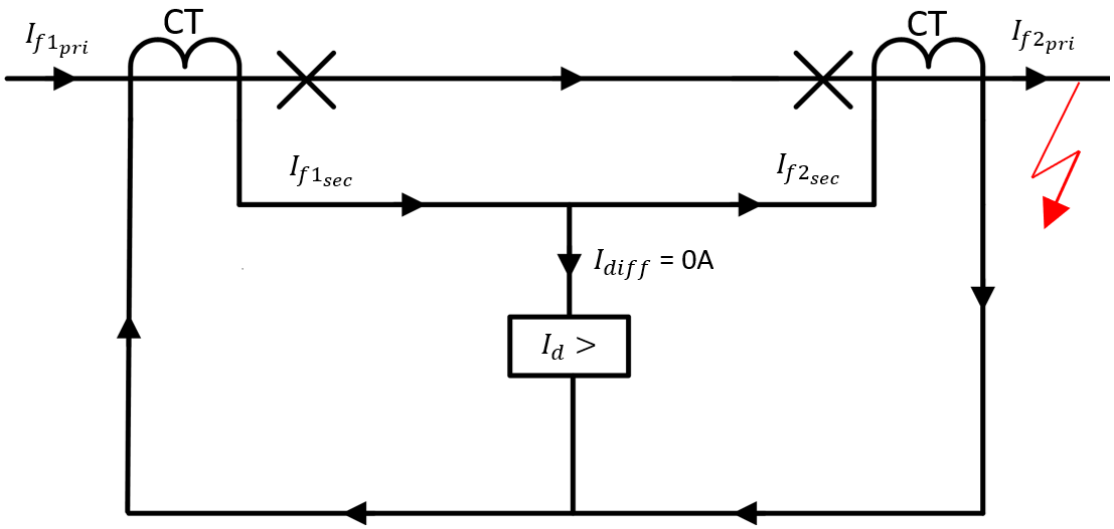

(a) External fault

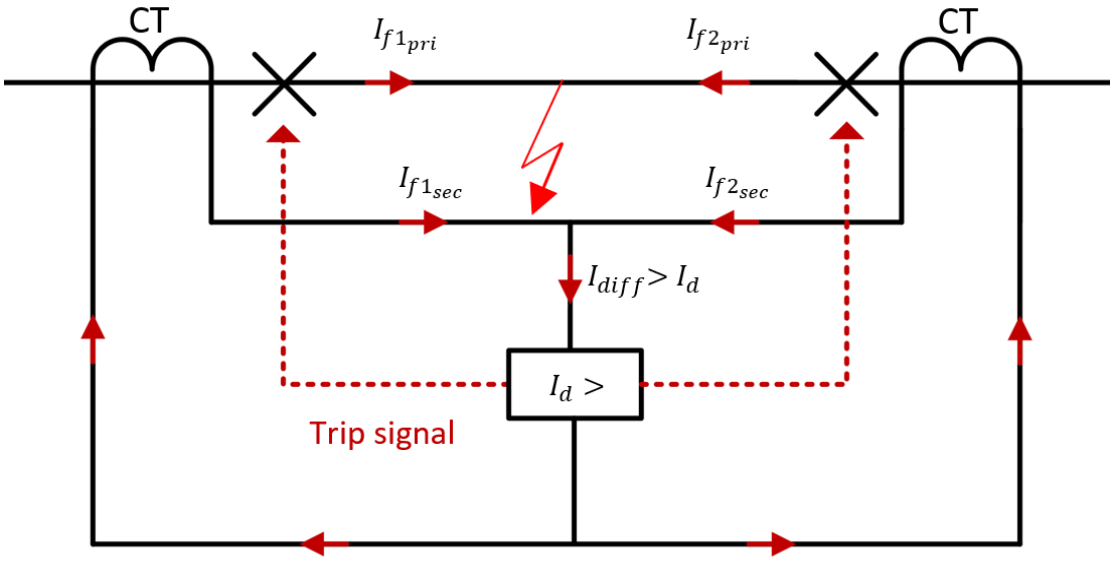

(b) Internal fault

Figure 3-6 Differential circulating current protection scheme

A biased operating characteristic is widely applied for the setting of I_d to avoid spill current (which can be down to errors/differences in CT outputs – particularly at high currents – for example when an external fault is located close to the differential protection scheme). A typical biased operating characteristic is demonstrated in Figure 3-7. The setting of I_d is based on the calculated value of I_{bias} (the average of the absolute value of the measured current I_1 and I_2). k_1 and k_2 are the slope factors for the

setting in different stages. When I_{bias} is smaller than the biased current threshold I_{s2}, I_{diff} is then compared with $k_1 \cdot I_{bias}$. When I_{bias} is larger than I_{s2}, I_{diff} is then compared with $k_1 \cdot I_{s2} + k_2 \cdot (I_{bias} - I_{s2})$. The above characteristic shall allow the system to be sensitive when the magnitude of fault current is low and secure when the system is working at a heavy load or experiencing external faults.

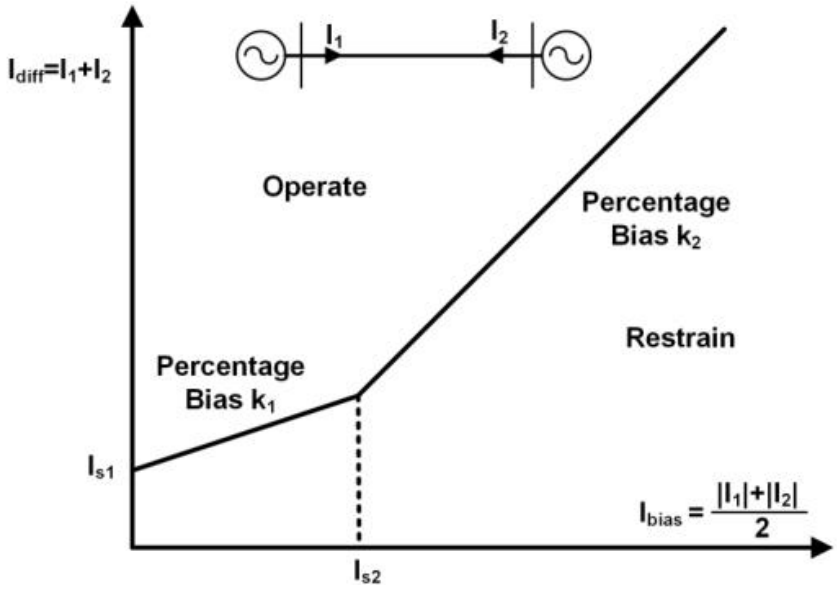

Figure 3-7 Biased characteristic of differential protection [53]

3.4.2 Overcurrent protection

Overcurrent protection is widely applied in GB as a form of backup protection for transmission-level power systems and as the main protection for MV/LV distribution systems. It is a type of non-unit protection. The operation of overcurrent protection is realised by monitoring the network current through CTs and comparing values with pre-set thresholds – often using characteristics where the tripping time reduces as the magnitude of measured current increases (above the threshold) – this is a valuable

characteristic (and is based upon original electromechanical relays) in those relays closer to the fault can be set up to trip more quickly than those further from the fault. Fault current typically reduces as distance to the fault from the measurement location increases and, therefore, this feature is sued to ensure that relays close to the fault trip before others further away from the fault would trip, therefore embedding backup operation in a fleet of relays and ensuring that if a relay or circuit breaker fails to operate, other relays (s) further from the fault will trip with a time delay to effect fault clearance in backup mode. The tripping time of the overcurrent relay can be varied by applying different current/time tripping characteristics [53]. As defined in IEC 60255 [54], commonly practised characteristics of Standard Inverse Definite Minimum Time (IDMT) overcurrent protection systems are classified as Standard Inverse (SI), Very Inverse (VI), Extremely Inverse (EI) and Definite Time (DT).

For DT, the relay's operation time is fixed, regardless of the value of the measured input current, with a preferred value when the measured current surpasses the threshold and will not change. For SI/VI/EI, the operation time depends on the level of the measured current – often with a reducing tripping time as the current increases above the minimum threshold required for operation – this allows relays "closest" to faults operate before those further from the fault – providing coordinated operation and clearance of fault via backup if the relay/circuit breaker closes to the fault fails. Examples of the operating curve for different characteristics are illustrated in Figure 3-8.

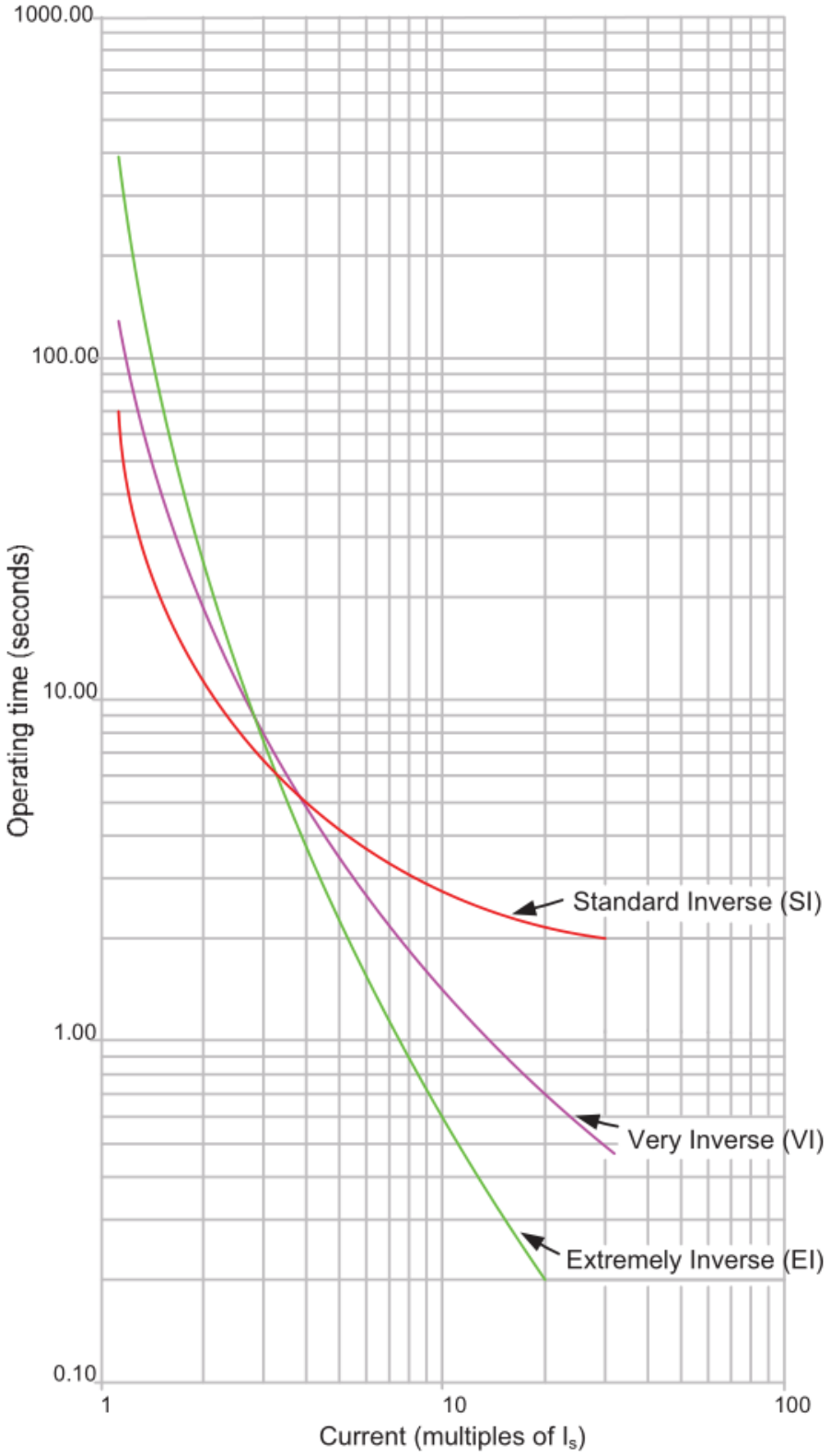

Figure 3-8 IEC 60255 IDMT relay characteristics with *TMS*=1 [53]

The corresponding equations for the above characteristics are shown in Table 3-1, where t is the operating time; TMS is the time multiplier setting, I is the measured current, I_s is the relay setting current.

Table 3-1 Standard relay characteristics [53]

Relay Characteristics	Equation
Standard Inverse (SI)	$t = TMS \times \frac{0.14}{(\frac{I}{I_s})^2 - 1}$
Very Inverse (VI)	$t = TMS \times \frac{13.5}{\frac{I}{I_s} - 1}$
Extremely Inverse (EI)	$t = TMS \times \frac{80}{(\frac{I}{I_s})^2 - 1}$

The setting of I_s will determine the threshold value at which the relay shall start to operate. The relay's final operating speed will be delayed/accelerated by manipulating the number of TMS. The selection of different characteristics is depending on the characteristic of the protected systems. For example, VI overcurrent relays are commonly practised in networks where the fault current is substantially reduced with distance, and EI relays are preferred to be applied in distribution feeder circuits where peak switching-in current occurs [53].

3.4.3 Distance protection

Distance protection is a non-unit type of protection which operates by measuring the voltage and current close to the relay's location. During faults, the voltage will typically drop, and the current will rise, which leads to a drop in the measured/calculated impedance at the relaying location. The corresponding impedance between the location of the fault and the relaying point can be calculated from the known line impedance and the corresponding fault distance from the relay can therefore be calculated (any additional fault resistance can also be catered for using the relay's zone characteristic shapes and other processing techniques – particularly in modern microprocessor-based relays). Using this, the relay can verify the fault location and act rapidly (operating times can be as low as 10 ms or less [53]). Compared to overcurrent protection, the operation of the distance protection is much more reliable since the calculated fault impedance is not varied by the source impedance/fault level in the system, and therefore operating times can be more consistent, even with varying system fault levels (which would clearly compromise and vary overcurrent relays' operating times).

Normally distance protection is set up with three or more protected zones with different values defined as zone reach for each zone. For each zone, the relay is set up with different operating times to ensure primary and backup protection functions. An example of the settings of three zones of protection for a distance relay is described as follows:

- Zone 1 setting: distance relays normally are set up with a zone 1 reach up to 80%-85% of the first/main protected line [53]. Selecting a value less than 100% of the protected line is necessary to provide a safety margin and ensure that the

relay does not react to faults outside the first protected line; the primary reason for this is to cater for CT/VT measurement errors, and also to provide some margin in relay processing of the input values.

- Zone 2 setting: The setting of zone 2 reach is at least 120% of the first protected line (although short connected "second" lines may change this value) to ensure full-coverage protection of the protected line and backup protection for an element of the adjacent "second" lines [53]. The operation of the relay for zone 2 must be configured with a time delay to ensure that the primary main relay for the adjacent circuits will always operate faster than the backup relay (and of course, if they fail, then other relays will operate in zone 2 to provide backup).

- Zone 3 setting: the zone 3 reach is normally set up with a value of 220% of the first protected line to provide a backup protection function for faults located at further locations (note that the number is for demonstration purposes only - different system operators might use different standards for specifying these reach/distances) [53]. The time delay of zone 3 operation must be longer than the setting of zone 2 to maintain the coordination between different relays.

A typical arrangement for a distance protection relay from [55] is demonstrated in Figure 3-9 where the relay is located at busbar A, measuring the voltage and current through transformers at TU and TI. The relays are set up to provide protection of zones with reaches of 80%, 120% and 220% of the first protected line In interconnected systems, sometimes the reach of zones 2 and 3 must be based on the shortest of the lines connected to the remote node from the main protected line to avoid overreaching into remote parts of the system – maximum load conditions must also be taken into account when setting zone 3 to avoid unwanted operation; although load power is usually mostly

"real", and detection of reactive power (via measuring an increased angle between voltage and current) can be used to further enhance discrimination and stability of distance schemes.

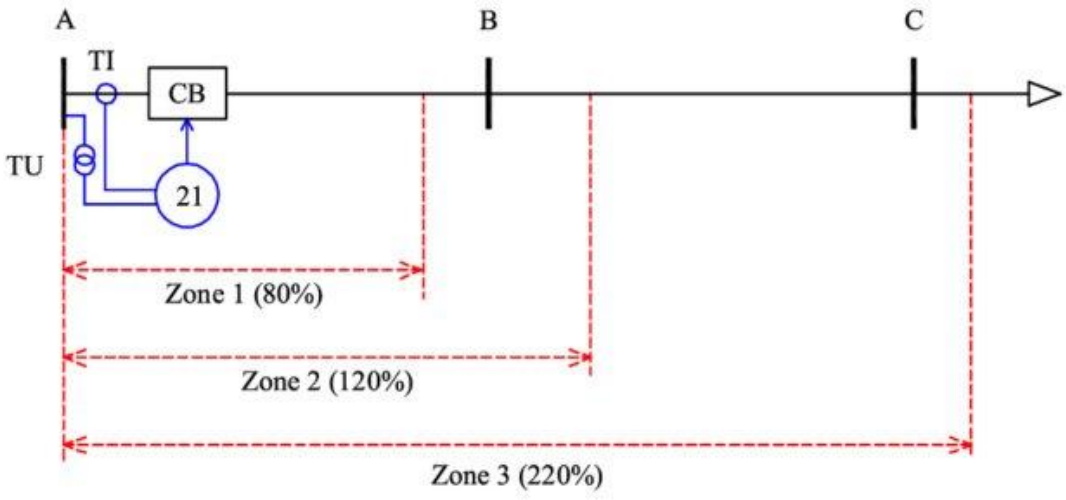

Figure 3-9 Setting up of distance protection relay [55]

For traditional distance relays (including electro-mechanical and analogue electronics-based static relays) the operation of the relay is achieved by comparing the calculated short circuit impedance with the protected line impedance for each zone. The resultant tripping/non-tripping zones can be illustrated on *R/X* diagrams as circles – although many modern relays use different shaped characteristics to enhance relay sensitivity, stability and discrimination. If the calculated (from measurements) impedance lies within the boundary of a circle (or other shapes) representing the corresponding zone in the complex impedance plane, then the relay shall operate – either instantaneously for zone 1 or with a time delay (during which the measured impedance must remain within the zone boundary). By manipulating the settings and software, the circle can be controlled to move around the impedance plane to achieve better resistive fault

coverage and the most common characteristic is the Mho-circle demonstrated in Figure 3-10.

In addition to the traditional Mho-circles, other shapes including rectangular, parallelogram, lenticular, and others, are also available and used. Typical quadrilateral characteristics as shown in Figure 3-10 are available [56].

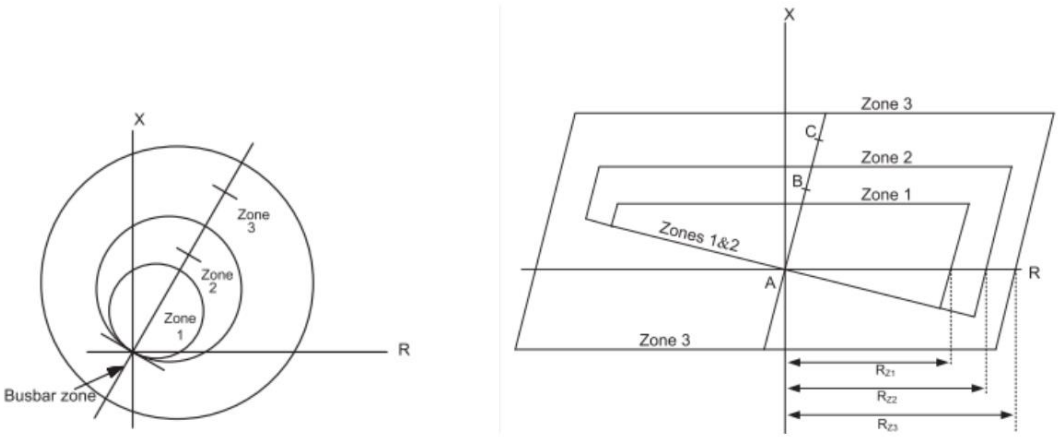

(a) Mho impedance characteristic (b) Quad impedance characteristic

Figure 3-10 Typical characteristics of distance protection [56]

3.4.4 Numerical distance protection

3.4.4.1 Starting, fault detection and phase selection

The operation of a numerical distance protection system is triggered by its initial starting system to initially detect and identify the presence of faults. The starting system can be classified as follows:

- Over-current starting:

- Under-impedance starting
- $U / I / \phi$ -starting (angle dependant under-impedance starting)
- Impedance starting

The starting system must ensure that the faults are correctly identified in the correct phase. An example of the selection of the faulted phase is demonstrated in Figure 3-11.

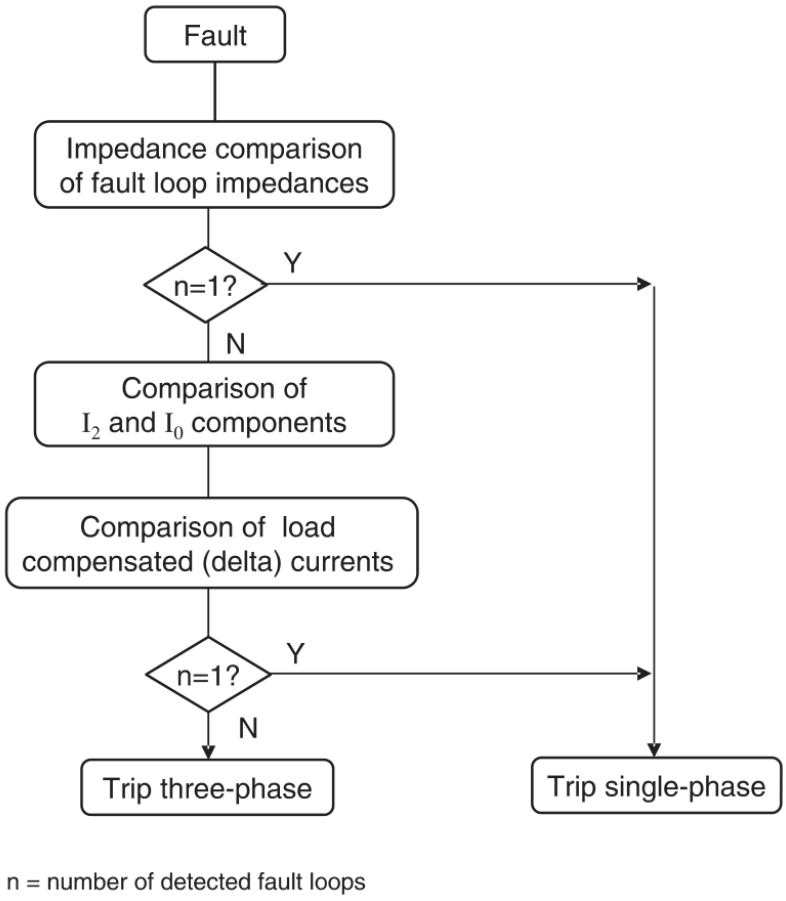

Figure 3-11 Selection of the faulted phase [56]

3.4.4.2 Features of modern distance protection systems

Numerical distance relays can provide much more convenient functions compared to traditional relays.

Load Blocking

Numerical relays typically offer load blocking zone functionality, or “load blinders” - a wedge-shaped area which is “cut out” of typical distance zones to reduce the reach for resistive (or real power dominated) loads and to allow higher loading of the system without inadvertent tripping [56], [57]. During faults, the system impedance typically moves from being highly resistive to highly reactive due to the line impedances being inductive in nature. Examples are shown in Figure 3-12.

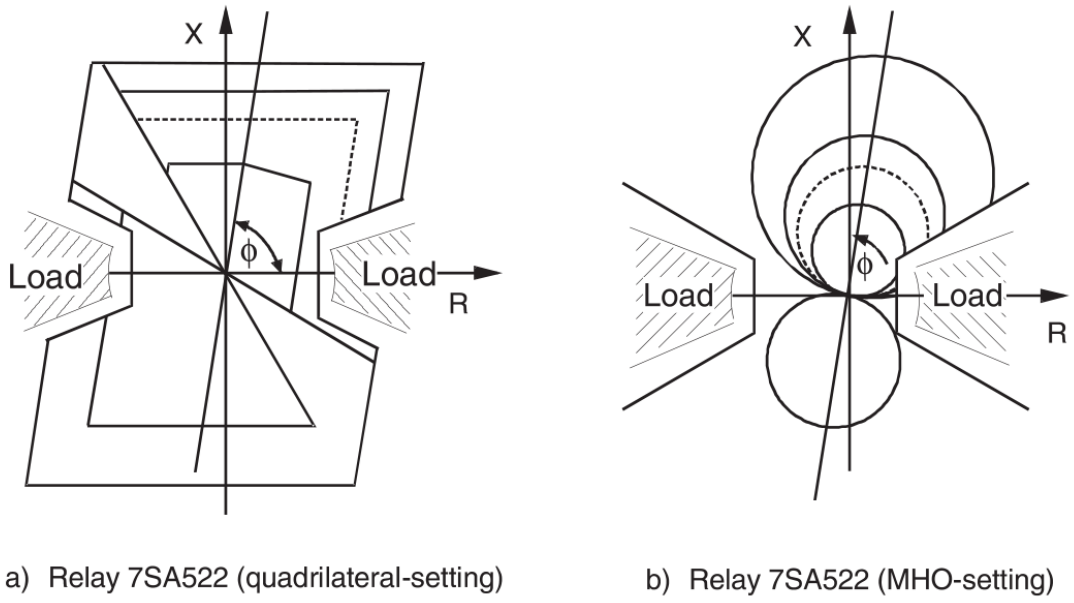

Figure 3-12 Typical characteristics of distance protection with load blocking/blinding [56]

Power Swing Blocking (PSB)

The operation of the PSB function is based on the principle that, when faults occur, the impedance typically changes very rapidly from a load/pre-fault impedance to the corresponding fault impedance, which may be located inside the zone(s) setting

characteristic shapes on an impedance diagram [58]. If one considers the system represented in Figure 3-13 as an example, it is evident that two equivalent sources E_1 and E_2, with source impedances Z_{s1} and $Z_{s2,}$ are transferring power through the transmission line with an impedance of Z_L. As shown in Figure 3-14, during power swing conditions (e.g. caused by a significant load change, the loss of a generator, or some other major event – but which the distance protection should not trip for) the corresponding measured impedance by the relay located at bus A may change and encroach temporarily inside zone boundaries as the system status transits from one state to another, but this change will be slower and more gradual in nature when compared to fault impedance transitions. The trajectories of the change of the calculated (or "seen") impedance depend on the voltage difference of the sources. The rate of change of impedance change will correspond to the prevailing power swing frequency in the system. By measuring dZ/dt or $\Delta Z/\Delta t$ and comparing it with a pre-determined threshold, it is possible to distinguish between actual faults and power swings and to block the operation of the relay if a power swing is detected, thus enhancing the stability of the protection system.

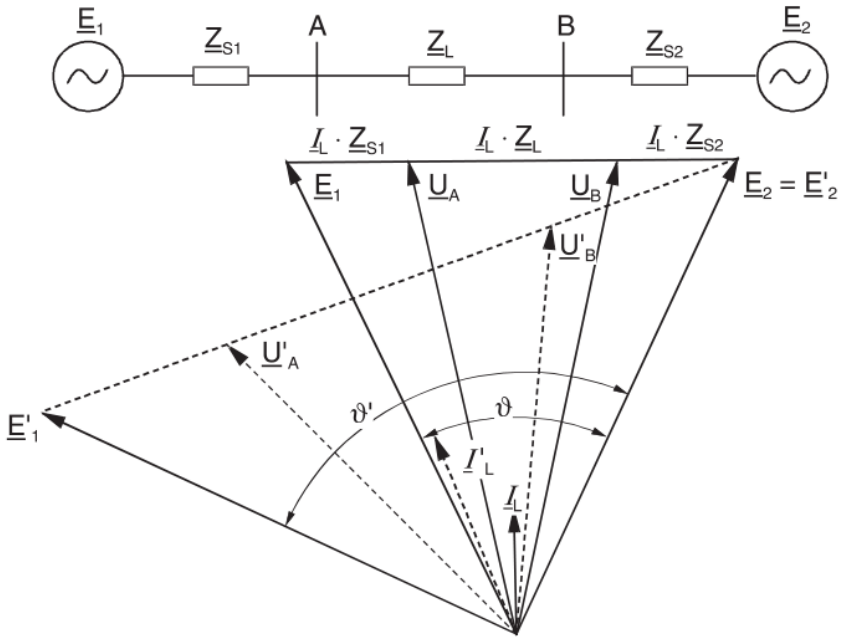

Figure 3-13 Power swing condition in a transmission system [56]

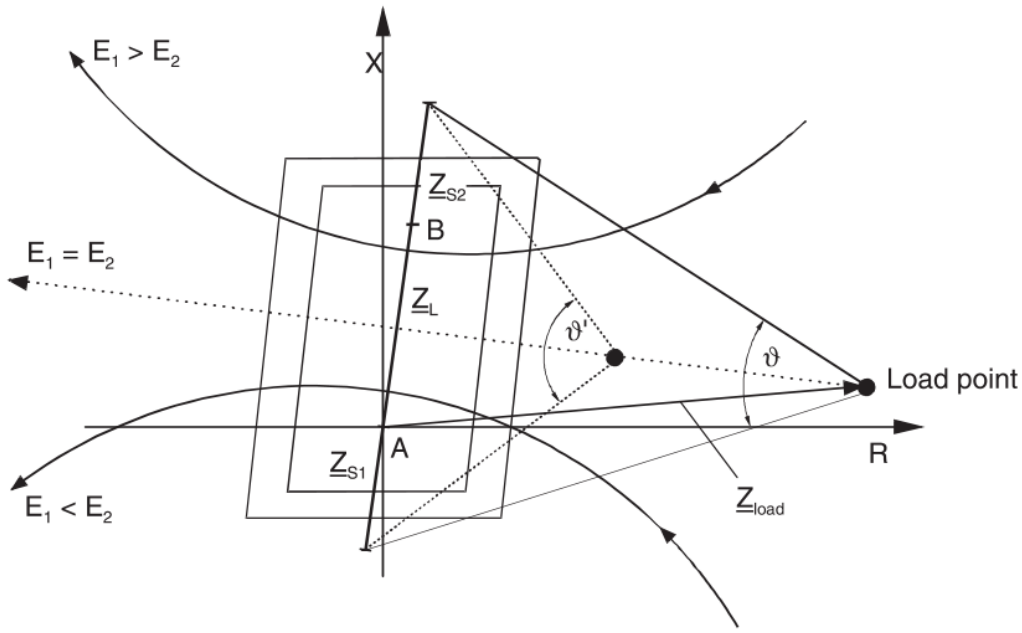

Figure 3-14 Impedance locus during power swing [56]

•Permissive inter-trip

Operation of numerical (and indeed previous generations of) distance relays can be further enhanced using communications channels – speeding up operation in some cases, or blocking/disallowing operation when it is known that the fault either does not exist or is in a part of the system for which operation (or to be specific, instantaneous zone 1 operation) is not desired. This can enhance the speed, sensitivity, discrimination capability, and security of the overall protection scheme. There are a number of different methods for doing this:

(1) Direct Under-Reach Transfer Trip (DUTT）

In this scheme, a local relay that detects a zone 1 fault would send a signal directly to the relay at the remote end(s) of the line instructing it (or them if a multi-ended circuit) to trip regardless of which zone they may be detecting a fault in – in an effort to speed up the fault clearance. This is valuable when, for example, a fault is located near one line end, which may be detected as a zone 2 fault by the relay at the other end of the line and therefore this relay may not issue an instantaneous zone 1 tripping command to its local circuit breaker – which would act to delay overall fault clearance. This scheme is useful, but can be prone to inadvertent operation – if an “accelerate” signal is incorrectly sent/received, then the incorrect operation of a local relay could ensure. There are alternative schemes that can address this by applying logic at the receiving relay to enhance security.

(2) Permissive Under-Reach Transfer Trip (PUTT)

In such schemes, if a relay detects a fault in zone 1, then it sends a signal to the relay at the remote end to request the remote relay to trip without delay (even if it is viewing the relay as a non-zone 1 fault). However, the remote end relay will only trip (it may

already detect a fault in zone 1 which means it would be tripping anyway) upon receipt of a remote tripping command *and* detects a fault in zone 2 (i.e. the fault is near the remote end of its line). Permissive schemes mean that other relays protect a line that can trip faster if they also detect a fault (in the correct direction and in zone 2) – hence they have "permission" to operate. This enhances the security of the system and negates the risk of a transfer trip being inadvertently sent and reacted to when no fault exists, as the relays would not operate unless they are also detecting a fault (in zone 1 or 2). The corresponding operation logic can be found in Figure 3-15 and Figure 3-16, where Z_1, Z_A and Z_{1B} represent the protection setting for zone 1, the corresponding fault starter zone and the corresponding time-independent over-reaching zone for the permissive protection scheme. Taking the PUTT scheme shown in Figure 3-16 as an example, when the fault F_1 is applied at the beginning part of the transmission line, the left relay will detect the fault as a zone 1 fault, trigger the circuit breaker immediately and send a permissive signal to the relay at the right-hand side. The relay on the right-hand side shall detect the fault that lies in the over-reaching zone and start to count to the configured timer, but with the help of the signal sent by the left-hand side relay, the right-hand side relay will trip immediately after receiving the signal. For fault F_2 located at the right-hand end of the transmission line, the right-hand relay shall trip immediately and send a permissive signal to the left-hand relay, which will allow the left-hand relay to trip faster, even though the left relay detected an overreaching fault.

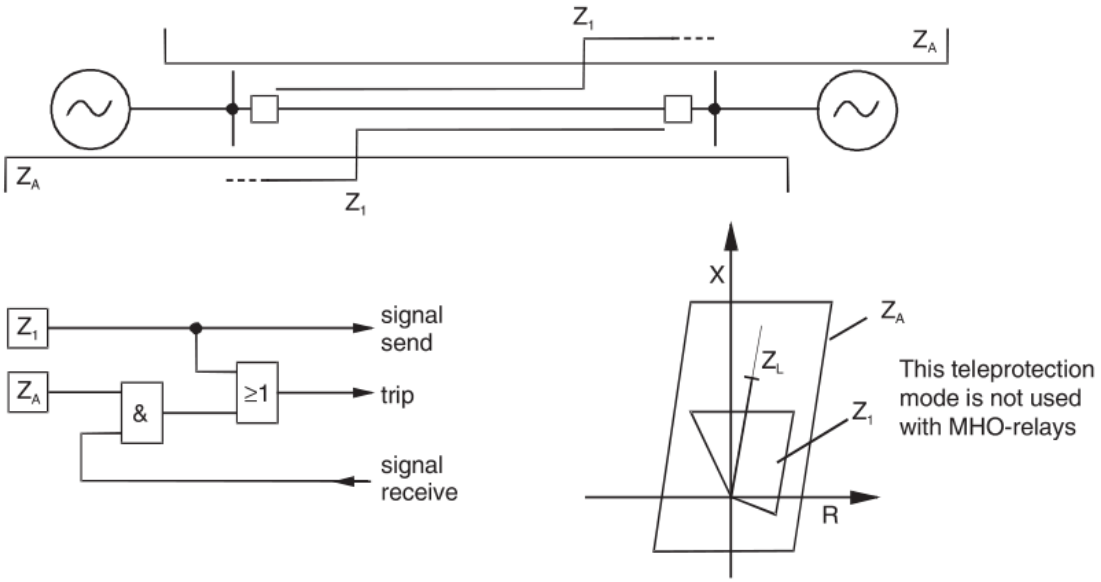

Figure 3-15 PUTT with starter [56]

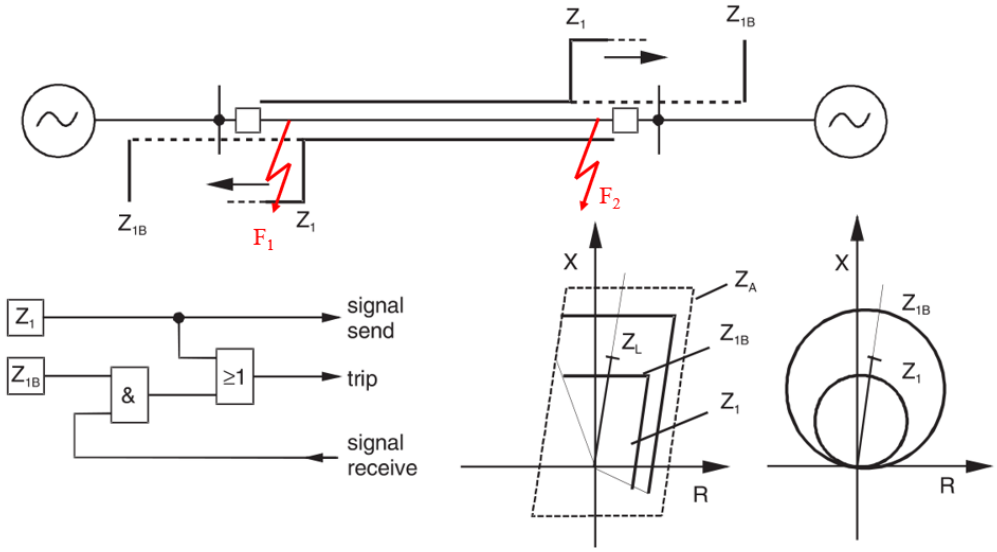

Figure 3-16 PUTT with overreaching zone [56]

(3) Permissive Over-Reach Transfer Trip (POTT)

This works to achieve fast tripping when the relays at either line end (or more in a multi-terminal configuration) of the feeder detect a fault in their over-reaching zones (i.e. beyond zone 1) and send a “permission to trip” signal to the other relay(s). The major

difference between PUTT and POTT is that in PUTT schemes the relay will only send the permissive signal when underreach faults (i.e. faults in traditional zone 1) are detected, while in POTT schemes the relay will only send signals when faults in the overreaching zone (beyond traditional zone 1) are detected – the actual zone 1 settings on the relay (Z_{1B}) overreach the end of the line, as there is no setting available to cover only 80% of the line as with traditional "longer line" schemes. This function is normally applied to short feeders where zone 1 cannot be applied with confidence, due to the relatively very short line length being protected, so the settings must be set to overreach – but the communications provide security as a zone 1 trip can only be initiated if the signal from the other relays is received (unlike the PUTT scheme, where zone 1 can operate without the permission signal from the other relay(s)). This type of scheme works both for mho and quad-type relay characteristics, and the operation of the scheme is illustrated in Figure 3-17 below, where Z_{1B} represents the overreaching setting zone 1 setting (the "traditional" but not used zone 1 is shown in a dotted line – this setting would be too low for short lines and could result in maloperation of the scheme – again, this scheme is only used for very short lines) and the time-independent over-reaching zone (applied in tele-protection scheme, faults in this zone can be selected to be cleared without time-delay as long as the communications signals are received) for permissive protection. With reference to the diagram, for fault F_1 which is in the middle of the protected short line, the relays at each end of the line will both see the fault and since the line is short, the fault can be detected as a zone 1B fault by each of the relays and they will therefore both send and receive permission to trip signals. After receiving the signals from their remote relay, the local relays then confirm that the fault is in Zone 1 and allow the circuit breaker to trip. For a fault F_2 which is outside of the line between the relays, the relay at the left end of the line will detect the fault located in Zone 1B,

send permission to trip signals to the other relay at the right-hand end of the circuit, but the relay at the right side will not detect the fault in the forward direction, and even though it receives the permission signal from the other relay, and therefore will not trip instantly – it may operate after a time delay if it has a "reverse-detecting" zone as shown in the quadrilateral characteristic in the following Figure.

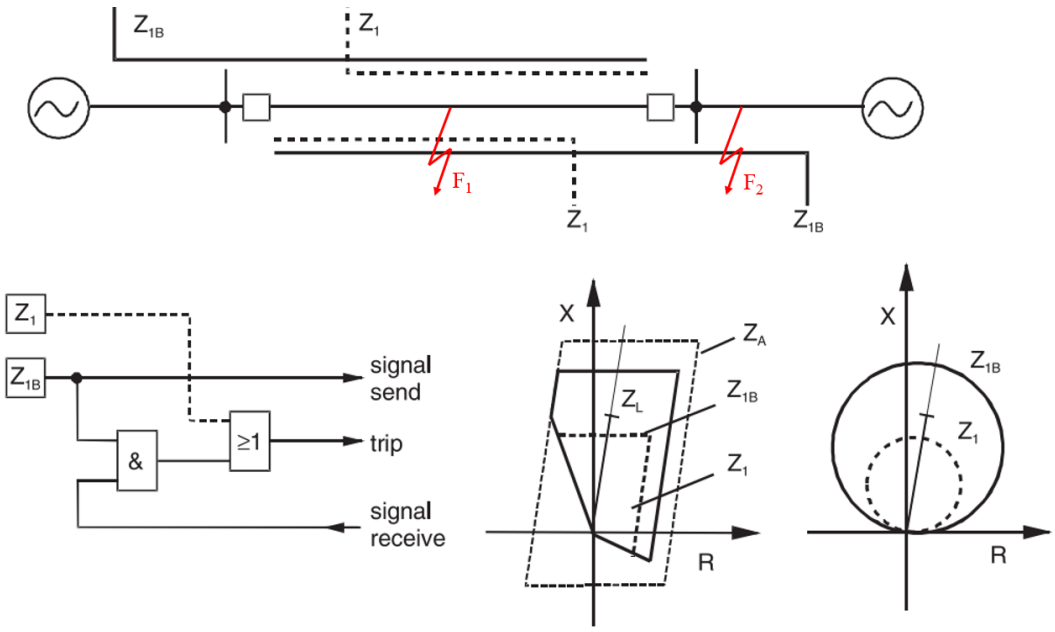

Figure 3-17 Distance protection with communication, POTT [56]

(4) Weak in-feed supplement function

Protection at the end of a circuit with a very weak in-feed may not "start" or pick up, as insufficient current flows from "behind" the relay to the faulted feeder.

To achieve fast tripping when a feeder is connected to a weak in-feed bus bar, an additional echo-circuit (as displayed in Figure 3-18, Z_A represents the protection setting for the fault starter zone) must be provided. This circuit operates as a supplementary function to the POTT scheme.

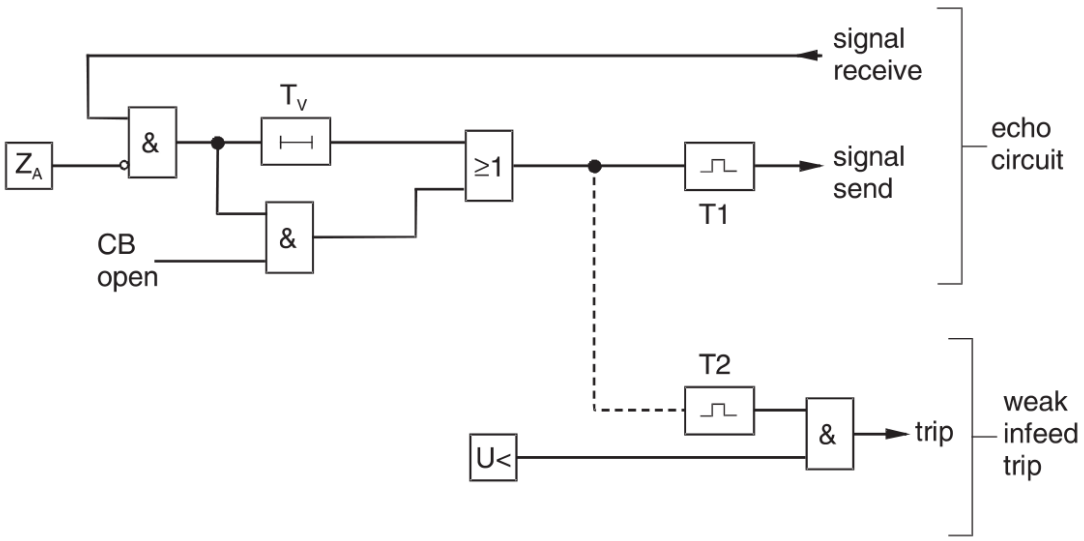

Figure 3-18 Weak in-feed echo-circuit [56]

When a fault is applied within the protected area, the protection at the weak in-feed end shall not open the circuit since the fault current is insufficient. However, the received signal at this end will be sent back and allow the strong in-feed end to trip instantaneously. By configuring the weak in-feed supplement function (with the aid of voltage drop detectors) at the weak in-feed end, the relay can also trip during the fault.

3.4.5 Travelling wave-based protection

It is worth noting that in the past years, modern travelling wave-based protection are considered to be providing a high standard of reliability, as the their operational principle will be less affected by the integration of renewable technologies [59]. Compared to the traditional protective devices the travelling wave relays are considered to be faster and more reliable, as their operation is less likely to be affected by the changed system behaviours introduced by the integration of renewables.

After faults, electromagnetic transient components shall start to propagate from the faulted point with a speed comparable to the speed of light, the transients shall travel in both directions and then be reflected back (with a loss governed by the attenuation constants) at each end of the line. The travelling wave-based protection devices can then collect the information from the captured transient at terminals.

The famous Bewley's lattice diagram explaining the basis of the operation principles of travelling wave relays is presented in Figure 3-19: After the occurrence of the fault at t_f, the transients start to propagate toward both ends of the line, arriving at each bus at t_A and t_B. The waves start to bounce back to the faults with attenuation, reflected and refracted again at the fault point, the second transients received at each end shall be detected at the time of t_{AR2} and $t_{BF1.}$ Based on such operating mechanisms, travelling wave-based protection devices are broadly classified into the following two categories: single terminal and two terminal. With the help of t_A and t_{AR2}, the fault location can be calculated from a single terminal, while by analysing t_A and $t_{B,}$ the fault location can be calculated from two terminals.

While the scope of this thesis is to examine the impact of converter-based energy sources on traditional protection systems, the focus is not on emerging protection technologies. However, future research can certainly explore effective protection alternatives to address the current challenges.

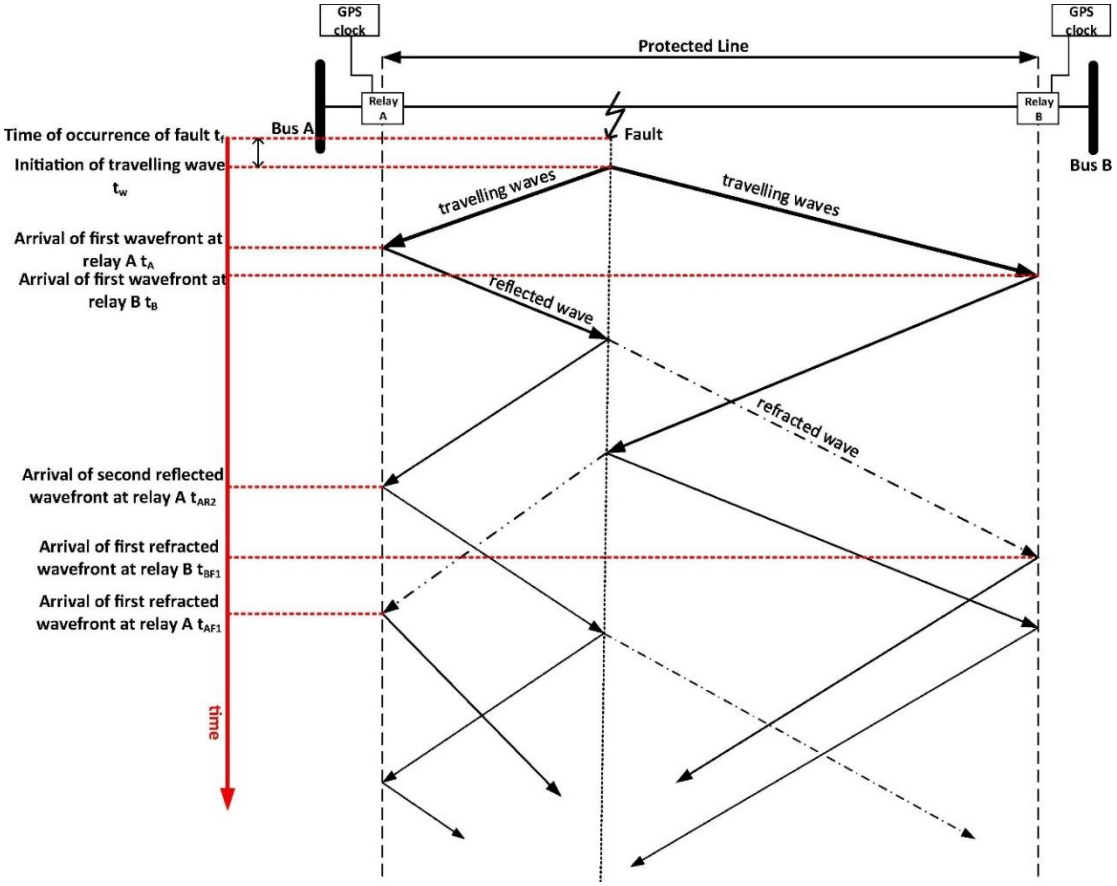

Figure 3-19 Bewley's lattice diagram [59]

3.6 Summary

This chapter has presented a comprehensive overview of power system protection principles and has addressed the challenges associated with converter-interfaced sources. The fundamentals of power system faults and the detailed operating principles of both traditional and emerging protection systems have been thoroughly studied. Furthermore, the chapter has investigated how changes in fault behaviour in future converter-dominated power systems can impact both power systems and protection systems.

Understanding the protection challenges that arise from the integration of converter-based energy sources requires a clear understanding of the nature of faults and the functioning of traditional protection devices that monitor them. In traditional protection systems, both unit and non-unit protection devices rely on measuring system voltage and current during faults. However, when a system is dominated by converter-based energy sources, the changed VI behaviour during faults introduces uncertainties.

The studies conducted in this chapter have led to the conclusion that a systematic study and testing methodology are crucial to examine the impact of changes in system behaviour, as explored in the previous chapter, on traditional protection systems. The primary focus of this thesis will be on distance protection, as the operating principles of differential/overcurrent protection systems are relatively more straightforward. However, future studies will encompass various types of protection devices, including emerging technologies such as travelling wave-based protection systems, to ensure comprehensive coverage of different scenarios.

Chapter 4

Review of related research activities

4.1 Introduction

This chapter presents a review of related research activities including literature that analyses converter fault responses, literature that analyses potential protection issues introduced by converters and literature that proposes potential solutions to identified issues and problems associated with network protection that may arise in converter-dominated power systems. The review also highlights identified gaps or shortcomings in related work that the research reported in this thesis addresses.

4.2 Overview of converter behaviour during faults

As mentioned previously in Chapter 2, a converter's fault response is directly defined and impacted by its control system. The detailed fault response of converters shall be guided by the grid/network codes [8], [14], [15], yet the requirements are somewhat non-specific in many instances (with the details of the exact specifications being left to national operators to define) and therefore it is important to systematically investigate systematically the impact of a range of credible converter outputs during faults upon protection systems.

Converters will provide relatively limited fault current contributions when compared with a synchronous machine of comparable rating. As has already been explained in detail in Chapter 2, synchronous machines can typically output 5-7 pu fault current immediately following close-up short circuits [18]. However, the fault current contributed by a converter-interfaced source may only be 1-2 times the rated current

[60]–[64]. During severe voltage depressions, converters may not even be capable of providing rated current [65].

The fault response of converters is guided, at least at a high level, by the appropriate and aforementioned grid codes. Converter sources can be considered as flexibly-controlled current sources capable of outputting current with both active and reactive components that can be independently controlled [66]. In some cases, it seems that converters may only provide fault current after an initial delay, during which there may be an initial reduction or dip in output current followed by a ramping up of current – this delay is most possibly due to measurement and control system-induced delays, could be due to "self-protection" within converters (e.g. crowbars) and the delay/dip may be more pronounced for faults with relatively higher voltage depressions [67].

Examples of the output voltage and current waveforms of a converter for a range of faults, with a range of voltage depressions, based on actual laboratory tests are displayed in the following Figures. Figure 4-1, Figure 4-2 and Figure 4-3 are results based on lab tests and Figure 4-4, and Figure 4-5 are results based on simulations.

It is clear from Figure 4-1. that for the fault with the most severe voltage depression (voltage down to 0.15 pu), then the converter takes around 4 cycles (80 ms) to reach the maximum output current, whereas for a fault with a voltage of 0.83 pu, the converter response is relatively quicker, and the current output reaches a maxim after around 1.5 cycles (30 ms). It is also notable that the output current waveform becomes more distorted as the voltage at the converter terminals reduces.

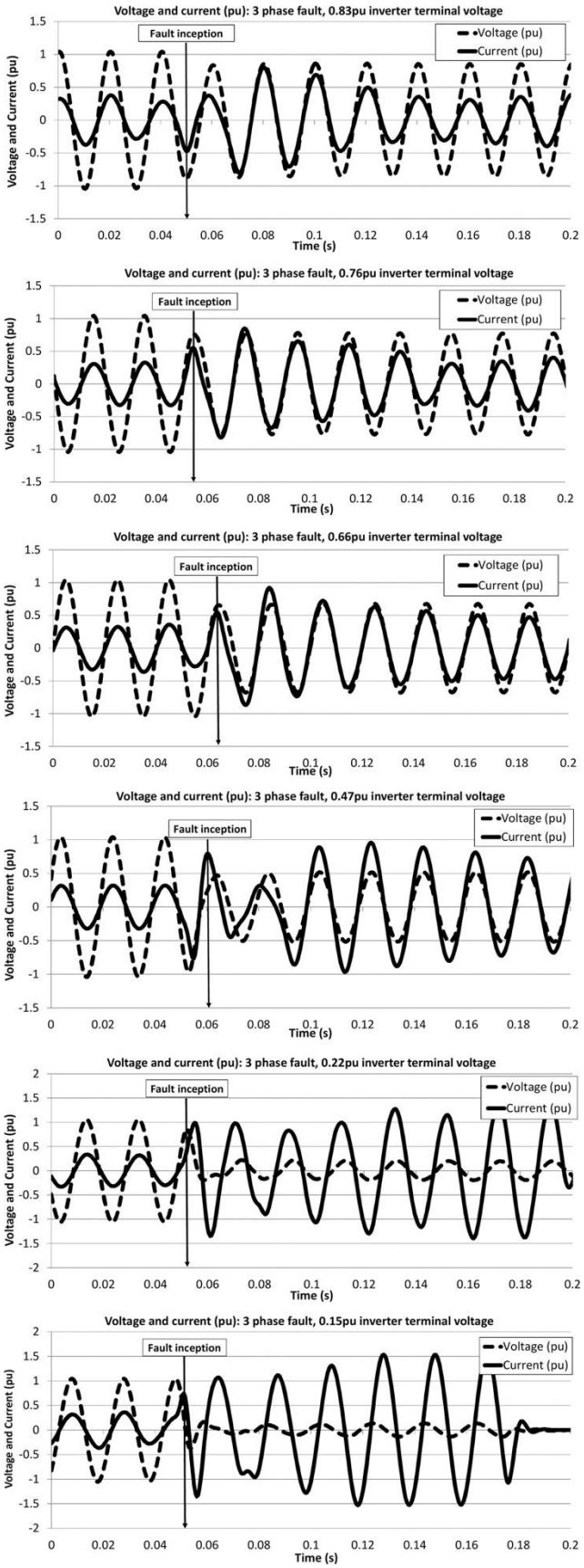

Figure 4-1 Inverter fault response during network faults [65].

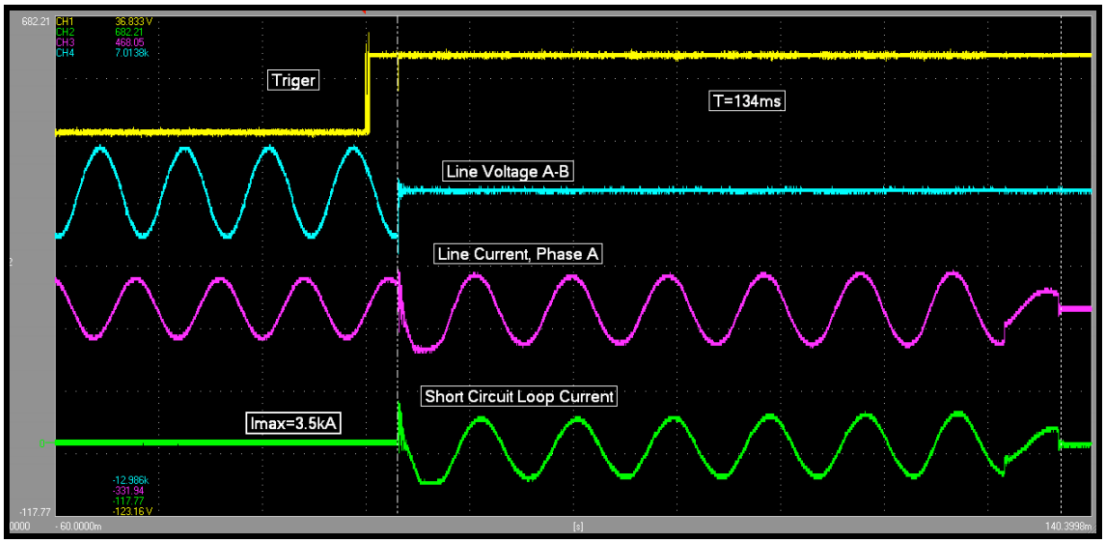

Figure 4-2 Manufacturer testing inverter for voltage ride-through [60]

Phase-to-phase faults are applied to a converter-based power source from the lab and the fault response is demonstrated in Figure 4-2. The trigger of the fault is recorded as the yellow trace (a delay of the starting time of the fault is induced by the contactor closing time). The response of the inverter's phase current is recorded as the purple trance and the line voltage is presented by the blue trace. These tests are for a 1 MVA converter, and it is clear that the response is almost instant, but that the fault current is not significantly larger than the pre-fault current.

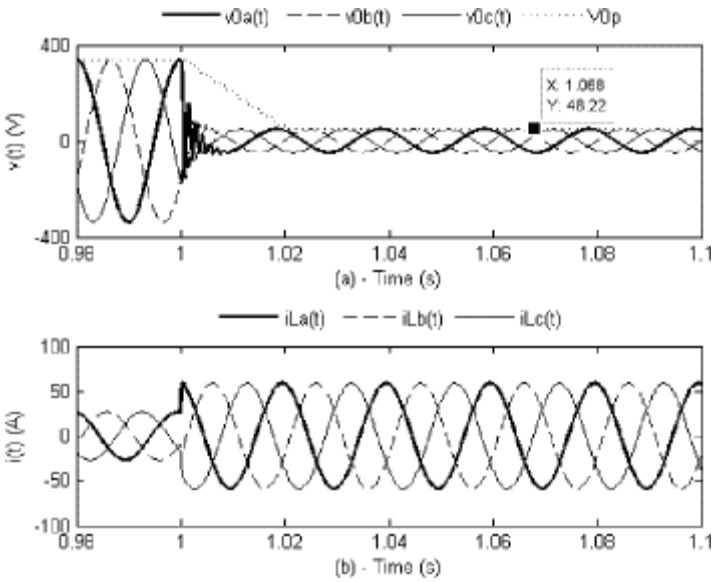

Figure 4-3 Response of inverter to three-phase fault (PSCAD simulation): (a) output filter phase and positive sequence voltages; (b) inductor phase currents [61]

The trace in Figure 4-3 illustrates “good” performance in terms of an instant and sustained current output, but as with all simulations, this must be treated with caution as it may not reflect actual behaviour in practice.

Figure 4-4 illustrates the performance (measured) of a three-phase 5kW converter that is subject to various network faults resulting in a retained voltage of 0.2, 0.18 and 0.17 pu. The faults are applied at 0.1 s and under normal conditions the inverter is outputting 0.5 pu active power and 0 pu reactive power. It is clear that all three phase currents increase for the first two cases, but for the final case, the output of the converter is very erratic with the current effectively reducing to zero rapidly after the first cycle, and this would clearly cause problems for the network protection, especially if such converters provided the majority of the fault current contribution to the fault on the network.

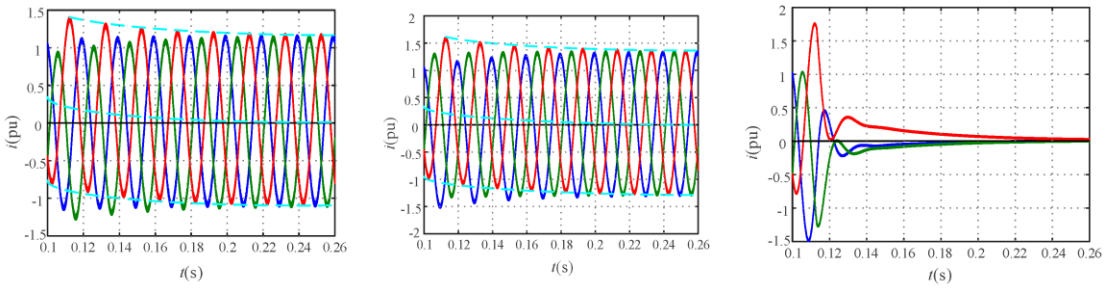

Figure 4-4 Measured three-phase short-circuit currents of an experimental platform of a 5 kW VSC-based renewable energy. (a) U′ = 0.2 pu; (b) U′ = 0.18 pu; (c) U′ = 0.17 pu [62]

As with Figure 4-4, the outputs in Figure 4-5 show “good” performance in terms of an instant and sustained current output, but as with all simulations, this must be treated with caution as it may not reflect actual behaviour in practice.

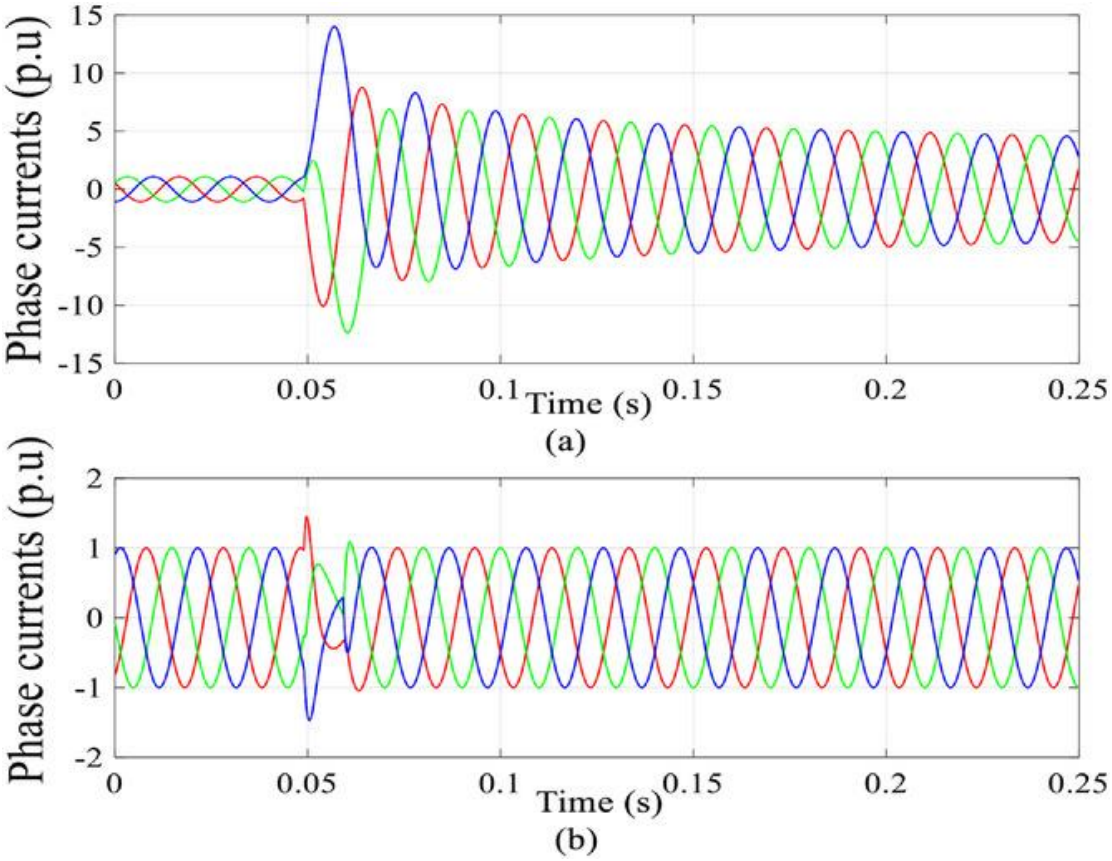

Figure 4-5 (DIgSILENT simulation) SC current from a 50 MVA generation unit in response to a three-phase bolted fault at the generator terminal (a) SG, (b) PE-based generator [9]

As with other simulated results, these results may be somewhat "ideal" and different from those that would be experienced in a practical installation. The examples that are related to actual tests (although the scale and voltages may not be reflective of transmission-level installations) show that the converter output, particularly for faults that impose severe voltage depressions on the converter output AC terminals, may be very erratic, with delayed responses, low levels of sustained fault current and in some cases, a complete failure of the converter to supply sustained fault current. All of this means that there is a degree of uncertainty over the converter responses during faults, particularly during the first 10s of milliseconds, which is the very critical period when

network protection is required to make decisions as to whether tripping or other action is required. This review of the literature indicates that there is still a great deal of work required to establish the behaviour of converters (and the potential impact on protection) immediately following short-circuit events on the network. The Network Code published by ENTSO-E [8] has specified how converters should provide "maximum" reactive current and "fast" fault current, but the terms maximum and fast are not defined explicitly and it is incumbent on national operators to define and quantify specific requirements at the national level.

In conclusion, there are many papers outlining and analysing the response of converters during network short circuits, and the majority of papers indicate that the output of converters will be significantly less in magnitude than a similarly-rated synchronous machine. Furthermore, it is clear that most converters may not provide a large amount of unbalanced (negative sequence) current during faults. It is also clear that the output of converters may be "delayed" and the ramp rate of outputs may not be fast (when compared to instantaneous ramped-up outputs of machines). All of these factors might impact negatively network protection (particularly distance protection) and therefore it is clear that there is a "gap" in the literature and a need for improving understanding of both converter responses during faults and the potential impact that this response may have on protection – which is the focus of the research reported in this thesis.

4.3 Review of research related to potential protection challenges in future systems

It can be concluded from the previous section that there will be noticeable and potentially-significant changes in power system fault behaviour in the future due to the penetration of converter-interfaced energy sources and infeeds. Concerns have been raised and different types of issues have been simulated, demonstrated and tested and verified in several research papers, which were cited and critiqued in the previous section.

Using dynamic models of power systems within an experimental arrangement consisting of both a protection relay model and an actual device (which is injected with the outputs from a flexible converter interface), discussions relating to converter responses during the period immediately following fault inception (when network protection would be required to detect and react to faults) are discussed in [68], which is a publication arising from this research project. This paper illustrates how converter-interfaced energy sources respond very differently to network faults when compared to synchronous machines and that these differences in responses could lead to network protection problems in the future, where converter-interfaced sources may proliferate. A range of fault scenarios, using both models of synchronous machines and a configurable converter-interfaced source model, have been studied and the results show that, potentially, there are several areas of concern associated with the protection of future systems. The conclusion of the paper reveals the importance of performing a complete and systematic range of studies with a mature testing system and methodology, to identify and quantify the challenges and therefore potential mitigation strategies.

While the paper has some case studies, it is stated that there is more comprehensive work required to evaluate many different relay types and to perform this evaluation of performance and response under a wider range of fault and system scenarios, and this future work is reported and included in this thesis.

Overreaching issues related to distance protection zone boundaries are discussed in [69]. The paper concluded that. when a transmission line experiences a three-phase SC fault in a combined ac/dc system, its backup protection relay tends to overestimate the distance to the fault from the measurement location due to the reactive power control scheme inherent in the VSC-HVDC converter. For example, Table 4-1 below shows the relays are overestimating the fault distance by relative magnitudes ranging from 5% to as much as 111.2%. To identify distance relays that are not properly coordinated in an ac grid with offshore wind HVDC network injections, an apparent impedance calculation method is proposed. The paper concluded that settings of the protective devices must be adjusted when VSC-HVDC sources are integrated, but it is unclear how exhaustive or more generally applicable the solutions proposed would be – and forms of adaptive protection can be difficult to maintain and risk management. While this is a promising solution, it is felt that more understanding and mitigation of the issue using a simpler method may be prudent – and further investigations are required using converters with different presumed and actual responses – as is carried out in this work.

Table 4-1 Comparisons Between Impedances Measured (stated as "Viewed" in the paper) by Distance Relays on Combined AC/DC System at Zone 2 Fault Clearing Time and Zone 2 Settings of Corresponding Relays [69]

Relay	Viewed impedance (Ohm)	Zone 2 setting (Ohm)	Difference (Over ±5%)
17 line 16-17	$20.00 \angle 96.96^{\circ}$	$19.04 \angle 97.58^{\circ}$	5.0%
24 line 16-24	$38.10 \angle 46.11^{\circ}$	$31.11 \angle 46.09^{\circ}$	22.4%
24 line 23-24	$56.63 \angle 92.09^{\circ}$	$50.95 \angle 96.09^{\circ}$	11.1%
27 line 17-27	$27.51 \angle 84.12^{\circ}$	$26.10 \angle 84.40^{\circ}$	5.4%
27 line 26-27	$51.60 \angle 94.14^{\circ}$	$47.73 \angle 94.21^{\circ}$	8.1%
28 line 26-28	$251.78 \angle 12.76^{\circ}$	$118.85 \angle 13.69^{\circ}$	111.2%
28 line 28-29	$57.19 \angle 109.99^{\circ}$	$41.86 \angle 124.44^{\circ}$	36.6%
29 line 26-29	$198.25 \angle 84.40^{\circ}$	$122.24 \angle 38.6^{\circ}$	62.2%

Issues associated with changing "directions" of fault currents for close-up faults next to wind farms are demonstrated in [70]. Conventional R-L differential equation-based algorithms experience difficulties in detecting the correct fault direction if the fault location is very close to the relay location (either in front or behind the measurement location) since the fault is so close that the voltage is measured as zero. The paper analyses the aforementioned problems by establishing an instantaneous value-equivalent model of a DFIG and analysing the characteristics of the transient electromotive force (EMF) produced by the DFIG during and immediately after faults. It is concluded that innovative algorithms are required to solve the aforementioned problems. Again, this paper is specific to a particular application on the fault direction issue, and it is clear that more comprehensive tests and studies would be required in practice – over a range of presumed converter-interface responses, and again this is addressed by this research.

Specific studies related to the calculation of fault impedance within power systems dominated by converter-interfaced sources and infeeds have been analysed in multiple publications. In [71], it is shown how a converter's control system and its limited current output during short circuits can affect the apparent impedance as "seen" by distance protection for resistive faults. Mathematical calculations of the apparent impedance measured by the distance relay during asymmetrical faults for a VSC-HVDC connected transmission line are performed and the paper reveals that limited positive and negative sequence fault current from the converter, zero sequence from the transformer, grid current and fault resistance impact the distance relay significantly. It is shown how the active current blocking algorisms of the converter's control system will lead to relay under-reach during both symmetrical and asymmetrical fault scenarios. Figure 4-6 from [71] illustrates that the measured and calculated impedance from the relay side is significantly affected by the increase of the fault resistance. This is relevant to this work, and again modelling a wide range of converter responses assists in furthering the knowledge as to the potential impact of converter-interfaced sources and infeeds (particularly when they dominate over synchronous machine-based source) upon protection, and distance protection specifically.

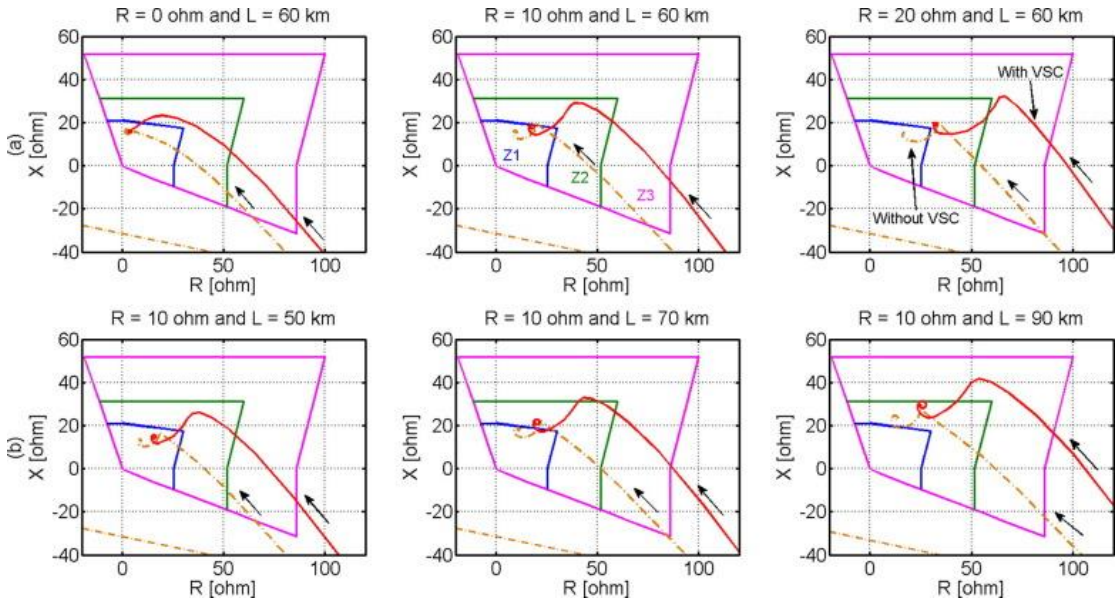

Figure 4-6 Impedance trajectory of ground AG element with and without VSC for phase-A to ground fault on Line 1. (a) Length = 60 km with Rf = 0, 10, 20 Ω. (b) Length = 50, 70, 90 km with Rf = 10 Ω. (Solid Red Line: with VSC; Dotted Orange Line: without VSC.) [71]

As summarised in [72], grid codes for HVDC connections, being compiled by organisations such as TenneT (the TSO in the Netherlands and Germany) and the European Network of Transmission System Operators for Electricity (ENTSO-E) suggest that VSC-HVDC sources should provide reactive current support during faults following a specific reactive current slope as demonstrated in Figure 4-7. Investigation regarding the effect of VSC based HVDC connection and its limited reactive current support during the fault as recommended by the grid code on the performance of the distance relay using closed-loop tests with the Real Time Digital Simulator (RTDS) under realistic conditions are then performed in the study. Results reveal that the reactive current provided by the converter may lead to the maloperation of the relay. However, the paper only focuses on the performance of protection relays without varying the controller settings or input current characteristics (which are carried

out in the research reported in this thesis) of the VSC source, which might further affect the protection devices.

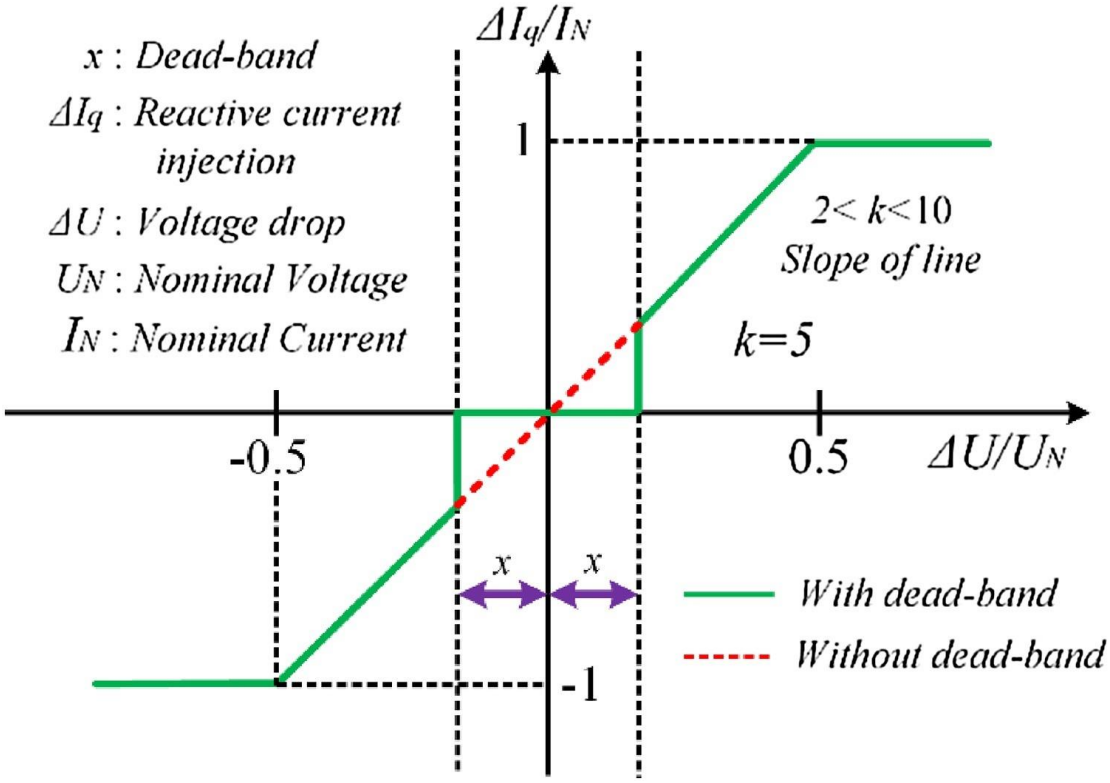

Figure 4-7 Reactive current slope for voltage support by the VSC-HVDC system. [72]

[73] introduces a converter-interfaced renewable energy power plant (CIREPP) model suitable for relaying studies, and outlines and explores operating scenarios that can lead to the malfunction of a distance relay that is located at a converter substation and protects the adjacent line. The system is demonstrated in Figure 4-8, where DS25 and DS52 represent the relays located at buses 2 and 5. These scenarios include in-zone short circuits that are not detected properly by the relay, and incorrect tripping for out-of-zone faults, which would, in turn, neutralise FRT schemes implemented within the converter. The above studies are related to the work reported in this thesis, but they are

somehow limited to evaluating how certain saturated currents with a narrow range of magnitudes (as output from the converters) influence the measured impedance by the relay for resistive faults based on calculation, and it makes several assumptions over the behaviour of the converter-interfaced source which may not always be valid in practice – the work reported in this thesis conducts a more thorough analysis of how different converter responses may impact protection to identify and quantity when and how problems may manifest. To have a more comprehensive understanding of how protective devices can be affected in future power systems under all types of different scenarios, a testing platform including both simulation and hardware-in-the-loop (HIL), as reported in this thesis, is required.

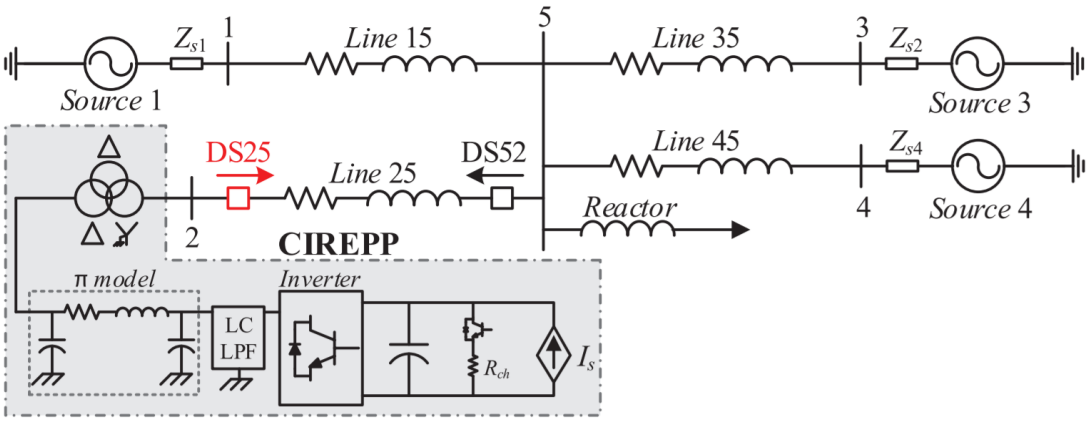

Figure 4-8 Power system model suitable for relaying studies [73]

Multiple studies have been performed by others to check whether converter-interfaced energy sources may lead to protection challenges or problems. The operation of relays located at grid-connected wind farms is studied in [74]. The work reported in the paper is focused on exploring how the protection supervisory elements (the elements responsible for detecting fault direction, fault impedance, the faulted phase(s), etc.) can be affected. The fault behaviour of a Doubly Fed Induction Generator (DFIG) is

different from a traditional synchronous generator as its output current is effectively limited according to specifications (crowbar protection or a chopper circuit is operated to limit its output during close-up/solid faults [75]). The simulation results (with examples from Table 4-2) reported in the paper reveal that the limited ability of DFIG to supply unbalanced currents shall lead to sensitivity issues for protection schemes and that this is influenced by the magnitudes of sequence currents supplied from the DFIG. The limited ability to provide zero-sequence current shall lead to changes in the measured fault impedances, coupled with negative impacts on the performance of the fault selection elements in the relays. It is clear that there are a number of issues with performance. In the table below:

- W - Wind turbine side relay
- G - Grid side relay
- 87LA/B/C - Line current differential elements in phase A/B/C
- 87LQ - Negative sequence element
- Z1G - Zone 1 Ground element
- Z2G - Zone 2 Ground element
- Z1P - Zone 1 Phase Distance element
- Z2P - Zone 2 Phase Distance element
- TRPPRM - trip permission element

Table 4-2 Responses of various zone protection elements in the presence of DFIG-supplied fault current [74]

Fault type	*Mode*	*Trip Issued by (trip time in cycles)*	*Operated*				
			Z1G	*Z2G*	*Z1P*	*Z2P*	*87*
AG	1	W: 87LA (1.5c)	N	N	N	N	Y
		G: Z1G (1.125c)	Y	Y	N	N	Y
	2	W: TRPPRM (3.25c)	N	N	N	N	--
		G: Z1G (1.125c)	Y	Y	N	N	--
ABG	1	W: 87LA (1.625c)	N	N	Y	Y	Y
		G: Z1P (1.875c)	N	N	Y	Y	Y
	2	W: Z2P (2.125c)	N	N	Y	Y	--
		G: Z1P (1.875c)	N	N	Y	Y	--
AB	1	W: 87LQ (1.375c)	N	N	Y	Y	Y
		G: Z1P (1.875c)	N	N	Y	Y	Y
	2	W: Z1P (2.125c)	N	N	Y	Y	--
		G: Z1P (2c)	N	N	Y	Y	--
ABCG	1	W: 87LA (1.75c)	N	N	N	N	Y
		G: Z1P (1.625c)	N	N	Y	Y	Y
	2	W: TRPPRM (4.125c)	N	N	N	N	--
		G: Z1P (1.625c)	N	N	Y	Y	--

[76] illustrates how converter control strategies may adversely impact relay performance by testing converters with specified control algorisms during faults. The system is tested through HIL tests on commercial relays. The paper advised that the performance of distance protection can be improved by ensuring that converters using constant active power and balanced current control strategies are used.

Studies presented in [58] and [59] show how traditional protection schemes using negative sequence current measurements are not always reliable in terms of fault detection and clearance when presented with fault currents that are supplied from converter-interfaced sources. In [77], protection schemes are studied together with actual recorded short circuit currents and voltages on transmission lines supplied from

converter-interfaced sources during actual faults experienced on an in-service system. Examples from this publication are presented in Figure 4-9, Figure 4-10 and Figure 4-11. The results demonstrate that negative sequence relaying to identify faults on converter-dominated systems is not fully dependable and line protection using negative sequence current to detect unbalanced faults could be compromised. It is clear from the diagrams below, that for all of the faults, the converter is not capable of providing the same types of sequence currents that would be provided by a synchronous machine. For example, in Figure 4-10 and Figure 4-11it is clear that the negative sequence voltage and current of the Type 3 wind turbine generator is largely different from the negative sequence *V/I* provided by a conventional source as shown in Figure 4-9 (especially the phase difference between the *V/I*). The change of the negative sequence *V/I* response may compromise the performance of relays that incorporate negative sequence current based schemes in order to detect and identify faults.

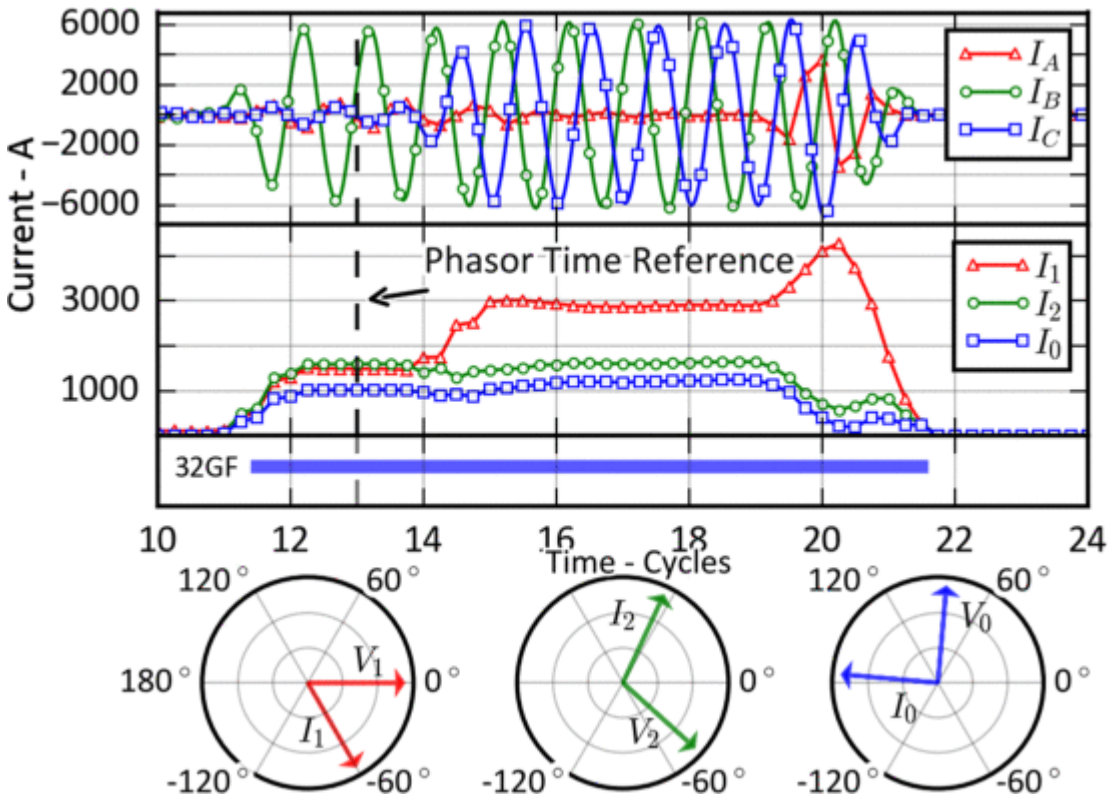

Figure 4-9 Relay records for forward ground fault contributed by conventional source [77]

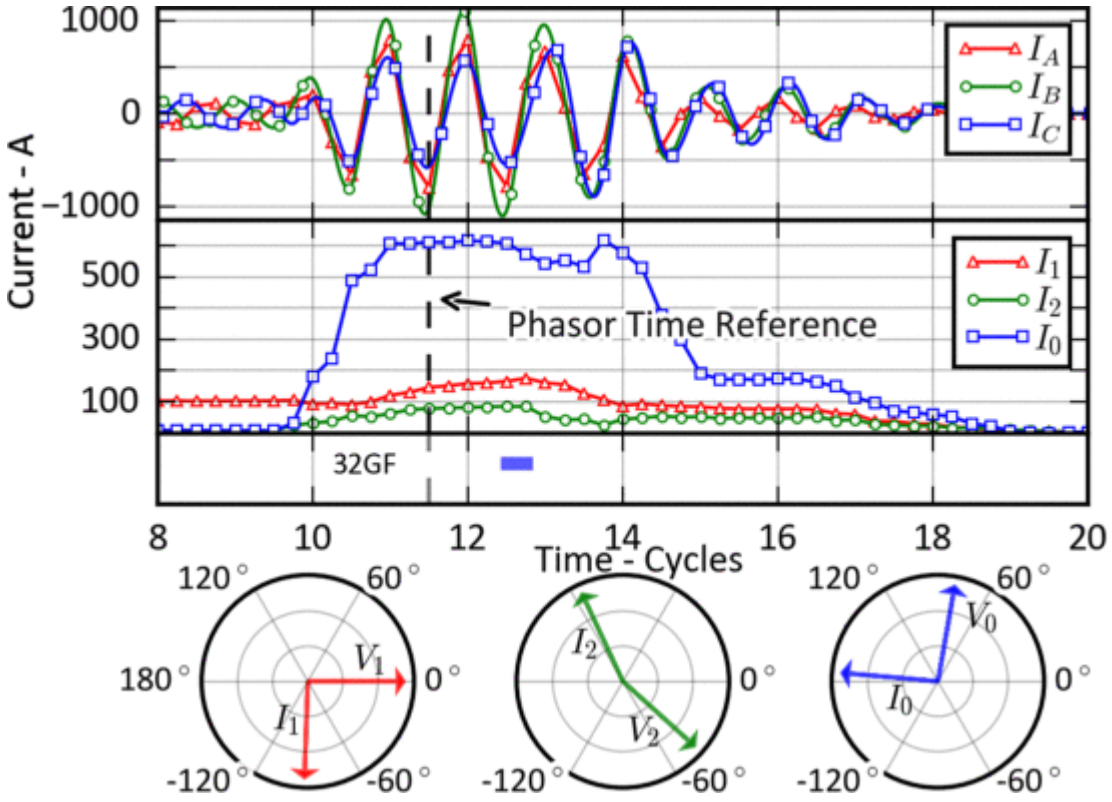

Figure 4-10 Relay records for forward ground fault contributed by Type 3 wind turbine generator [77]

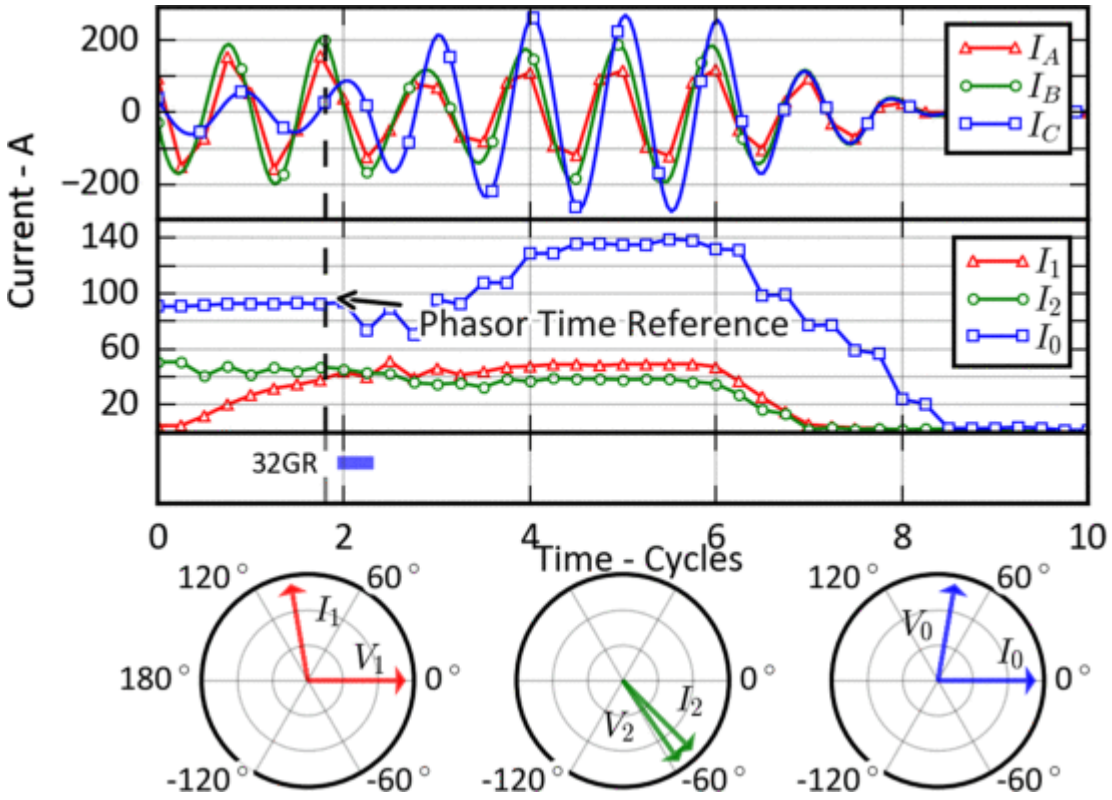

Figure 4-11 Relay records for reverse ground fault contributed by Type 3 wind turbine generator [77]

[78] is focused on the impact of various factors such as WTG (wind turbine generator) type (Type-III/Type-IV) and Type-IV WTG control schemes (including traditional coupled sequence control and decoupled sequence control schemes). Simulation cases are presented showing the maloperation of network protection schemes (including incorrect operation of the directional element and mal-operation of the phase selector) in the vicinity of high penetrations of these WTGs. Through a real-time, hardware-in-the-loop simulation arrangement using a physical relay, the impact on directional elements is also investigated and validated. As with other publications, this paper concentrates on a small number of specific cases. As presented in this research and

stated on several occasions previously, there is a need for a testing platform with comprehensive and flexible testing capabilities to enable a large range of studies to be conducted so that protection challenges and potential solutions for future systems can be fully investigated, understood tested and validated.

4.4 Review of research on potential protection solutions for future power systems

While a range of issues relating to different aspects of protection performance in a future system context has been identified, there are also various studies related to potential solutions for the protection of future systems, and these are reviewed in this section.

To address overreaching issues related to distance protection zone boundaries, the authors in [69] propose that, the specific HVDC system parameters to which the AC system being protected is interfaced, must take into consideration for the setting of the distance protection. The paper stipulates those specific settings for relays must be applied to avoid miscoordination and incorrect zone settings/reaches as the introduction of VSC devices will change the apparent impedance viewed by relays during short circuit faults. It should be noted that the paper is only focused on specified issues associated with the potential for coordination problems between relays on a specific system arrangement. Further investigations and solutions would be required to address other potential issues, such as problems in fault detection and identification, speed of decision-making and potentially slow/delayed operation, etc., as is highlighted in this research work and reported in this thesis.

Table 4-3, reproduced from [69], shows that the difference between the calculated impedance in a system with converter infeeds and the actual impedance settings can differ by significant amounts (differences of up to 134.5%). The differences between the measured/apparent impedance and the actual impedance setting are due to the influence of the reactive power control system of the VSC-HVDC during the fault. This is again clear evidence of the potential for problems with distance relays in a system dominated by converter-interfaced sources and infeeds and further validates the requirements for the research reported in this thesis.

Table 4-3 Comparisons Between Calculated Impedances Viewed by Distance Relays on Combined AC/DC Grid at Zone 2 Fault Clearing Time and Zone 2 Settings of Corresponding Relays [69]

Relay	Calculated impedance (Ohm)	Zone 2 setting (Ohm)	Difference (over ±5%)
1 line 1-39	198.00 ∠ 75.99°	163.31 ∠ 79.98°	21.4%
2 line 2-25	22.75 ∠ 65.83°	19.61 ∠ 70.62°	16.0%
5 line 5-6	8.82 ∠ 101.10°	6.92 ∠ 105.32°	27.4%
7 line 6-7	20.76 ∠ 93.71°	17.25 ∠ 96.14°	20.3%
9 line 9-39	318.54 ∠ 79.64°	267.85 ∠ 79.75°	18.9%
11 line 6-11	15.48 ∠ 84.19°	14.29 ∠ 83.65°	8.3%
13 line 10-13	6.92 ∠ 84.80°	6.52 ∠ 93.00°	6.1%
17 line 16-17	21.01 ∠ 90.00°	19.04 ∠ 97.58°	10.3%
21 line 21-22	33.83 ∠ 86.99°	28.96 ∠ 109.42°	16.8%
22 line 22-23	62.49 ∠ 92.89°	58.21 ∠ 94.98°	7.4%
24 line 16-24	40.09 ∠ 61.05°	31.11 ∠ 46.09°	28.8%
24 line 23-24	57.78 ∠ 92.55°	50.95 ∠ 96.09°	11.8%
26 line 26-29	87.15 ∠ 90.27°	81.82 ∠ 89.30°	6.5%
27 line 26-27	50.12 ∠ 87.35°	47.73 ∠ 94.21°	5.0%
28 line 26-28	278.60 ∠ 9.59°	118.85 ∠ 13.69°	134.5%
28 line 28-29	56.82 ∠ 101.87°	41.86 ∠ 124.44°	64.3%
29 line 26-29	211.14 ∠ 37.90°	122.24 ∠ 38.60°	72.7%

Distance relay: i line i-j means bus i side relay on line i-j, and j line i-j means bus j side relay on line i-j.

[70] proposes a new type of distance relay, based on the R-L differential-equation algorithm, which is claimed to be suitable for systems with high amounts of wind power integration. It is stated that this new type of relay/algorithm can deal with issues associated with changes and errors in the detected “directions” of fault currents (with

respect to the relay's measurement location) for close-up faults in close proximity to wind farms. The relay's algorithm is designed to deal with zero-voltage fault conditions (i.e. faults very close to the relay's measurement location) by analysing a "memorised" voltage drop and actual voltage drop with the assistance of a differentiated correlation coefficient. The corresponding operation logic is presented in Figure 4-12, where U_{set} is the threshold voltage, l_{set} is the setting value of the protected distance, $\tau_{ui,uj}$ is the calculated correlation coefficient and τ_{set} is the setting used for the correlation coefficient. As with several other publications, the paper is focused on solving a specified problem related to the directional detection unit; further studies and investigations are required to identify and address the full range of potential protection challenges (and solutions) under a comprehensive set of operational scenarios.

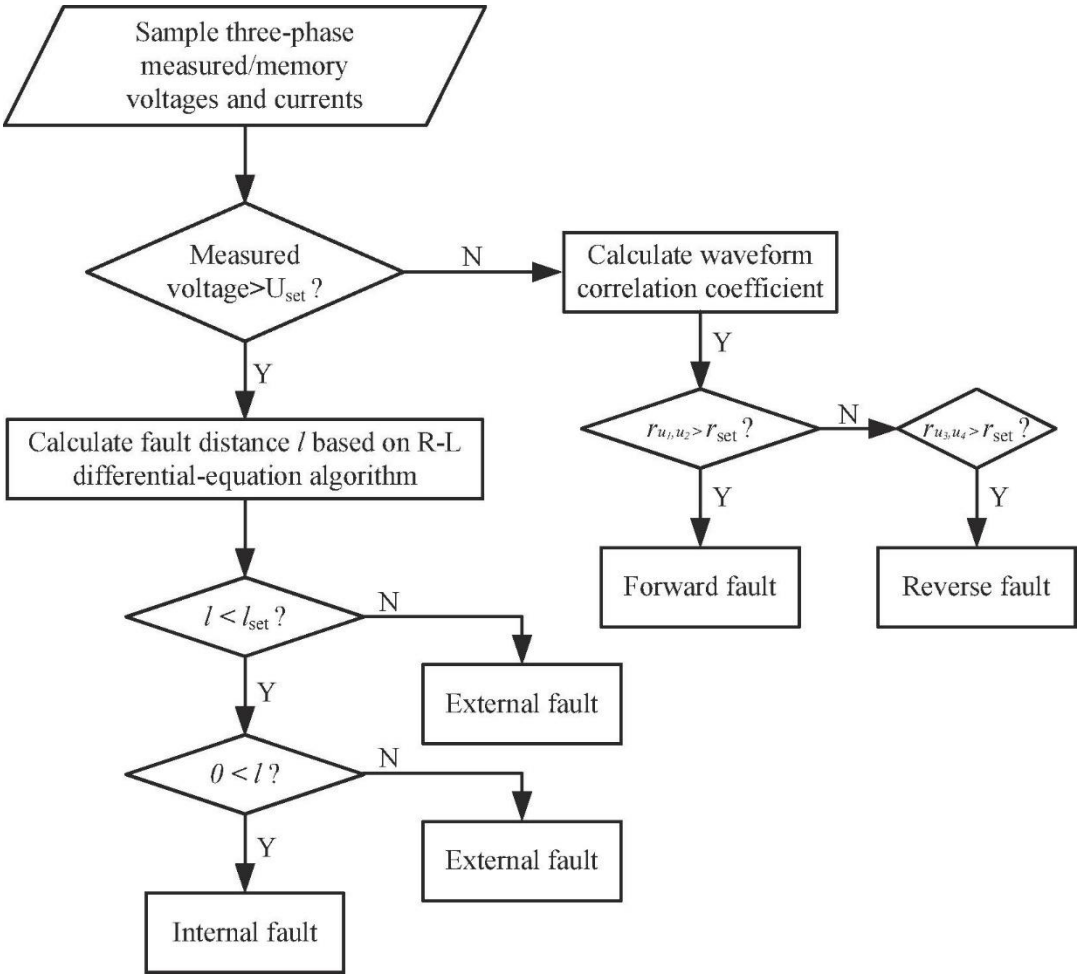

Figure 4-12 Flow chart of the operation of a proposed distance relays [70]

To counter the issues related to changes in impedance measured by relays in converter-dominated systems, [79] proposes a set of solutions including the derivation of a formula to calculate impedance in the phase elements of the relay to prevent maloperation in the event of line-to-line to ground faults (which incidentally is a really rare and unusual type of fault); proposal of a communications-assisted method requiring minimal bandwidth to deal with balanced and line-to-line faults. Again this paper is focused on addressing the issues of relay's miscoordination and incorrect zone settings. [80] proposes a method using local voltage and current data and calculates the

line impedance up to the fault point from the relay by determining the phase angle associated with the current in the faulted loop to obtain an accurate measure of impedance and a subsequent correct distance protection decision. The flow diagram is demonstrated in Figure 4-13, where Z_{app} is the apparent impedance calculated by relay, Z_{MF} is the line impedance up to fault point from the relay, and Z_{SP}^{pf} is the pre-fault equivalent impedance of the source. The method is assessed and compared to traditional distance protection systems, showing that the performance of the relay is improved. Like the previously listed articles, this paper is also focused on how to avoid incorrect zone reaching issues of distance relays.

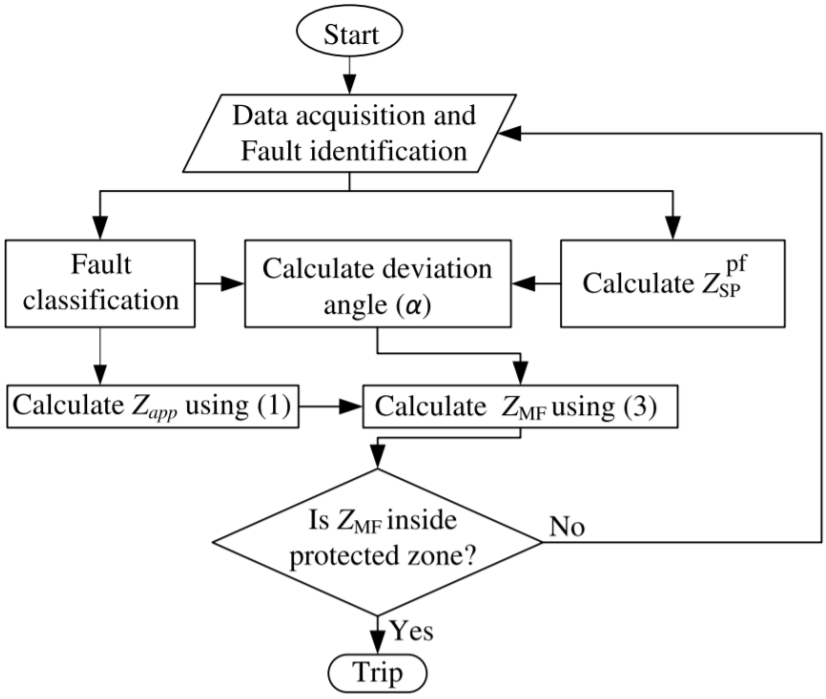

Figure 4-13 Flow diagram for the adaptive relaying technique developed in [80]

It is clear that there are several methods and potential solutions proposed, focusing on a range of different and specific protection problems associated with converter-dominated power systems. While they are useful and do make contributions to

addressing issues, there remains the requirement for a comprehensive testing platform and a systematic testing method to ensure a thorough range of studies can be conducted, enabling a range of insights to be made to support the development of guidance and solutions for the protection of future power systems.

4.5 Summary

This chapter has provided a comprehensive review of the behaviour of converters during faults in the AC system. It has also reviewed publications conducted by other researchers in the field, addressing protection challenges and proposing potential solutions. While these publications focus on specific issues and offer possible solutions, there is a lack of wide-ranging and systematic studies on the overall influence of converter-interfaced sources, specifically on transmission protection and distance protection.

Therefore, it is necessary to investigate the potential effects of introducing converter sources with different fault response characteristics on protection systems. Despite various efforts to identify and address protection issues, there has not been a fully detailed and comprehensive analysis of the impact of converter-interfaced sources on distance protection. Specifically, the ability to modify converter responses and consider different assumed scenarios remains unexplored.

Chapter 5

Development of A Converter Model to Produce Flexible and User-Defined Fault Current Responses

5.1 Introduction

This chapter presents and describes the design and operation of a comprehensive, flexible and credible converter-interfaced generation/infeed model that is capable of reproducing appropriate voltage and current output waveforms, that can be modified depending on the type of response required by configuring various model parameters, during grid network faults.

5.1 VSC-HVDC control system layout

Figure 5-1 demonstrates how the VSC system used as the basis for the converter model producing fault current in this thesis is arranged. A phase-locked loop (PLL) connected to the connection point (CP) is used to track the AC voltage's angular speed and this is used as input to Park and Inverse Park transformations, which underpin the VSC control scheme [27]. In this system, a dual sequence controller is implemented, as this permits the VSC to output both balanced and unbalanced three-phase currents; and facilitates stable, non-oscillating real and reactive power control and output; while minimising DC link voltage ripple during unbalanced network conditions [28]. By varying positive and negative sequence current output, duel sequence schemes can enable the response of the converter to be similar to a synchronous generator, albeit with a lesser relative magnitude of fault current, during unbalanced fault conditions [29], which obviously is desirable in terms of complying with grid code requirements.

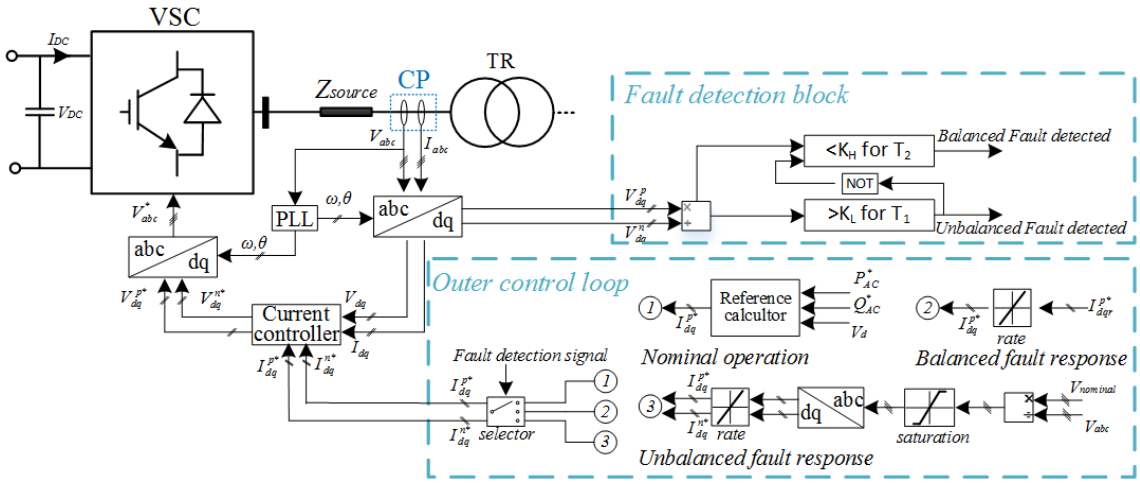

Figure 5-1 Overall layout of the VSC system

The control system consists of inner and outer controllers. The inner current controller computes VSC output voltage references in order to regulate VSC output currents. The three-phase voltages v_{abc} and currents i_{abc}, as measured at the connection point are transformed into dq values ($v_{dq}^{p}, v_{dq}^{n}, i_{dq}^{p}, i_{dq}^{n}$) by one positive sequence rotating reference frame and one negative sequence frame, both of which rotate mutually in opposite directions with identical fundamental frequency. The process is displayed in the following equations:

$$v_{dq}^{p} = v_{d}^{p} + \mathrm{j}v_{q}^{p} = \frac{2}{3} j e^{-j\omega t}\left(v_a + e^{j\frac{2}{3}\pi} v_b + e^{-j\frac{2}{3}\pi} v_c\right) \quad \text{Equation 5-1}$$

$$v_{dq}^{n} = v_{d}^{n} + \mathrm{j}v_{q}^{n} = \frac{2}{3} j e^{-j\omega t}\left(v_a + e^{-j\frac{2}{3}\pi} v_b + e^{j\frac{2}{3}\pi} v_c\right) \quad \text{Equation 5-2}$$

$$i_{dq}^{p} = i_{d}^{p} + \mathrm{j}i_{q}^{p} = \frac{2}{3} j e^{-j\omega t}\left(i_a + e^{j\frac{2}{3}\pi} i_b + e^{-j\frac{2}{3}\pi} i_c\right) \quad \text{Equation 5-3}$$

$$i_{dq}^{n} = \ i_{d}^{n} + \mathrm{j}i_{q}^{n} = \frac{2}{3} j e^{-j\omega t}(i_a + e^{-j\frac{2}{3}\pi} i_b + e^{j\frac{2}{3}\pi} i_c)$$ Equation 5-4

The magnitudes of i_{dq} are regulated by the PI controllers with the inner current control according to the reference values. To achieve the control of i_{dq}, the VSC output voltage references v_{dq}^{p*}, v_{dq}^{n*} are computed, taking account of the coupling effect of the VSC phase reactor and transformer.

The relationship between the grid voltage v_{abc}, converter output voltage v_{abc}^{*} and current value i_{abc} is as follows:

$$v_{abc}^{*} = L\frac{di_{abc}}{dt} + Ri_{abc} + j\omega Li_{abc} + v_{abc}$$ Equation 5-5

Expressing Equation 5-5 above in the dq positive and negative sequence forms yields:

$$v_{d}^{p*} = L\frac{di_{d}^{p}}{dt} + Ri_{d}^{p} - \omega Li_{q}^{p} + v_{d}^{p}$$ Equation 5-6

$$v_{q}^{p*} = L\frac{di_{q}^{p}}{dt} + Ri_{q}^{p} + j\omega Li_{d}^{p} + v_{d}^{p}$$ Equation 5-7

$$v_{d}^{n*} = L\frac{di_{d}^{n}}{dt} + Ri_{d}^{n} + \omega Li_{q}^{n} + v_{d}^{n}$$ Equation 5-8

$$v_{q}^{n*} = L\frac{di_{q}^{n}}{dt} + Ri_{q}^{n} - j\omega Li_{d}^{n} + v_{d}^{n}$$ Equation 5-9

For the outer controllers, the VSC output current control can be transformed into other forms for regulating *P, Q, V_{DC} or V_{AC}*, and the outer controllers can be configured to achieve various objectives. Detailed operating principles for such controllers are reviewed in Chapter 3.

5.2 Flexible and controllable fault response capability

To enable the converter model to emulate a range of different fault response characteristics, a fault detection logic function (as shown in Figure 5-2) has been developed to automatically detect the types of faults that have occurred and subsequently select the corresponding fault response mode. When the fault type has been detected, the outer control loop as shown in Figure 5-1 will feed forward the corresponding fault current reference signals as input to the current controllers, which will then regulate the fault current output from the converter.

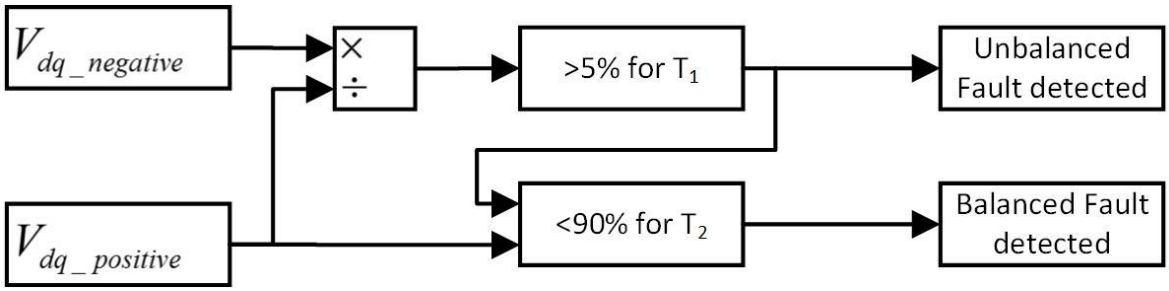

Figure 5-2 Fault detection logic

Fault detection is achieved by monitoring the per-unit value of positive and negative sequence voltages ($|v_{dq}^{p}|$,$|v_{dq}^{n}|$) at the connection point where:

$$|v_{dq}^{pn}| = \sqrt{(v_d^{pn})^2+(v_q^{pn})^2}$$ Equation 5-10

For the detection of balanced faults, the controller will monitor both positive sequence voltage $|v_{dq}^{p}|$ and negative sequence voltage $|v_{dq}^{n}|$. Balanced faults will typically lead to a positive voltage depression (i.e. $|v_{dq}^{p}|$ will drop below the normal operating range, which is typically 94%), while $|v_{dq}^{n}|$should remain to be negligible. Therefore, the controller will conclude that there is a balanced fault if $|v_{dq}^{p}|$ drops below a threshold K_H and $|v_{dq}^{n}|$ is within a limit of K_L.

For unbalanced faults, significantly larger values of $|v_{dq}^{n}|$ will be measured, compared to their values with normal operating conditions, so the magnitude of $|v_{dq}^{n}|$ is monitored, and if it is greater than the threshold K_L, it is considered that there is an unbalanced fault present in the system. The thresholds K_H and K_L are configurable to ensure that there is an appropriate balance between the sensitivity and stability of the fault detection element of the system.

The time delays T_1, T_2 are applied to avoid incorrect operation due to system transient behaviour. T_1 is selected to be longer than T_2 in order to make sure that the total time for the production of a positive fault detection output signal is dependent on T_1. For a close-up fault, which will result in a severe voltage depression as measured at the converter's AC terminals, the PLL unit may not be capable of determining phase and frequency information, as the voltage measurement inputs to the PLL drop to near-zero values. Consequently, the converter may not be able to correctly inject current into the grid and the controller may shut down. In order to ride through such fault conditions,

the fault detection function is essential to be developed in this model. After the detection of faults, the PLL unit will retrieve the pre-fault phase and frequency information recorded from historical data immediately before the fault in order to sustain current injection into the grid. Although this may mean that it will not follow the true system frequency or inject the correct current phase angle relative to the voltage during the fault, it will mimic the converter's AC voltage waveforms under assumed steady state conditions and sustain continuous AC current injection to the system in order to facilitate fault ride-through as required by the grid codes [8], [14], [15].

The converter's fault response is varied by modifying the initial response delay, current ramp rate and final sustained fault level – all of which can be configured by the user of the model. The corresponding parameters and how they can be modified are demonstrated (using an exaggerated representation for illustrative purposes) in Fig. 9. After a fault is detected, the converter will begin to respond to the fault. Several characteristics of the fault response can be manipulated within the model. The setting of T_1 from Figure 5-2 dictates the initial response delay time.

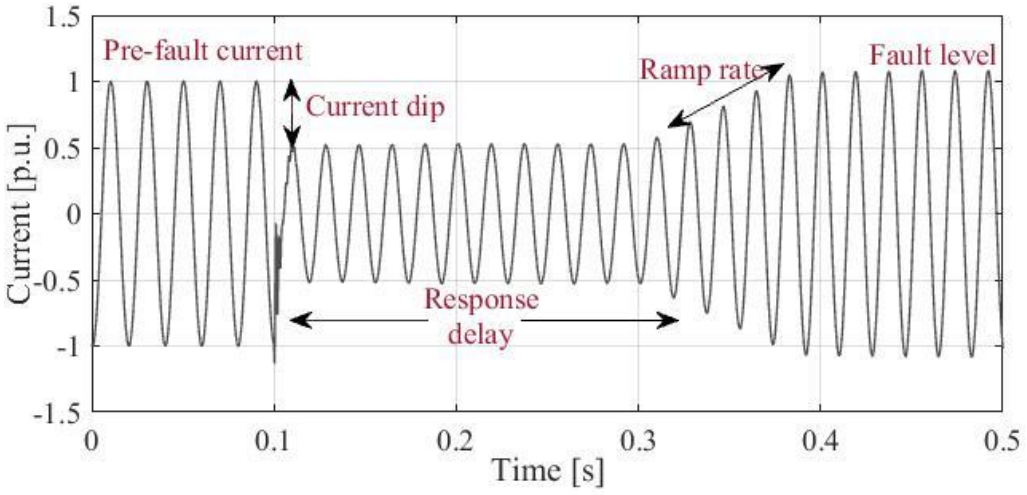

Figure 5-3 Controllable output current provided by the converter

For balanced fault situations, where the desired sustained fault level has been specified by the user, the corresponding i_{dq} reference value for the converter's current control loop can be calculated using equations Equation 5-3 and Equation 5-4. During the fault, the output current is regulated to reach its final fault level with a controlled current ramp rate by the limiter.

During an unbalanced situation, the fault detection block shall identify the type of fault and then configure the outer controller to enable the unbalanced fault response mode. The corresponding reference values for the current outputs shall begin to be calculated. The corresponding i_d and i_q are selected to allow the converter to output its maximum reactive current (with ramp rate defined by the limiter) for the faulted phase(s) while the current in the healthy phase(s) shall be maintained at nominal values (or load values if less than nominal).

The process is divided into the following parts:

1) Detect the fault and the faulted phase(s).

2) Calculate the corresponding ABC currents individually and ensure that the current in the non-faulted phase(s) remains as per pre-fault values and the current in the faulted phase(s) shall begin ramping up to maximum value.

3) Disassemble the ABC current into positive sequence and negative sequence components, then calculate the corresponding *dq* value using a Park transformation.

4) Allocate the calculated *dq* value of the reference current for the inner current control loop to guide the converter's output current.

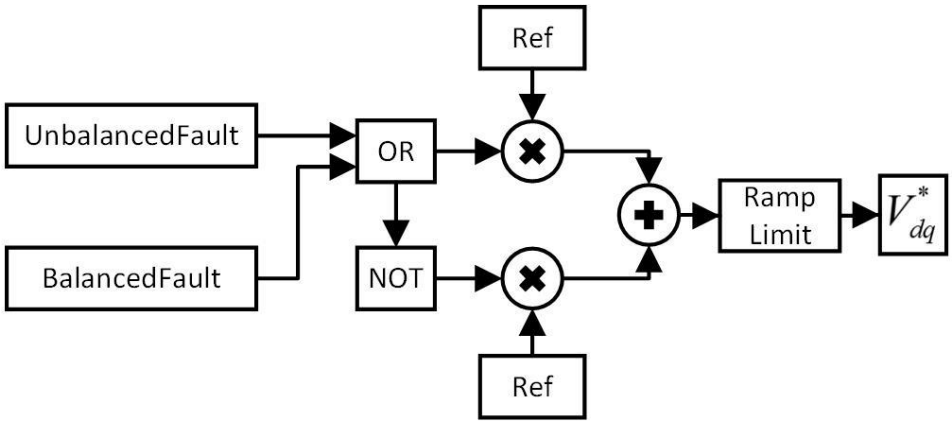

Figure 5-4 Fault response logic

5.3 Validation and case studies of converter model output

To validate the model, fault responses from the converter model are generated to represent the example provided from realistic results from [60] which is displayed in Figure 4-2, where the converter is configured to produce a 2 ms response delay, a 1.4 GVA/cycle ramp rate and a 1.2 GVA sustained fault current:

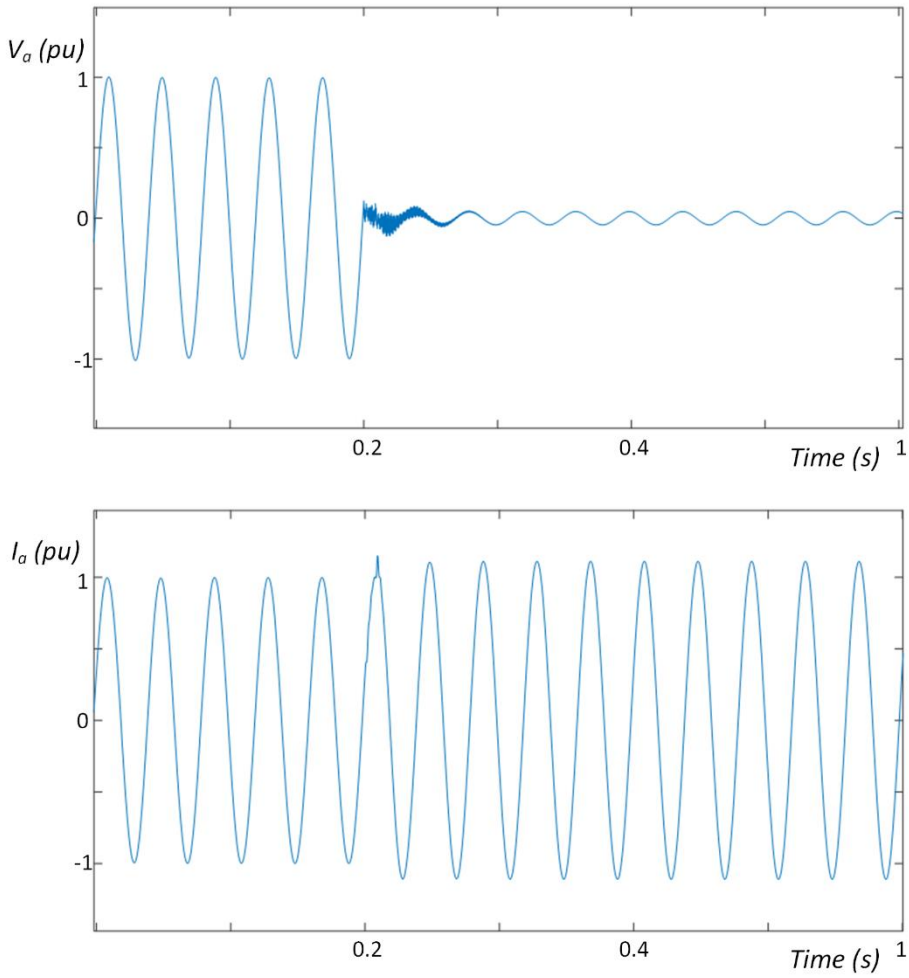

Figure 5-5 generated fault response to represent the example provided from realistic results from [60]

The generated result aligned with the previously published realistic research.

In addition to the above validation processes, examples of the output provided by the converter have also been simulated and analysed. Note that the setting of the reference values of the current limitation for the VSC sources in this section is for theoretical analyses only, in order to demonstrate the difference between the developed model and a traditional synchronous machine.

As presented in Figure 5-6 and Figure 5-7, the generating source is connected to the transmission system and solid faults are applied to the protected transmission line.

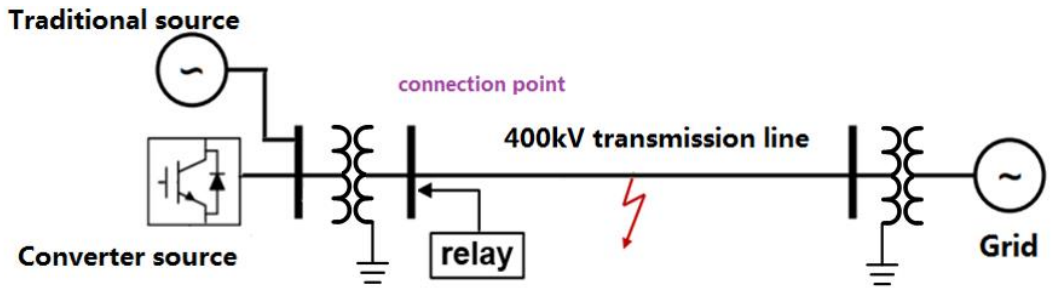

Figure 5-6 Transmission system model example

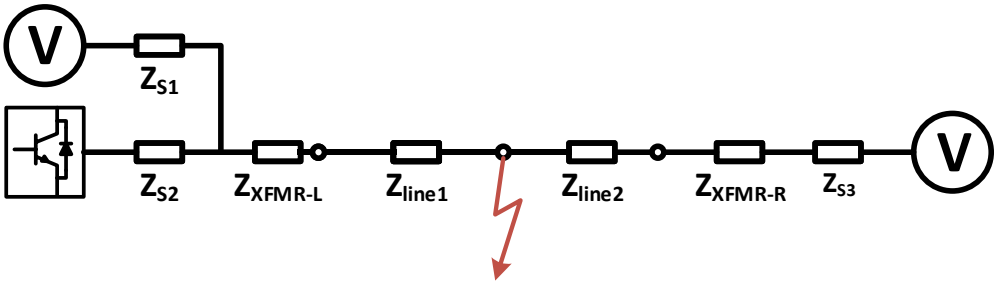

Figure 5-7 Single-line diagram

When balanced three-phase faults are applied, the corresponding fault response from differently-configured sources is shown in Figure 5-8, Figure 5-9 and Figure 5-10. Two extreme cases of the VSC sources are selected here to demonstrate the result of varying the converter's controlling algorithm. The VSC in Figure 5-9 is configured to have a low response delay (2 ms), a high ramp rate (1.4 GVA/cycle) and a relatively large sustained fault current (2.4 GVA – which is twice the nominal output current rating – again, as stated earlier, this is relatively high and in practice may be less, but this value is chosen so that the results are clearer and more easily compared). The VSC in Figure

5-10 is set up with a relatively longer 50 ms response delay, a relatively lower ramp rate (0.45 GVA/cycle) and a relatively low level of sustained fault current (1.2 GVA which is equal to the nominal rating).

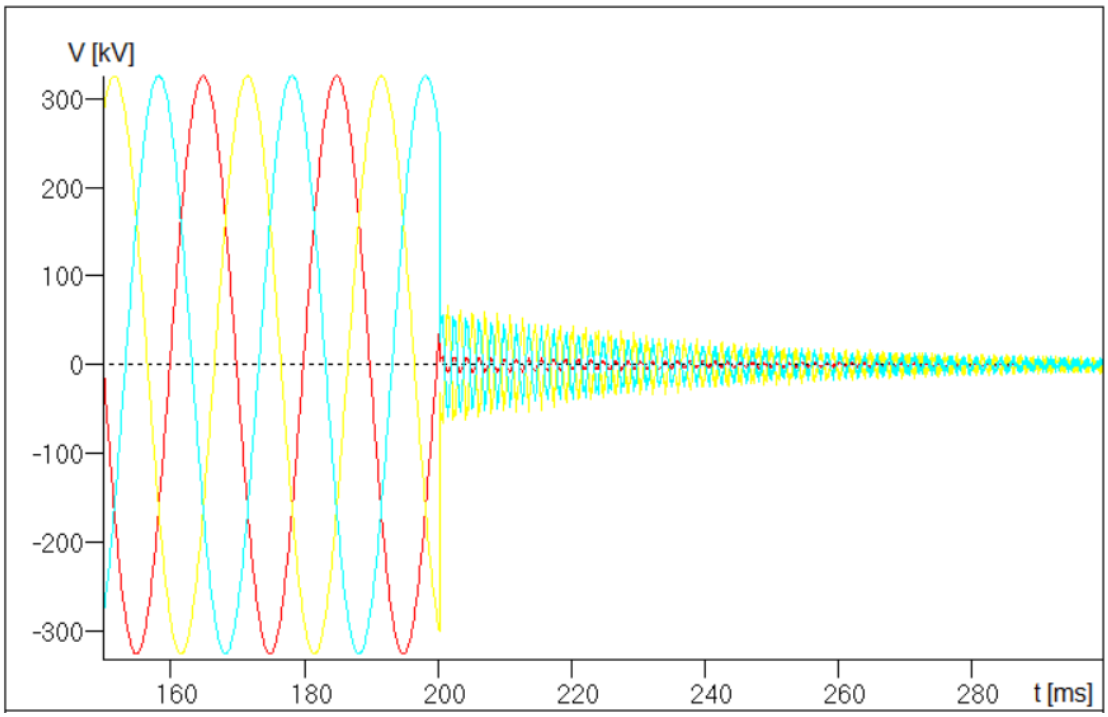

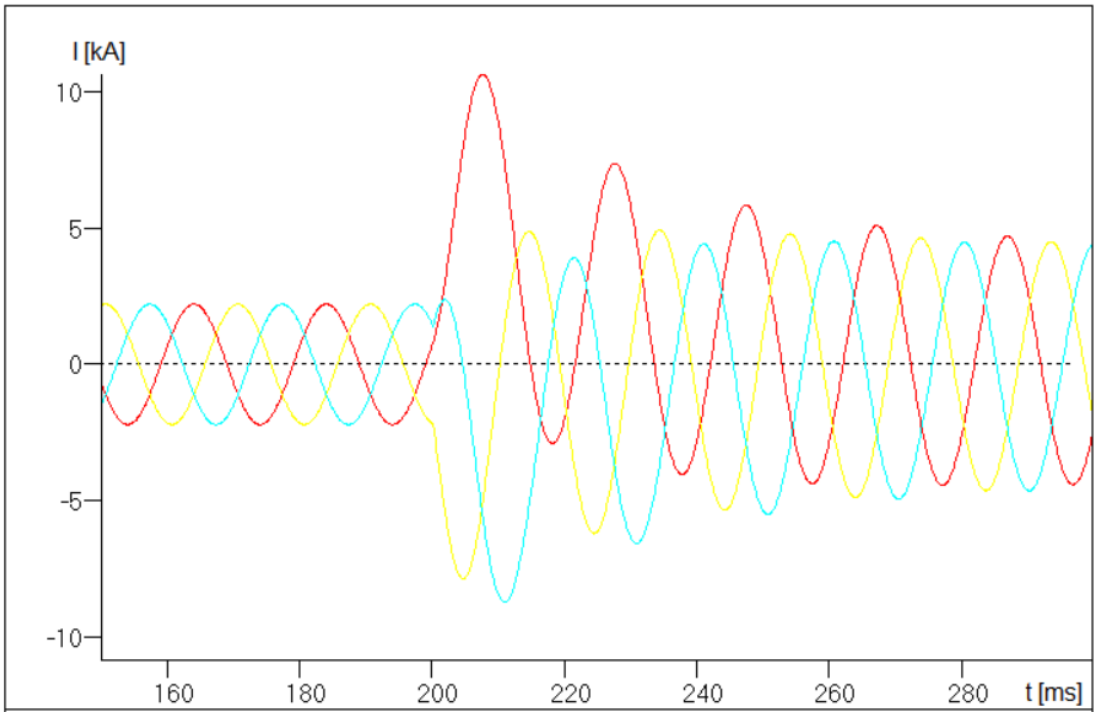

Figure 5-8 Fault V/I provided by synchronous machine only under balanced three-phase faults

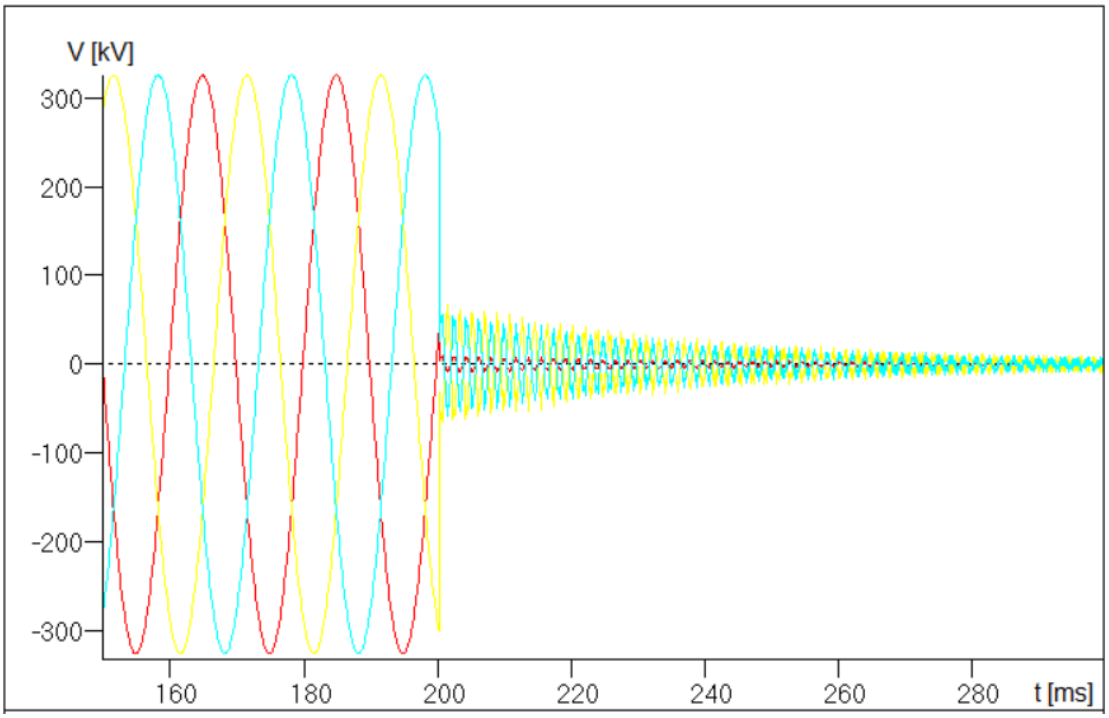

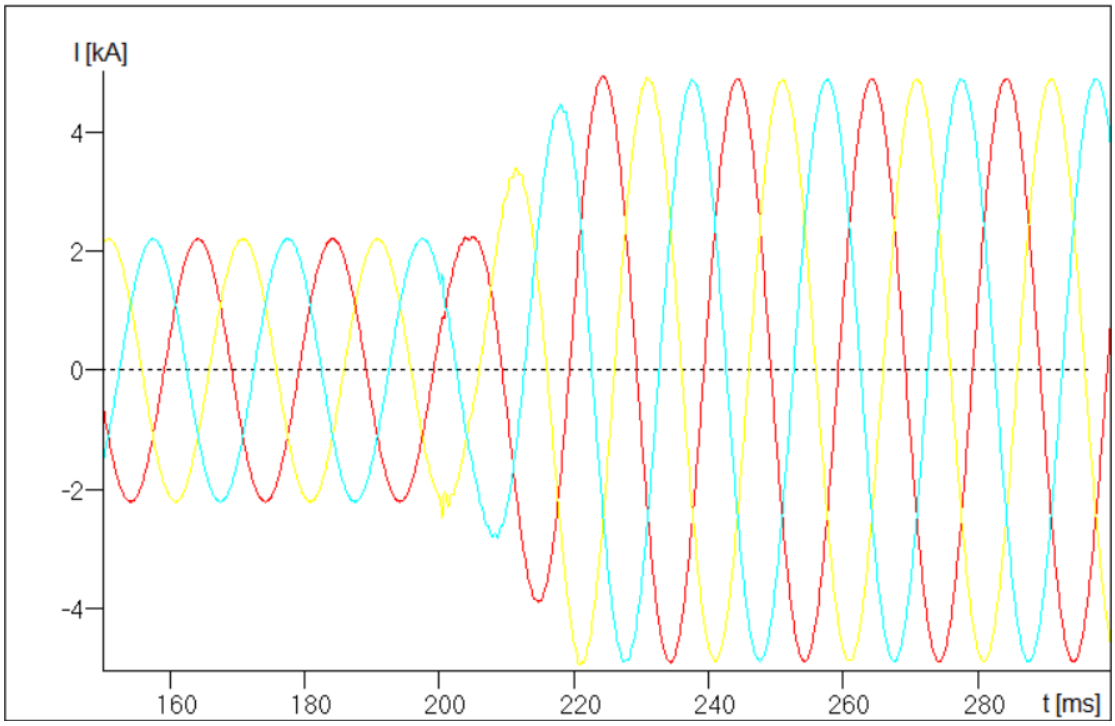

Figure 5-9 Fault V/I provided by VSC only with fast fault response for a balanced three-phase fault

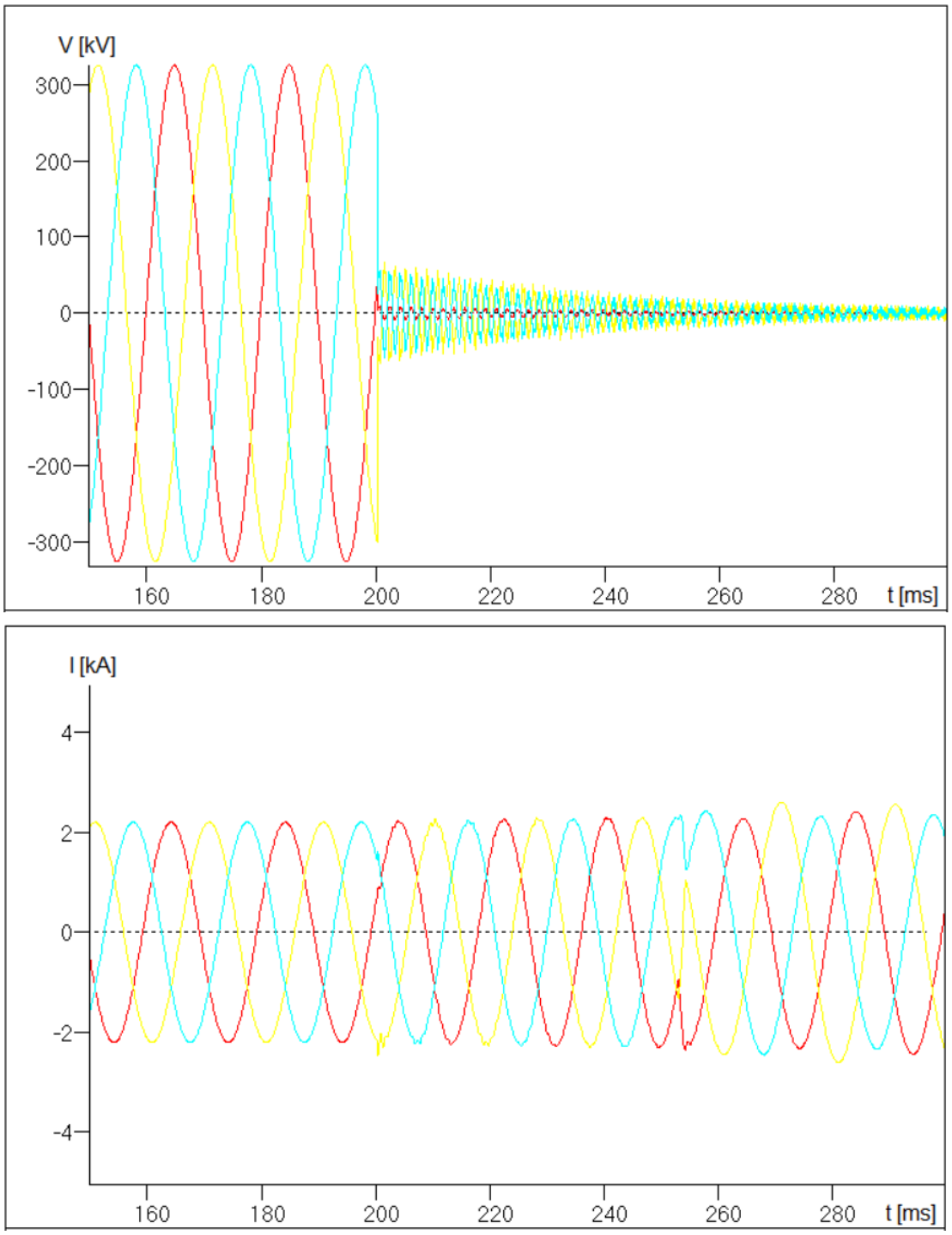

Figure 5-10 Fault V/I provided by VSC with slow fault response for a balanced three-phase faults

When unbalanced faults are applied, the corresponding output currents from the VSC source are further varied by its positive and negative sequence control algorithm. Taking single phase to earth fault as an example, with systems dominated by different

source types, the post-fault sequence network of the transmission system shown in Figure 5-7 from this study can be represented in Figure 5-11:

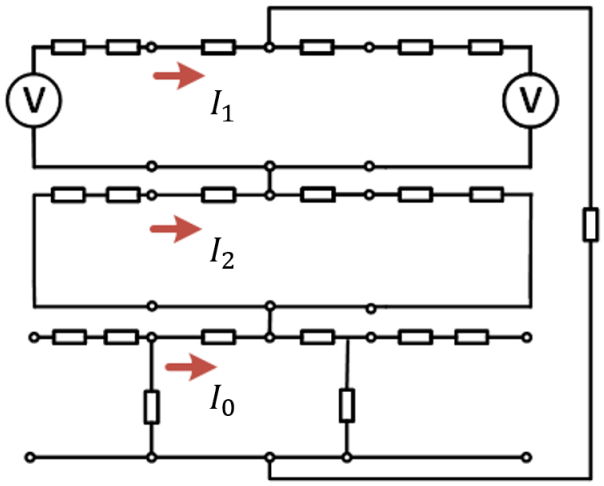

(a)System dominated by synchronous machine

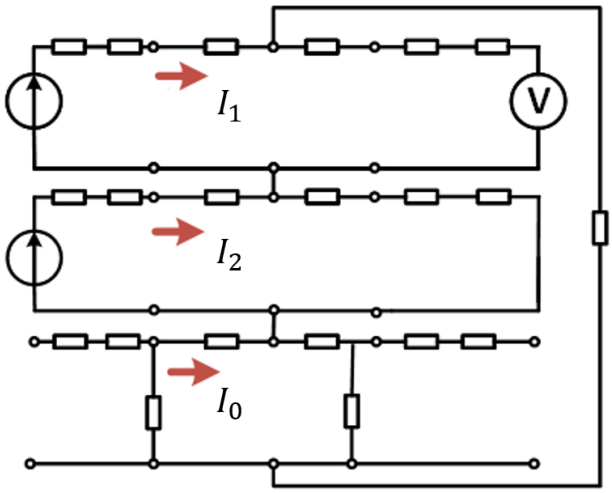

(b) System dominated by VSC

Figure 5-11 Post-fault sequence network

When the system is dominated by synchronous machines, the solid phase-to-earth fault shall create a fault loop where the positive, negative and zero sequence fault currents are instantaneously supplied by the source voltage. When the system is dominated by VSC, the converter shall behave like a current source during the fault and the positive

and negative sequence currents can be manipulated individually within the controller's algorithm.

When specific requirements are not provided, the corresponding fault current might only have the positive and zero sequence components when VSC is configured to output balanced currents during an unbalanced fault. When the VSC is configured to output unbalanced currents by manipulating the negative sequence current, the VSC shall share a similar fault response with a conventional synchronous machine during the sustained fault stage as demonstrated in

Figure 5-12 and Figure 5-13 (for the purpose of demonstration only, both VSC is configured with a low 2 ms response delay, a high 1.2 pu/cycle ramp rate, the balanced fault current is set as 2 pu and the unbalanced fault current set as 3.3 pu).

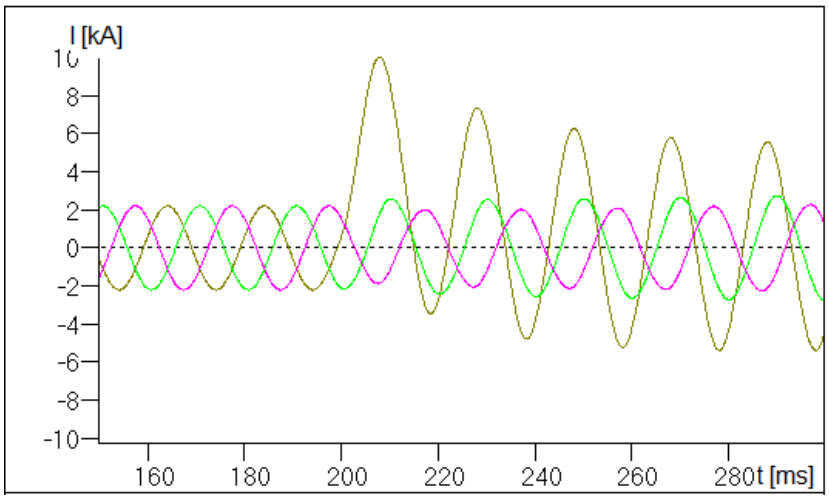

(a) Fault current recorded at the relay when the system is dominated by synchronous machine sources

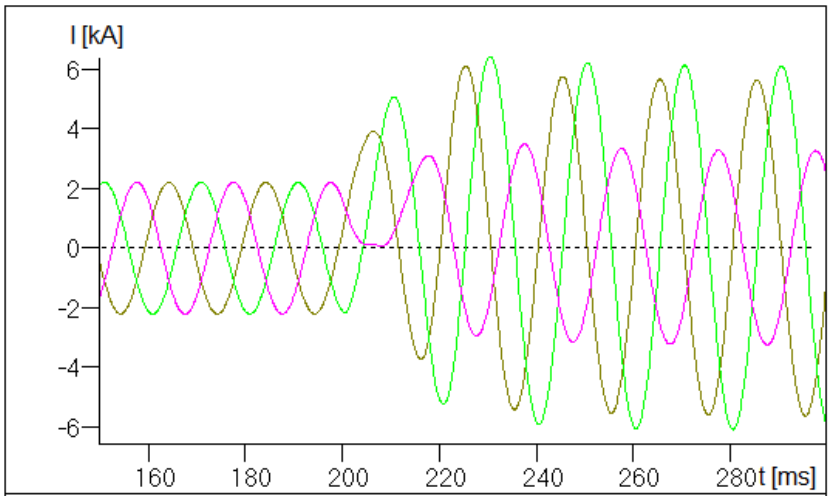

(b) Fault current recorded at the relay when the system is dominated by VSC with balanced output

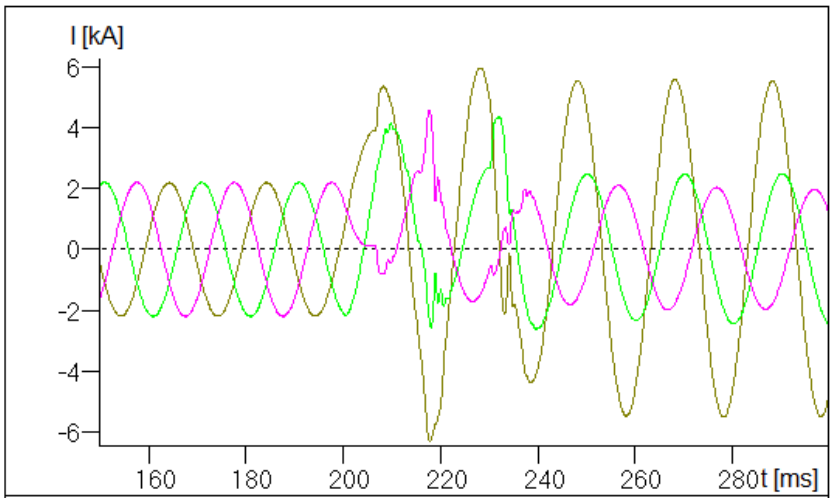

(c) Fault current recorded at the relay when the system is dominated by VSC with unbalanced output

Figure 5-12 Recorded fault response

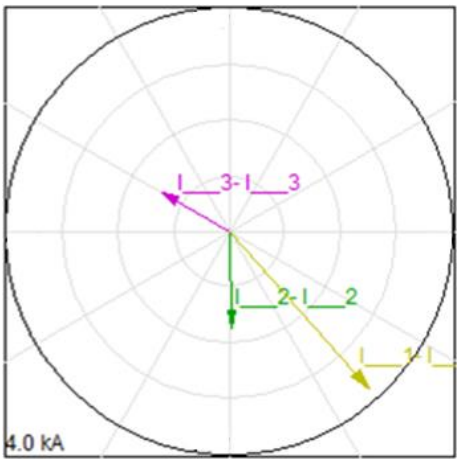

(a)Fault current provided by synchronous machine

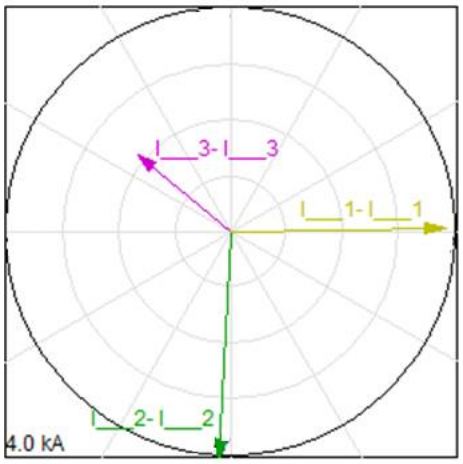

(b) Fault current provided by VSC with balanced output

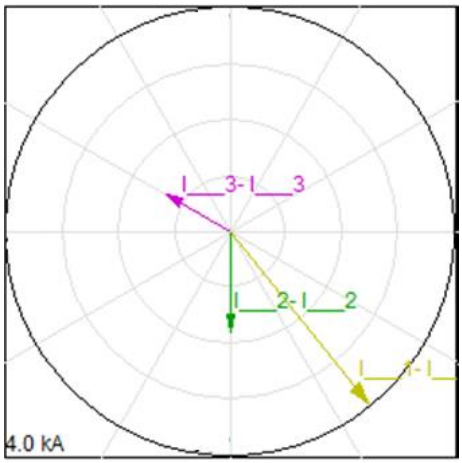

(c) Fault current provided by VSC with unbalanced output

Figure 5-13 measured phaser diagram of the steady post-fault current

In summary, this section has shown, with example waveforms, the range of different fault current responses that can be produced by varying the parameters associated with the converter model – using these variable characteristics, the operation (or not) of protection in systems that are dominated by converter-interfaced sources can be studied in detail under a range of assumed responses.

5.5 Summary

In this chapter, a comprehensive, flexible, and credible converter-interfaced generation/infeed model has been presented and described. The model is capable of reproducing accurate voltage and current output waveforms during grid network faults. Various model parameters can be configured to modify the type of response required. The overall system layout has been displayed.

To enhance the system's flexible and controllable fault response capability, a fault detection block and a fault response block have been developed. The results have been validated, and testing examples have been provided to demonstrate the range of different fault current responses achievable by varying the parameters associated with the converter model. By utilizing these variable characteristics, the operation (or lack thereof) of protection systems in converter-dominated sources can be thoroughly studied under a range of assumed responses.

Throughout the chapter, the significance of the converter-interfaced generation/infeed model in investigating protection system behaviour has been emphasized. The provided examples, along with their accompanying waveforms, illustrate the model's capabilities and the potential impact on protection systems in converter-dominated environments.

Chapter 6

Relay Performance Testing Methodology

6.1 Introduction

This section presents the overview and description of the setting up of the hardware testing platform to aid the systematic study of investigating the protection challenges led by the introduction of converter-based energy sources, the comprehensive overview and description of the testing methodology, the configuration of the system together with the selection of protection relays.

6.2 Configuration of the modelled transmission system

A transmission line model and an actual protection relay device with appropriate settings have been used as the basis for investigations, the overall layout of the test facilities is displayed in Figure 6-1.

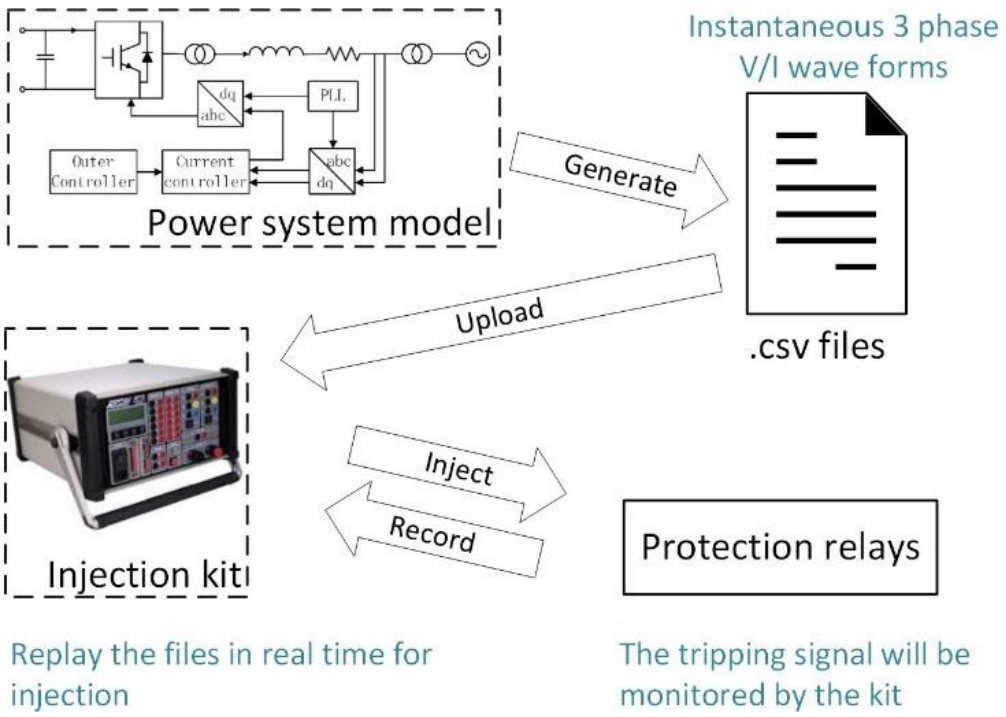

Figure 6-1 Secondary injection testing facility

A single transmission line model is used – more complex (e.g., multi-ended) arrangements could easily be incorporated, but for clarity and simplicity this model is used. The focus of the investigations in this thesis is on the main protection operation (i.e., testing zone 1 performance, and the reach associated with zone 1) for faults on the "main" protected line. The system could be easily extended to investigate zone 2/3 reaches and performances, and therefore the potential for impact on the performance of backup protection, including other converter-interfaced infeeds at remote nodes – this is outlined as future work and described in Chapter 8.

The layout of the system is depicted in Figure 6-2 and a photograph of the actual laboratory set-up is included in Figure 6-3.

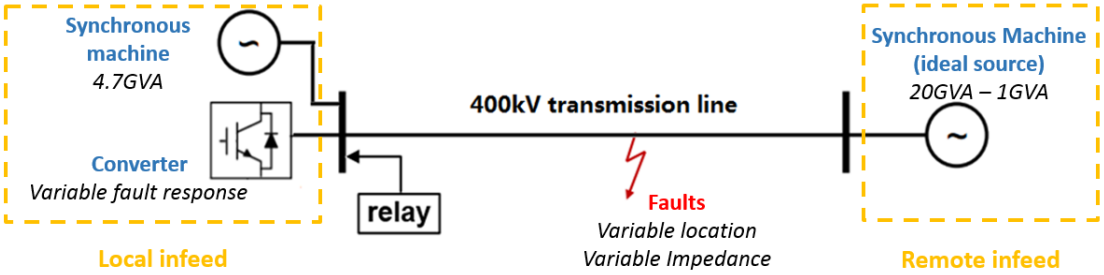

Figure 6-2 Model of the transmission line system

Figure 6-3 Actual laboratory set-up

The system is supplied by a combination of SG and VSC-based generation sources. The power generated from each source (P_{VSC}, P_{SG}) is fully configurable. Note that the fault level from the generation sources is directly affected by their rated power. To avoid confusion, the power generated from each source prior to any fault is set to be at their rated power level in this system. Based on the rating of each source (i.e., the converter and synchronous generator respective ratings), the penetration level (PL) of the VSC is defined as shown in the equation below:

$$PL = \frac{P_{VSC}}{P_{VSC} + P_{SG}} \times 100\% \qquad \text{Equation 6-1}$$

Since only bolted/solid short circuit faults are applied in the case studies, to ensure that the developed testing and evaluation scheme can be applied to different transmission systems with different conditions (and also to facilitate faults at variable distances along lines to be tested), the transmission line model (representing the transmission system with a length of 80 km) has been disassembled into four different components as shown in Figure 6-4.

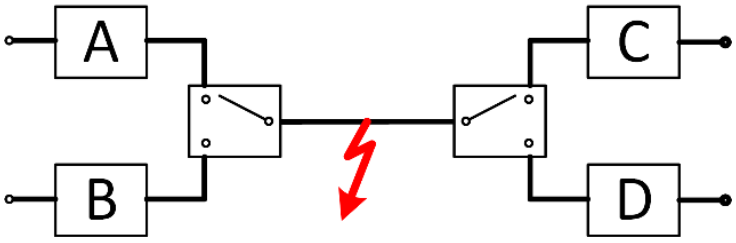

Figure 6-4 Model of the transmission line

Line components A and C uses a pi model, while B and D use an RL model which can be switched to operate based on the length of each part of the transmission line separated by the fault with the logic from Table 6-1:

Table 6-1 Selection of the transmission line components

	Fault location L(km)		
Section	L<20	20<L<60	L>60
A	Off	On	On
B	On	Off	Off
C	On	On	Off
D	Off	Off	On

The faulted phase(s) of the transmission line is divided into left and right elements when a fault occurs. When the line length is longer than 20 km, the pi model is selected to represent the system to ensure model fidelity, and when the line length is less than 20 km, the RL model is used to reduce the calculation burden without excessively compromising accuracy. More information on transmission line modelling, which has been used as guidance for the approach adopted here, is contained in [18].

6.3 Testing methodology

The detailed testing arrangement for the assessment of a distance relay's performance is presented in Figure 6-5. To initiate the testing, the corresponding details (line parameters/nominal voltage/power rating) for the transmission system are required. Then the corresponding relay equipment can be set up and configured with the

appropriate settings. Following this the selection of the fault response parameter of the VSC model, faults with selected type and location.

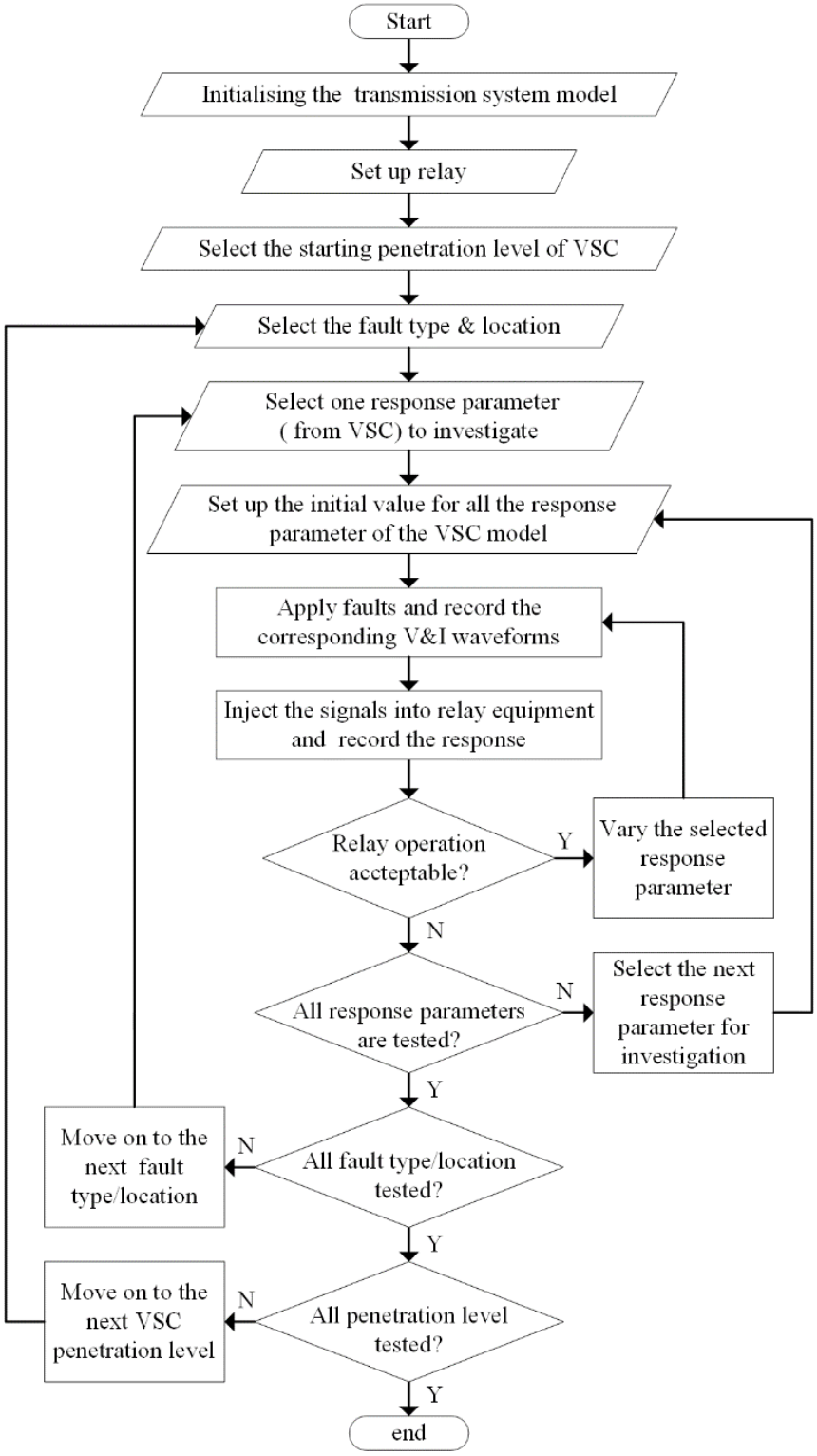

Figure 6-5 Relay testing methodology

In the next stage, a .csv file containing discrete values for the three-phase instantaneous voltage and current waveforms (sampled at a frequency of 10 kHz) is created and replayed in real-time into the protection relay using secondary injection equipment. The performance of the relay can therefore be recorded and assessed.

In the particular studies in this thesis, the nominal power flows (1.2 GVA) and fault levels provided by the local infeed for the transmission line are sourced from NGESO documents [81]. When the system is supplied solely by SG sources, the fault level is set to be 4.7 GVA to represent minimum fault levels as outlined in [81]; a relatively weak local infeed. The remote-end infeed is assumed to comprise SG sources with a 20 GVA fault level (i.e. relatively strong remote infeed, sourced from [81]). The selection of the transmission system including its generation rating and fault level data is based on a 'worst case' strategy and used NGESO's electricity ten-year statement [81], system operability framework [7] and the future energy scenarios [3] documents, with a particular transmission line being selected from the GB system due to the low fault levels in that area; however, as already mentioned, any line/fault infeed could be characterised easily by changing parameters.

6.4 Selection of protection relays

As clarified in Chapter 3, only distance protection has been selected due to its complexity and the altered behaviour of the *VI* waveform in converter-dominated power systems. In comparison to distance protection systems, the operating principles of differential and overcurrent protection are relatively more straightforward. However, future research is necessary to investigate the impact of converter-based energy sources

on all types of protection devices. Two distance relays (from two different manufacturers) have been tested in this study using secondary injection. The main protection schemes applied to lines within transmission networks are distance protection schemes and differential protection schemes. When compared with differential protection, which possesses absolute selectivity [56], distance protection is commonly arranged to protect multiple zones and requires a higher number of settings, with more complex settings and user input required when configuring. Their operating principles can be summarised as follows.

During network faults close to a distance relay, with the fault current being supplied by conventional generation sources, the current measured by the relay shall rise immediately and the corresponding voltage shall simultaneously drop. The sudden change in the measured data will trigger the relay's starting function to identify the faulted phase. Then the measured ratio of *V/I* shall indicate the distance between the relay and the faulted point. As a non-unit protection, the distance relay is configured to act to disconnect the fault within its primarily protected zone as quickly as possible, and act in a delayed manner when the fault is outside zone 1 as a backup function.

The setting of the relays in this study is displayed in Table 6-2.

Table 6-2 Setting of the distance relays

Operation characteristic	Quad
Zone 1 reach	80% of the protected line
Zone 1 response delay	0ms
Zone 2 reach	120% of the protected line
Zone 2 response delay	300ms

The relays' operation speed, in response to different fault types and locations with different generation sources supplying the fault current, will be tested and presented in detail in the next chapter.

6.5 Summary

This chapter has provided a complete and comprehensive overview and description of the testing system and methodology used to emulate different converter responses and inject the resulting waveforms directly into protection relays or relay models. This experimental setup operates in a "hardware in the loop" arrangement, where the relay responses are monitored and recorded.

The configuration and parameters of the modelled transmission system, along with the detailed testing arrangement, have been explained in great detail. Additionally, the selection of protection relays has been thoroughly discussed, ensuring the appropriate relays are utilized in the testing process.

By employing this testing system and methodology, it becomes possible to accurately assess the performance and behaviour of protection relays under various converter response scenarios. The recorded relay responses provide valuable data for evaluating the effectiveness of the protection schemes and further understanding the impact of converter-based energy sources on the overall system protection.

Chapter 7

Case studies

7.1 Introduction

This chapter presents detailed case studies aimed at systematically evaluating the impact of integrating converter-based generation sources on traditional distance protection relays. Four primary scenarios are introduced, encompassing the analysis of changing converter responses, fault locations and types, converter penetration levels, and varying remote infeed. Key findings are derived from the results, and corresponding solutions based on these findings are presented.

7.2 Scenario 1: impact of changing converter fault response

The relay responses to a fault (at a fixed location) with local infeed consisting of a SG only, and then consisting of converters only, and using a range of different converter response characteristics, are monitored and analysed in each scenario. Values for the initial delay, ramp rate and sustained fault levels have been selected based on a combination of evidence [60] [64], and through consultation with experienced engineers. As mentioned in Chapter 6, two distance protection relays (from different manufacturers that are commonly used in the GB transmission system) have been tested and are referred to as relay 1 and relay 2 in this thesis. Table 7-1 presents relay tripping times for the first scenario (testing ABC faults with balanced converter output). The system is 100% dominated by SG in case 1.1, and then 100% dominated by VSC converters in case 1.2-1.14.

T_1 and T_2 are the tripping times (from the inception of faults to the generation of the tripping signal) of relays 1 and 2.

As already explained in detail in Chapter 5, the converters are controlled to react to faults with a fixed initial delay, ramp rate and sustained fault level (note that the current dip function as mentioned in section 5.2 is not employed here as it is an additional option which can be applied when required). In case 1.2, the converter is configured to provide a relatively fast response (detailed parameters are shown in the table) and therefore it is selected to be a reference case as a starting point and will be used for comparison with other cases that consider different converter responses. In case 1.3-1.6, the initial delay is increased gradually from 2ms in case 1.2 up to 100 ms in case 1.6, while all other parameters remain fixed. In cases 1.7-1.10, the ramp rate is decreased from 1.5 GVA/cycle to 0.1 GVA/cycle while all other parameters stay the same (with the values as for case 1.2.). Similarly, in cases 1.11-1.14, the effects of changing the sustained fault level, with all other parameters remaining as per case 1.2., are studied.

As an extension of Table 7-1, results regarding solid faults applied at a location of 50 % of the distance of the transmission line are included for all scenarios and the results are presented in Figure 7-1 (for clarity, instances of non-operation are shown as white columns topped with a red X). The trip times for each relay are measured for four fault types with two converter response modes: for solid 3-phase ABC faults with balanced converter output (T_{ABC}); for solid AB faults with balanced converter output (T_{AB}); for solid AN faults with balanced converter output (T_{AN}); for solid AN faults with unbalanced converter output (using a dual sequence controller) (T_{AN}^{*}). The plots a), b)

and c) show the trip times for relay 1, while d), e) and f) are related to the operating times for relay 2.

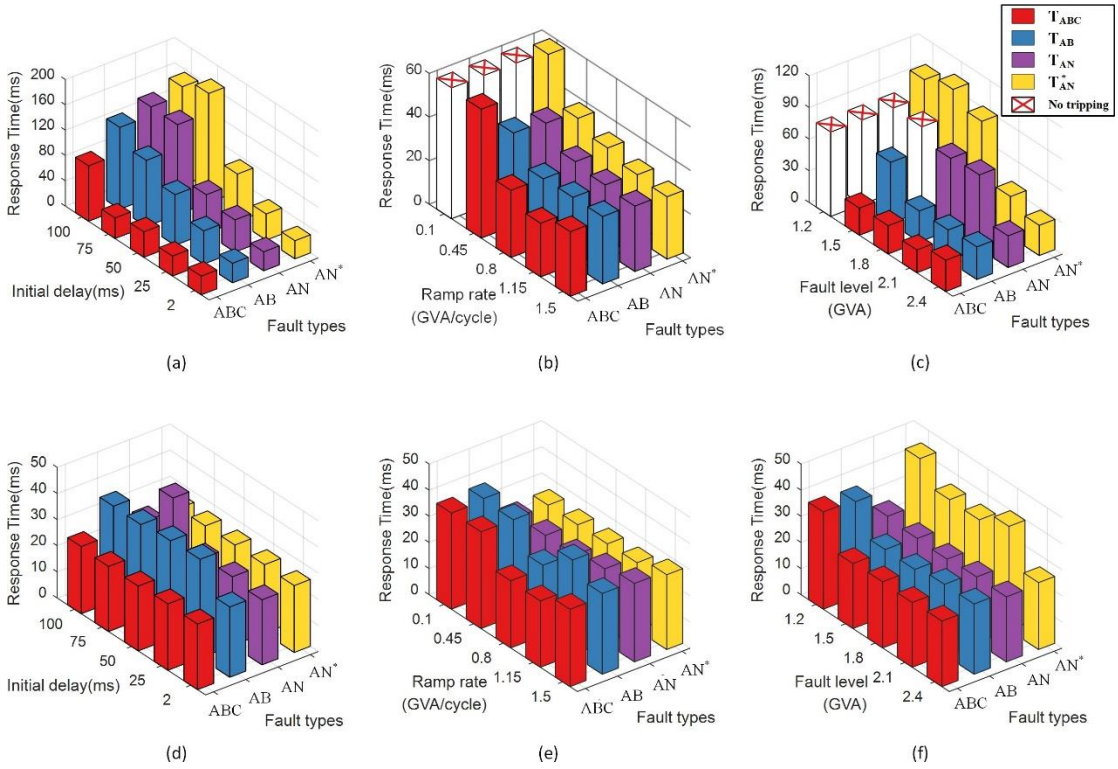

Figure 7-1 Impact of varying converter response parameters – Relay 1: a) initial response delay, b) fault current ramp rate, c) sustained fault level; – Relay 2: d) initial response delay, e) fault current ramp rate, f) sustained fault level

Table 7-1 Relay tripping times (ms) for three-phase solid faults

No.	Energy source	Initial delay	Ramp rate	Final fault level	Fault location			Fault location		
		(ms)	(GVA /cycle)	(GVA)	1%	50%	99%	1%	50%	99%
					T_{trip1} (ms)	T_{trip1} (ms)	T_{trip1} (ms)	T_{trip2} (ms)	T_{trip2} (ms)	T_{trip2} (ms)
1	SG only	\	\	4.7	18.3	19.2	328.4	20.9	22.4	344.8
2	VSC only	2	1.5	2.4	35.1	29.6	329	25.2	25.1	349.9
3	VSC only	25	1.5	2.4	59.7	31.6	329.5	25.4	25.4	365.8
4	VSC only	50	1.5	2.4	58.9	40.2	329.7	25.1	24.8	455.3
5	VSC only	75	1.5	2.4	86.6	32.5	328.6	25.3	24.9	334.8
6	VSC only	100	1.5	2.4	87.3	87.5	329.7	25.8	25.7	339.1
7	VSC only	2	1.15	2.4	37.4	24.6	322.9	25	25.4	335
8	VSC only	2	0.8	2.4	58.5	30.8	328.1	25	25.7	337.6
9	VSC only	2	0.45	2.4	67.2	59.1	356.9	37	37	335.8
10	VSC only	2	0.1	2.4	∞	∞	∞	37.6	36.8	334.7
11	VSC only	2	1.5	2.1	36.1	21.6	327.2	25.5	24.8	346
12	VSC only	2	1.5	1.8	34	26.8	327.1	25.2	25.3	339.8
13	VSC only	2	1.5	1.5	∞	25.7	327.9	25.5	24.9	343.9
14	VSC only	2	1.5	1.2	∞	∞	∞	37.7	37.2	339.8

In the above table, the cells with green highlighting indicate behaviour that is deemed to be acceptable, and those with amber highlighting indicate where the performance may be suspect or not ideal (but tripping is still achieved – perhaps with a delay – any delay of up to approximately 20 ms from the expected time is deemed to be amber) and those on red indicate examples of incorrect and undesirable operation (or non-operation). In addition, the following general and specific conclusions have been drawn based on Table 7-1 and Figure 7-1:

1) For the different relays (with the same settings), certain trip times vary. For the benchmark case study (SG fault infeed), both relays operate similarly with a delay of approximately 20 ms (as shown in case 1.1 from Table 7-1). However, when converters are introduced, the relays' performance may be compromised to an extent in the majority of cases. Figure 7-1 demonstrates that the operation time of both relays can be impacted seriously in some cases (non-operation of relay 1 in Figure 7-1.b-c and a 20ms delay in the operation time of relay 2 in Figure 7-1.e).

2) When the system is supplied by converters with relatively fast fault responses and relatively high fault currents, the trip time of relay 1 can be delayed by up to 150 ms (Figure 7-1.a) compared to the benchmark case (SG fault infeed). When the ramp rate and sustained fault level magnitude are decreased beyond certain values, relays may not trip at all (Figure 7-1.b-c). The overall performance of relay 2 is not affected as much as that of relay 1, but it is still compromised as its operation is delayed in most cases (Figure 7-1.d-e).

3) The contribution of negative sequence currents from converters (which is only possible for some converters and is dependent on the controller) can lessen the

negative impact on relay performance. As shown in Figure 7-1.b and Figure 7-1.c, without negative sequence current injection (shown as red, blue and purple columns), relay 1 can no longer operate when the VSC is not providing current with sufficient ramp rate/ sustained level. It is clear that, in general, there are many instances of delayed (and in some cases non-) operation.

The The findings reveal that the introduction of converters has an impact on the performance of relays, but this impact varies depending on the internal algorithms of the relays. The detection of faults is closely tied to the starting system of the relays, and different starting systems result in different performances. In converter-dominated systems, factors such as fault level, initial delay, and ramp-up rate of fault current from VSC sources significantly influence the performance of traditional distance protection schemes. The ability of VSC to provide sufficient negative sequence current also has a significant impact on relay performance. Therefore, it is concluded that solutions to mitigate these issues can be pursued from both the VSC side and the relay side. This may involve implementing faster responses from VSCs and modifying fault detection/calculation logic blocks in relays.

7.3 Scenario 2: impact of changing fault locations

The purpose of this scenario is to investigate relay performance to different fault locations with the local infeed consisting of solely SG then with converters with different response characteristics (“strong” and “weak” converters VSC_1 and VSC_2 as defined below).

The two somewhat extreme examples of converter response were chosen to illustrate protection performance under markedly different and presumed "grid code" stipulations that may dictate the fault responses of the converters. VSC1 has a relatively low response delay (2 ms), a high ramp rate (1.4 GVA/cycle) and a high level of sustained fault current (2.4 GVA). VSC2 has a long response delay (50 ms), a low ramp rate (0.45 GVA/cycle) and a low level of sustained fault current (1.5 GVA). As for scenario 1, the relays' responses are tested for four fault types. The following findings are summarised based on the results presented in Figure 7-2 and Figure 7-3:

1) Three-phase solid faults: As shown in Figure 7-2.a-b, the performance of relay 1 is acceptable as the zone 1 reach boundary is around 80% of the line length, as expected when synchronous machines supply fault current. When the system is supplied by VSC_1 ("strong"), zone 1 reach remains relatively unaffected. When supplied by VSC_2 ("weak"), the operation of the relay is impacted and a reached error of almost 10% is introduced. The overall performance of relay 2 is similar to relay 1. The relay's performance is acceptable when synchronous machines or VSC_1 supply fault current. However, when VSC_2 is used, the zone 1 reach is shortened by at least 5%.

2) Phase-phase solid faults: From Figure 7-2.c-d, the performance of relay 1 is acceptable when either synchronous machines or VSCs provide the local infeed. However, for relay 2, zone 1 reach is extended by at least 7% when the system is supplied by VSC_1 (which is believed to be more "protection-friendly"). This is most likely due to the balanced fault current from the converter, discussed further in the next scenario.

3) Phase-to-ground solid faults: Figure 7-3 illustrates results for phase-to-ground faults. In this case, the non-operation points are demonstrated as faults which are not responded to in 500 ms.

4) When the converter provides a balanced fault current (demonstrated in Figure 7-3.a-b), it can be seen that when the system is supplied by VSC_1, zone 1 reach is acceptable for both relays. When supplied by VSC_2, relay 1 loses its ability to detect zone 2 faults. In the meantime, relay 2 suffers from zone 1 overreach.

5) However, when the converter is capable of producing negative sequence current (Figure 7-3.c-d), both relays' performance is improved. Relay 1 is now able to detect all faults outside zone 1, meanwhile, the overreach of relay 2 is reduced (to approximately 5 % in this case). The ability to supply unbalanced output currents can clearly benefit the performance of the relays.

Similar to the previous scenario, it can be concluded that the introduction of VSC sources will have a significant impact on the performance of traditional distance protection systems. In the studied cases, it is obvious that not only the fault detection systems but also the fault calculation and locating systems are affected, and the performance varies among different relay manufacturers. The findings matched the previous studies reviewed in Chapter 4, as the seen impedance from the relay shall be impacted by the introduction of converters due to the changed system behaviours. A similar conclusion can be drawn that mitigations can be implemented from both the VSC and relay perspectives. This includes the VSC providing faster responses of fault current and unbalanced current during unbalanced system conditions, as well as relays modifying their internal algorithms to accommodate the changed system behaviours.

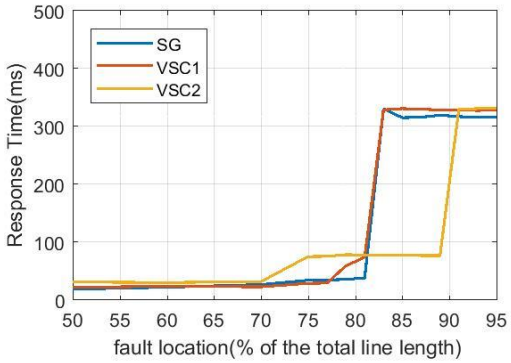

(a) Relay 1: A-B-C faults

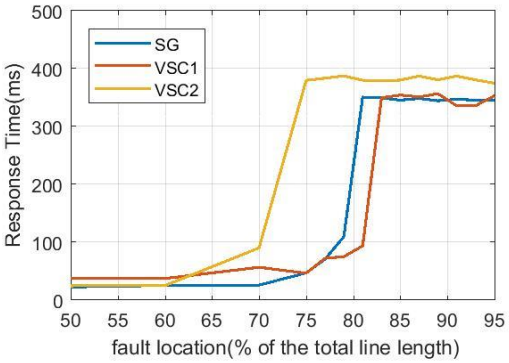

(b) Relay 2: A-B-C faults

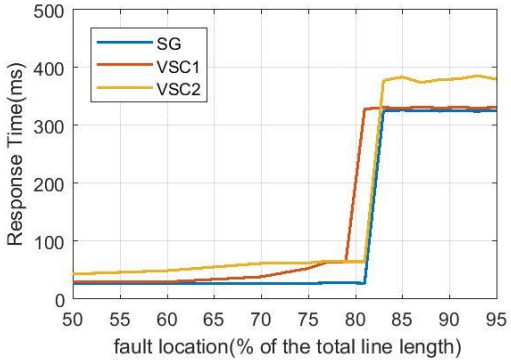

(c) Relay 1: A-B faults

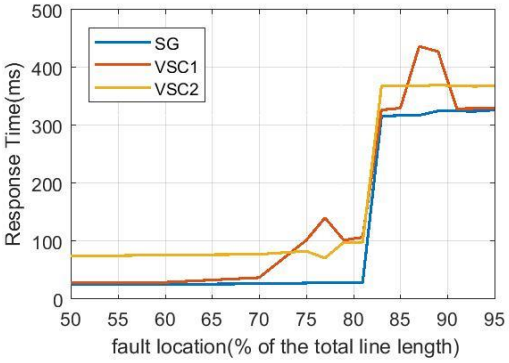

(d) Relay 2: A-B faults

Figure 7-2 Relay tripping time against fault location (% of the total line length

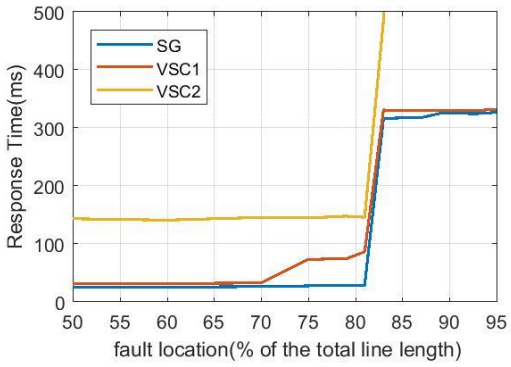

(a) Relay 1: A-N faults

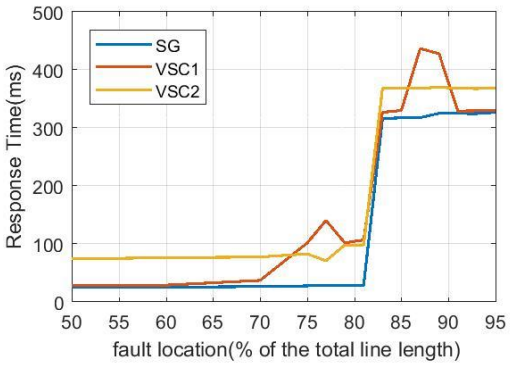

(b) Relay 2: A-N faults

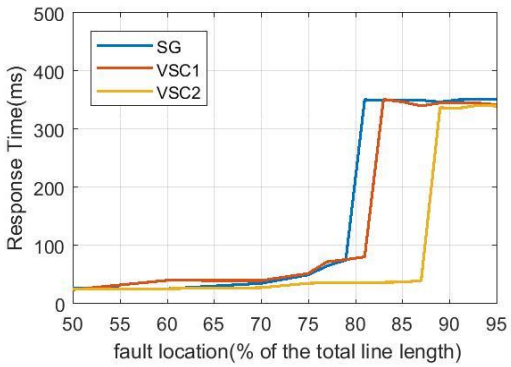

(c) Relay 1: A-N faults (input 2)

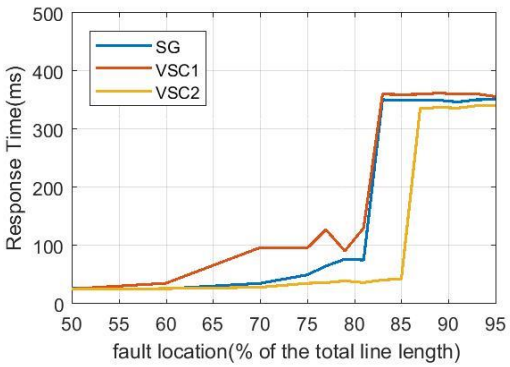

(d) Relay 2: A-N faults (input 2)

Figure 7-3 Relay tripping time against fault location (% of the total line length)

7.4 Scenario 3: impact of changing converter penetration level

Investigations have been performed to investigate the "tipping point" where the performance of relays shall be significantly compromised by the introduction of converters into the "mix" of generators' supply fault currents. In this scenario, relay responses to different converter *PL* using VSC_1 and VSC_2 are investigated.

In the four sub-scenarios, both converters' *PL* range from 0 % to 100 % in steps of 25 %. Selected results are presented in Table 7-2. The following figure is provided as an example to demonstrate how the penetration level shall impact the performance of the relays in this study.

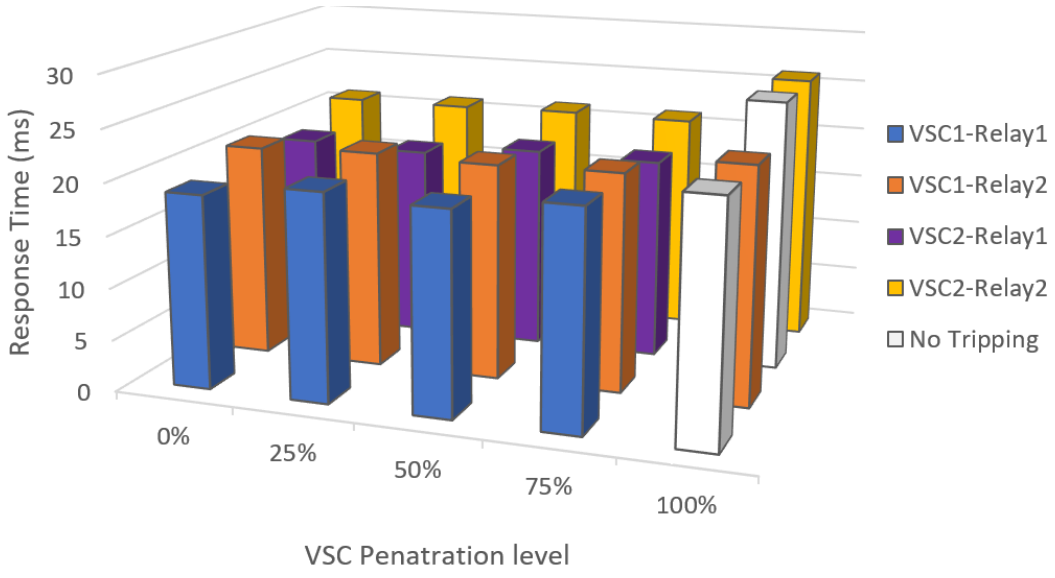

Figure 7-4 Impact of varying penetration level at fault location of 50% for phase-ground fault

From Figure 7-4 it can be seen that the relays' trip times are not significantly affected when the converter's *PL* is lower than 75 %. A similar conclusion can be made by examining the entire set of data in each sub-scenarios, when the protection performance can hardly be impacted when converter's *PL* is lower than 75 %

This shows that even a relatively small amount of SG may assist in minimising the impact of converters upon protection operation (which may show promise for the introduction of synchronous compensators, presently being trialled via the PHOENEX project in GB [82]).

Table 7-2 Relay tripping times (ms) for phase-ground solid faults

No.	Penetration Level	Fault location			Fault location		
		1%	50%	99%	1%	50%	99%
		T_{trip1} (ms)	T_{trip1} (ms)	T_{trip1} (ms)	T_{trip2} (ms)	T_{trip2} (ms)	T_{trip2} (ms)
1	0% - VSC1	18.7	18.6	319.8	20.6	25.8	335.8
2	25% - VSC1	20	20.5	322.5	21	25.6	345
3	50%- VSC1	19.5	22.5	324.9	20.8	26.3	336.2
4	75%- VSC1	20.8	23	323.9	21	37	340
5	100%- VSC1	∞	∞	∞	22.7	50	341.2
6	0% - VSC2	18.9	18.6	319.8	21.1	26	342.5
7	25%- VSC2	18.6	20	312.2	21.1	25.7	338
8	50%- VSC2	19.6	21.2	325.2	21.3	26.3	335.3
9	75%- VSC2	19.4	23	325.8	21.2	26.1	336.3
10	100%- VSC2	∞	∞	∞	26.1	26.2	338.2

7.5 Scenario 4: impact of varying remote infeed

Additional tests were also performed to investigate how the relay at the local end of the line (with converter infeed) might be affected by varying the remote infeed fault level. In this case, the local infeed shall be set as 100% dominated by synchronous machines, VSC1 and VSC2 in order to compare. The fault location, fault type and penetration level of each source are fixed at a certain value while the remote end fault level is varied from 20 to 1 GVA. Selected examples of results can be found in Table 7-3

Results demonstrate that for most cases (other than when the local end is very weak) the performance of relays is not affected by the remote end infeed and behaves similarly for all cases as before (with issues still introduced by the converters as outlined previously).

Table 7-3 Relay tripping times (ms) for phase-ground solid faults

No.	Energy source	Remote end infeed (GVA)	Fault location			Fault location		
			1%	50%	99%	1%	50%	99%
			T_{trip1} (ms)	T_{trip1} (ms)	T_{trip1} (ms)	T_{trip2} (ms)	T_{trip2} (ms)	T_{trip2} (ms)
1	SG only	20	18.7	19.5	319.9	25	25.7	362.4
2	SG only	15	18.7	20.2	321.2	25.6	25.9	356.1
3	SG only	10	18.9	20.8	319.7	25.6	25.8	464.7
4	SG only	5	18.7	20.4	320.2	25.5	25.3	362.7
5	SG only	1	39.3	90.7	∞	21.1	26.7	343.8
6	VSC1	20	27.9	28.9	327.5	25.2	26	343.7
7	VSC1	15	28.4	28.1	329.5	25.4	26.1	339.6
8	VSC1	10	27.3	28.3	329.5	25.8	26.1	341.9
9	VSC1	5	26.2	25.4	332.1	25.3	25	340.8
10	VSC1	1	∞	∞	∞	21.8	25.4	399.8
11	VSC2	20	87.1	86.4	380	25.2	25.8	341.3
12	VSC2	15	87.5	86.7	379.8	26.1	26	337.2
13	VSC2	10	87.5	80	376.8	25.5	25.5	334.8
14	VSC2	5	83.7	79.2	375.9	22.2	25.2	335.7
15	VSC2	1	123.3	123.1	610.4	22.3	25.2	400

7.6 Possible solutions

7.6.1 Solutions from a protection relaying perspective

It has been shown already on multiple occasions that different relays from different manufacturers perform differently even though they have identical settings. According to the relay user guides, it appears that the main difference lies in the initial fault detection or “starter” functions. Relay 1 has a system based solely on measured current, while Relay 2 has a starter that measures both current and voltage. The current-based starter is adequate for traditional strong power systems, but may not be adequate in future, as there may not be an “impulse” of current at fault inception to initiate relay fault detection (and subsequent tripping) functions.

Accordingly, for converter-dominated power systems, relays may need to use alternative starting systems based on both voltage and current.

In addition, the main protection function algorithms of relays also affect trip times according to the nature of the fault current provided by sources. Emerging protection technologies such as travelling wave protection devices can also be considered viable alternatives which require further investigation. As stated in Chapter 2, a standard relay testing system regime to emulate worst-case scenarios can be developed and may be viewed as necessary by system operators to prove that protection will operate under all scenarios in future power systems.

7.6.2 Solutions from a converter perspective

Along with the requirements specified in Grid codes, more specific detail can be achieved and guided by testing, using arrangements similar to those used in this research (indeed there is ongoing and related work concerned with this being conducted at the University of Strathclyde presently). Provision of unbalanced fault currents when appropriate has also been shown to assist in ensuring adequate relay performance. Some converters only provide balanced currents (regardless of the impedance of the system being supplied) and this may require to be changed in future. For instance, converters operating with a "Class 1" Grid-Forming performance as per [16] can provide an "instant" fault current response [1] and balanced or unbalanced fault current as required [83].

As for the worst scenarios with relays that can be severely impacted, it can be reasoned that the protection system can operate slower than 30 ms when the converter's fault contribution even with a 2.1 p.u. based on the worst case presented or the converter fault response is delayed by more than 25ms. These numbers may be interpreted as being quite radical and perhaps difficult/costly to achieve by converter manufacturers. However, the situation can also be improved by using relays applied with enhanced fault detection systems and/or operating algorithms. There remains ongoing research that is investigating solutions for future converter-dominated power systems, including injecting specific harmonic components from the converters when faults are detected to assist other devices in identifying the presence and location of faults [84] and using the synchronous compensators to provide a contribution of fault current to enable more conventional protection systems to remain fit-for-purpose [85].

7.7 Summary

In this chapter, the model and hardware testing platform setup mentioned earlier is utilised to conduct investigations into the impact of different types of converters on protection performance. The objective is to assess how different converter responses, as well as a combination of converter and synchronous sources supplying fault current, affect the overall performance of protection systems. A range of systematic tests are performed to evaluate network protection performance under various scenarios. These scenarios include different fault locations and types, such as single-phase, phase-to-phase, and three-phase faults.

The results have demonstrated that relays, even when set up with identical operating principles and settings, exhibit varied behaviour and are subject to different forms of compromise. Findings have been presented that integration of converters that lack the ability to provide "fast" ramping rates and "high" sustained maximum output current during faults poses a high risk of compromising relay performance. These compromises may manifest as delayed relay responses, compromised zone discrimination, and unexpected inoperation under specific incidents. As an example of the issues that may be experienced, the following excerpt of results is highlighted for illustrative purposes:

As an example of the issues that may be experienced, the following excerpt of results is highlighted for illustrative purposes:

- Though identical settings are applied, the performance of relays from different manufacturers is often different. Examples to provide evidence of this can be

found in Table A - 1 and by comparing the relay tripping times recorded in case 5 from relay 1 and relay 2.

- When the system is dominated by converters, the response times of the relay can be delayed by up to 131.1 ms compared with the responses in the synchronous machine-based cases (example data can be found in Table A - 4 and by comparing cases 1 and 5).

- When the ramp rate and the final fault level are decreased to at or below certain values, the relays will not trip at all. Detailed data to support this finding can be found in Table A - 1 and by observing cases 1, 9 and 13.

- The contribution of negative sequence currents from converters can generally improve the performance of relays in the presence of unbalanced faults. This conclusion is supported by an analysis of the recorded relay tripping times for case 9 from Table A - 3 and Table A - 4.

- When the system is supplied solely by VSCs, the zone 1 reach for solid ABC faults is affected. This conclusion is supported by observing the recorded data from Table B - 1.

Based on the analysis of experimental results and findings, a range of suggested solutions have been proposed, encompassing both protection relaying and converter perspectives. Future research works focused on upgrading fault detection algorithms in relays to account for the changed system behaviours introduced by converters can be performed to address the challenges arising from converter-based energy sources, together with the utilisation of emerging technologies such as travelling wave protection systems. Collaboration with converter manufacturers is recommended to

encourage the development of "protection-friendly" fault responses, such as providing fast and high-magnitude of fault currents,

Chapter 8

Conclusions and Future Work

8.1 Conclusions

This thesis has presented a systematic methodology for assessing power system protection performance in future scenarios where HVDC and other converter-interfaced generation is widely used within systems, which will significantly change the behaviour of power systems during faults (and therefore potentially challenge the protection systems in terms of properly identifying and responding to faults). The proposed approach utilises a flexible and configurable model and hardware-in-the-loop environment that has been developed.

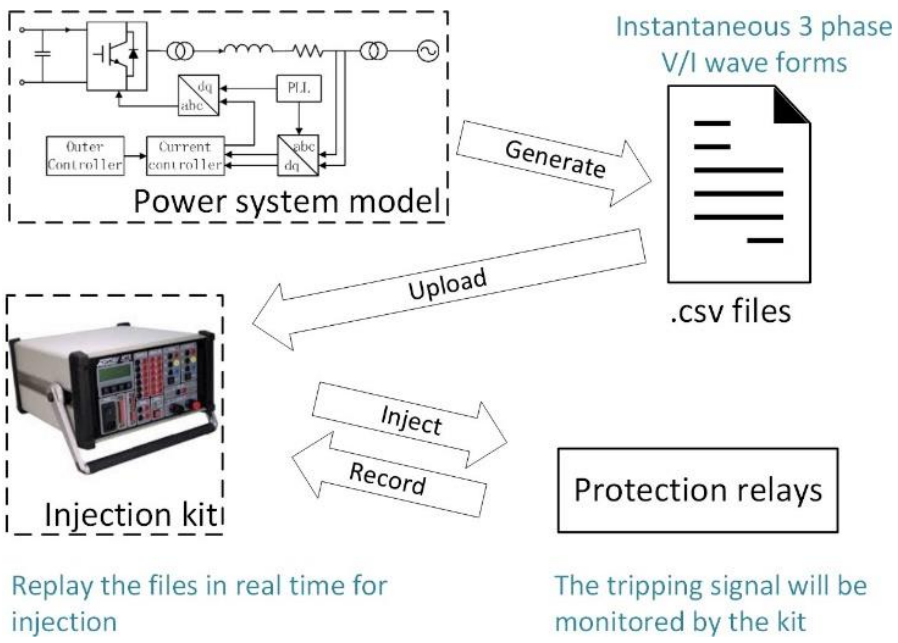

Figure 8-1 Simulation-testing environment

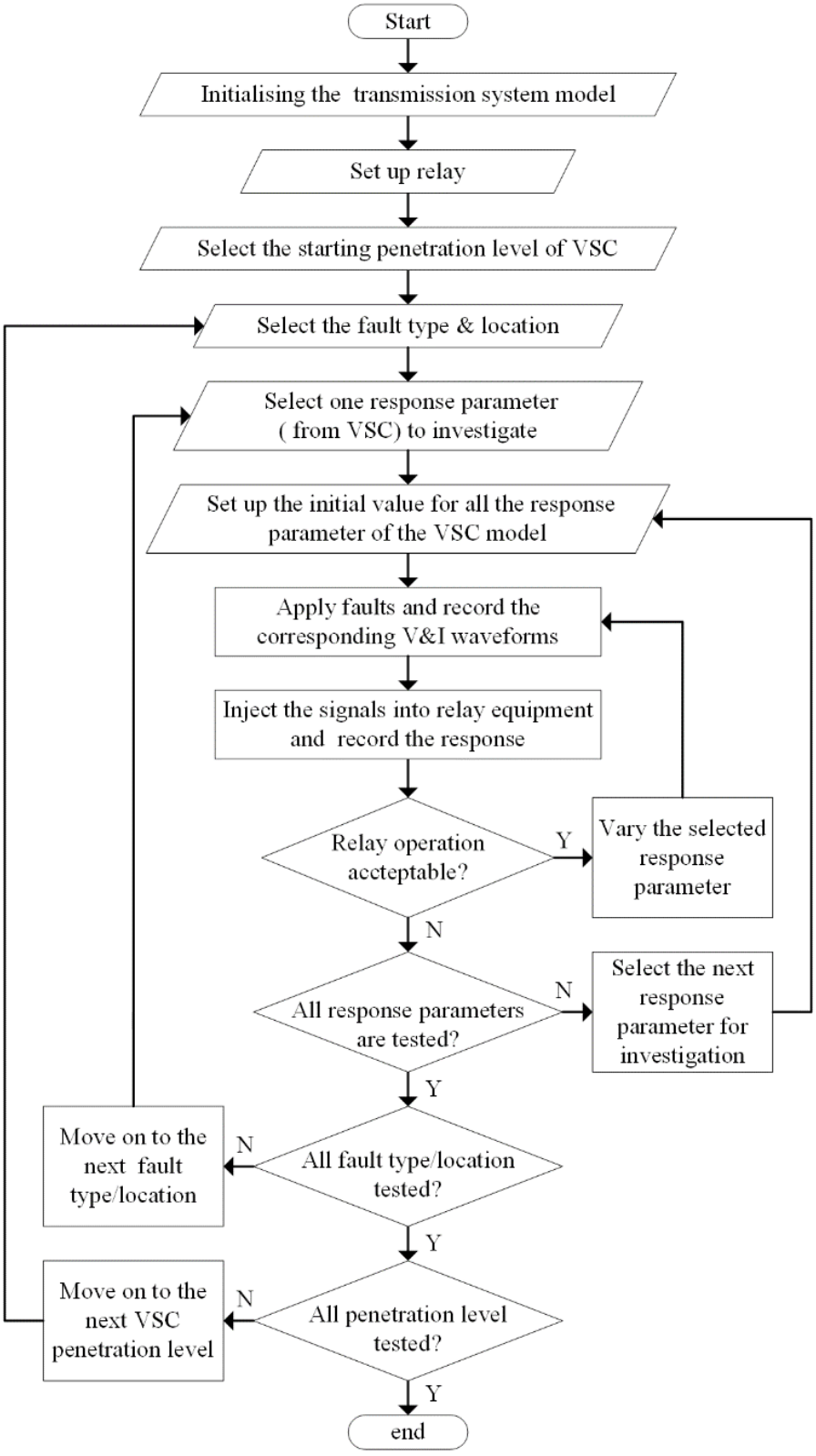

Figure 8-2 Relay testing methodology

This environment (as presented in Figure 8-1) allows several characteristics of the fault response of converters (e.g. the delay in responding initially to a fault, the magnitude of any "dip" in current/voltage output following the fault inception and accompanying system voltage collapse, the rate of increase in output current to sustained maximum levels, the maximum level itself, etc.) to be modified and can be used in conjunction with conventional power system models to vary the "mix", or penetration, of all generation that is feeding into the fault to represent scenarios with varying overall penetration levels of converter-interfaced generation as a proportion of the overall generation mix encompassing synchronous and non-synchronous (typically converter-interfaced) generation technologies.

This environment has been used to conduct a comprehensive set of tests exploring distance protection response under various fault levels and a range of anticipated converter-interfaced infeed and penetration scenarios (the testing methodology is presented in Figure 8-2). Varying levels of converter penetration, and variations in the aforementioned response characteristics of the converters to faults, have been simulated and the hardware testing platform and real-time simulation facility have been employed to conduct experiments whereby the simulated data has been injected into actual commercially available protection relays using both voltage and current injection. The results have confirmed concerns related to protection system performance caused by the increased utilisation of converter-interfaced generation and interconnectors.

It has been demonstrated that different relays, with the same operating principles and settings, behave differently and are compromised in a number of different ways. It can be stated with a high degree of confidence that the introduction of converters that are incapable of contributing "fast" (ramping rate) and "high" (sustained maximum output

current) current during faults introduces a high risk of compromising the performance of relays to some extent, including delayed relay response, loss of zone discrimination and, in some cases, a complete loss of ability to detect certain faults – all details of the various tests and associated results are contained in Chapter 7 and Appendix A-D.

Furthermore, with specific reference to the relays that were tested (which represent relays commonly used on the GB transmission system), the reliance on impulse starters for some distance protection relays and the observed consequent inadequacies of performance leads to a desire to investigate the performance of unit protection relays that are similarly reliant upon impulse starters.

8.2 Further work

As this work has resulted in the creation of a robust, flexible and realistic simulation and hardware injection facility, performance testing regarding a wide range of protection relays should be conducted in the future as outlined below:

1) Comprehensive studies (using injection and the developed system/converter models) of a range of faults/infeeds/converter mixes with a wide range of protection relays including distance, differential, overcurrent and emerging technologies such as travelling wave protection should be undertaken. These studies could be simple/generic in nature, or the system could be set up to represent specific elements of the transmission system (for example areas where large installations of renewable generation are planned to be connected in the future) in order to investigate general or system and relay-specific performance and issues. Ongoing work at the University of Strathclyde is presently being conducted in this respect with transmission and

renewable energy companies where a total of seven different relay types from specific manufacturers are being tested to ascertain their future performance and suitability for converter-dominated power systems.

2) Development of a standard testing/commissioning method (and possibly inputting to an industry standard) for evaluating the performance of protection relays in a future low-carbon power system scenario.

3) Work in conjunction with the manufacturers of converter devices to establish the most "protection-friendly" responses to faults, and how these might be achieved (e.g. to use synchronous condensers to perhaps "boost" the output from converters on the ac side when faults are being experienced [86]).

4) Considering the performance and response of future converter-dominated power systems (which may have very much lower fault levels and response characteristics during faults), develop novel protection algorithms and schemes that can recognise faults on such future systems using different criteria (and perhaps with a relaxation of operating times) – this is a longer-term piece of work, but still worth considering when power systems may change beyond recognition in terms of their fault behaviour and stability characteristics (which are largely based around synchronous machine-dominated systems, with high fault levels and stability constraints based around the electro-mechanical nature of the machines throughout the system – if synchronous machines for generation were to decrease markedly in number, the requirement for protection may change and "traditional" protection schemes may no longer be required).

References

[1] ENTSO-E, ‘Fault current contribution from PPMS & HVDC’, 2016. [Online]. Available: https://eepublicdownloads.entsoe.eu/clean-documents/Network%20codes%20documents/NC%20RfG/161116_IGD_Fault%20Current%20Contribution%20from%20PPMs%20%20HVDC_for%20consultation_for%20publication.pdf

[2] V. Telukunta, J. Pradhan, A. Agrawal, M. Singh, and S. G. Srivani, ‘Protection challenges under bulk penetration of renewable energy resources in power systems: A review’, *CSEE Journal of Power and Energy Systems*, vol. 3, no. 4, pp. 365–379, Dec. 2017, doi: 10.17775/CSEEJPES.2017.00030.

[3] National Grid, ‘UK Future Energy Scenarios 2020’, National Grid, 2018.

[4] H. Urdal, R. Ierna, J. Zhu, C. Ivanov, A. Dahresobh, and D. Rostom, ‘System strength considerations in a converter dominated power system’, *IET Renewable Power Generation*, vol. 9, no. 1, pp. 10–17, 2015, doi: 10.1049/iet-rpg.2014.0199.

[5] National Grid ESO, ‘Zero carbon operation of Great Britain’s electricity system by 2025 | National Grid ESO’, Apr. 2019. Accessed: Apr. 05, 2019. [Online]. Available: https://www.nationalgrideso.com/news/zero-carbon-operation-great-britains-electricity-system-2025

[6] R. Li, C. Booth, A. Dyśko, A. Roscoe, H. Urdal, and J. Zhu, ‘Protection challenges in future converter dominated power systems: Demonstration through simulation and hardware tests’, in *International Conference on Renewable Power Generation (RPG 2015)*, Oct. 2015, pp. 1–6. doi: 10.1049/cp.2015.0392.

[7] National Grid, ‘System Operability Framework’, National Grid, 2016.

[8] ENTSO-E, ‘Network Code on HVDC Connections’, ENTSO-E, Aug. 2016.

[9] R. Li *et al.*, ‘Impact of low (zero) carbon power systems on power system protection: a new evaluation approach based on a flexible modelling and hardware testing platform’, *IET Renewable Power Generation*, vol. 14, no. 5, pp. 906–913, 2020, doi: https://doi.org/10.1049/iet-rpg.2019.0518.

[10] ‘Electrical Power System Essentials, 2nd Edition | Wiley’, *Wiley.com*. https://www.wiley.com/en-gr/Electrical+Power+System+Essentials%2C+2nd+Edition-p-9781118803479 (accessed Apr. 15, 2021).

[11] K. Rahimi and P. Famouri, ‘Performance enhancement of automatic generation control for a multi-area power system in the presence of communication delay’, in *2013 North American Power Symposium (NAPS)*, Sep. 2013, pp. 1–6. doi: 10.1109/NAPS.2013.6666928.

[12] P. Kundur, ‘Power system stability’, *Power system stability and control*, pp. 7–1, 2007.

[13] N. Tleis, ‘1 - Introduction to power system faults’, in *Power Systems Modelling and Fault Analysis (Second Edition)*, N. Tleis, Ed., Academic Press, 2019, pp. 1–39. doi: 10.1016/B978-0-12-815117-4.00001-1.

[14] ENTSO-E, ‘Network Code on Requirements for Grid Connection applicable to all Generators’, ENTSO-E, 2016.

[15] National Grid, ‘The Grid Code’, National Grid, 2021.

[16] ENTSO-E, ‘High Penetration of Power Electronic Interfaced Power Sources (HPoPEIPS)’, ENTSO-E, Mar. 2017.

[17] ‘Network Code on Requirements for Grid Connection applicable to all Generators’. ENTSO-E, Mar. 2013. [Online]. Available: http://networkcodes.entsoe.eu/wp-content/uploads/2013/08/130308_Final_Version_NC_RfG1.pdf

[18] J. D. Glover, M. S. Sarma, and T. Overbye, *Power System Analysis & Design, SI Version*. Cengage Learning, 2012.

[19] T. G. Wilson, ‘The evolution of power electronics’, *IEEE Transactions on Power electronics*, vol. 15, no. 3, pp. 439–446, 2000.

[20] D. C. Prince, ‘Mercury arc rectifier phenomena’, *Journal of the A.I.E.E.*, vol. 46, no. 7, pp. 667–674, Jul. 1927, doi: 10.1109/JAIEE.1927.6535536.

[21] R. G. Arns, ‘The other transistor: early history of the metal-oxide semiconductor field-effect transistor’, *Engineering Science & Education Journal*, vol. 7, no. 5, pp. 233-240(7), Oct. 1998.

[22] O. Hashimoto, H. Kirihata, M. Watanabe, A. Nishiura, and S. Tagami, ‘Turn-On and Turn-Off Characteristics of a 4.5-kV 3000-A Gate Turn-Off Thyristor’, *IEEE Transactions on Industry Applications*, vol. IA-22, no. 3, pp. 478–482, May 1986, doi: 10.1109/TIA.1986.4504746.

[23] N. Iwamuro and T. Laska, ‘IGBT History, State-of-the-Art, and Future Prospects’, *IEEE Transactions on Electron Devices*, vol. 64, no. 3, pp. 741–752, Mar. 2017, doi: 10.1109/TED.2017.2654599.

[24] M. Kitagawa, I. Omura, S. Hasegawa, T. Inoue, and A. Nakagawa, ‘A 4500 V injection enhanced insulated gate bipolar transistor (IEGT) operating in a mode similar to a thyristor’, in *Proceedings of IEEE International Electron Devices Meeting*, Dec. 1993, pp. 679–682. doi: 10.1109/IEDM.1993.347221.

[25] P. Steimer, O. Apeldoorn, and E. Carroll, ‘IGCT devices-applications and future opportunities’, in *2000 Power Engineering Society Summer Meeting (Cat. No.00CH37134)*, 2000, pp. 1223–1228 vol. 2. doi: 10.1109/PESS.2000.867555.

[26] B. Wu and M. Narimani, *High-Power Converters and AC Drives*. John Wiley & Sons, 2017.

[27] A. Alassi, S. Bañales, O. Ellabban, G. Adam, and C. MacIver, ‘HVDC Transmission: Technology Review, Market Trends and Future Outlook’, *Renewable and Sustainable Energy Reviews*, vol. 112, pp. 530–554, Sep. 2019, doi: 10.1016/j.rser.2019.04.062.

[28] D. Jovcic, *High Voltage Direct Current Transmission: Converters, Systems and DC Grids*. John Wiley & Sons, 2019.

[29] ‘Offshore Transmission Techonology’. Entso-E, Nov. 24, 2011. Accessed: Oct. 09, 2014. [Online]. Available: https://www.entsoe.eu/fileadmin/user_upload/_library/publications/entsoe/SDC/European_offshore_grid_-_Offshore_Technology_-_FINALversion.pdf

[30] Z. Wei, W. Fang, and J. Liu, ‘Variable Extinction Angle Control Strategy Based on Virtual Resistance to Mitigate Commutation Failures in HVDC System’, *IEEE Access*, vol. 8, pp. 93692–93704, 2020, doi: 10.1109/ACCESS.2020.2994245.

[31] N. Mohan, T. M. Undeland, and W. P. Robbins, *Power electronics: converters, applications, and design*. John wiley & sons, 2003.

[32] O. E. Oni, I. E. Davidson, and K. N. I. Mbangula, ‘A review of LCC-HVDC and VSC-HVDC technologies and applications’, in *2016 IEEE 16th International Conference on Environment and Electrical Engineering (EEEIC)*, Jun. 2016, pp. 1–7. doi: 10.1109/EEEIC.2016.7555677.

[33] R. L. Sellick and M. Åkerberg, ‘Comparison of HVDC Light (VSC) and HVDC Classic (LCC) site aspects, for a 500MW 400kV HVDC transmission scheme’, in *10th IET International Conference on AC and DC Power Transmission (ACDC 2012)*, Dec. 2012, pp. 1–6. doi: 10.1049/cp.2012.1945.

[34] N. Flourentzou, V. G. Agelidis, and G. D. Demetriades, ‘VSC-Based HVDC Power Transmission Systems: An Overview’, *IEEE Transactions on Power Electronics*, vol. 24, no. 3, pp. 592–602, Mar. 2009, doi: 10.1109/TPEL.2008.2008441.

[35] S. Ji, Z. Zhang, and F. Wang, ‘Overview of high voltage sic power semiconductor devices: development and application’, *CES Transactions on Electrical Machines and Systems*, vol. 1, no. 3, pp. 254–264, Sep. 2017, doi: 10.23919/TEMS.2017.8086104.

[36] J. M. Maza-Ortega, E. Acha, S. García, and A. Gómez-Expósito, ‘Overview of power electronics technology and applications in power generation transmission and distribution’, *Journal of Modern Power Systems and Clean Energy*, vol. 5, no. 4, pp. 499–514, Jul. 2017, doi: 10.1007/s40565-017-0308-x.

[37] R. Li, C. D. Booth, A. Dysko, A. J. Roscoe, and J. Zhu, ‘Development of models to study VSC response to AC system faults and the potential impact on network protection’, in *Power Engineering Conference (UPEC), 2014 49th International Universities*, Sep. 2014, pp. 1–6. doi: 10.1109/UPEC.2014.6934696.

[38] J. Zhu, C. D. Booth, G. P. Adam, A. J. Roscoe, and C. G. Bright, ‘Inertia Emulation Control Strategy for VSC-HVDC Transmission Systems’, *IEEE Transactions on Power Systems*, vol. 28, no. 2, pp. 1277–1287, May 2013, doi: 10.1109/TPWRS.2012.2213101.

[39] T. Qoria and X. Guillaud, ‘Chapter 8 - Control of power electronics-driven power sources’, in *Converter-Based Dynamics and Control of Modern Power Systems*, A. Monti, F. Milano, E. Bompard, and X. Guillaud, Eds., Academic Press, 2021, pp. 193–234. doi: 10.1016/B978-0-12-818491-2.00008-0.

[40] D. Liu, Q. Hong, M. A. U. Khan, A. Dyśko, A. Egea Alvarez, and C. Booth, ‘Evaluation of Grid-Forming Converter’s impact on distance protection performance: The 16th International Conference on Developments in Power

System Protection', Mar. 2022. Accessed: May 03, 2022. [Online]. Available: https://dpsp.theiet.org/

[41] M. G. Taul, X. Wang, P. Davari, and F. Blaabjerg, 'Current Limiting Control With Enhanced Dynamics of Grid-Forming Converters During Fault Conditions', *IEEE Journal of Emerging and Selected Topics in Power Electronics*, vol. 8, no. 2, pp. 1062–1073, Jun. 2020, doi: 10.1109/JESTPE.2019.2931477.

[42] L. R. Almobasher and I. O. A. Habiballah, 'Review of Power System Faults', *International Journal of Engineering Research & Technology*, vol. 9, no. 11, Nov. 2020, Accessed: Apr. 09, 2021. [Online]. Available: https://www.ijert.org/research/review-of-power-system-faults-IJERTV9IS110036.pdf, https://www.ijert.org/review-of-power-system-faults

[43] 'IEEE Recommended Practice for Protection and Coordination of Industrial and Commercial Power Systems (IEEE Buff Book)', *IEEE Std 242-2001 (Revision of IEEE Std 242-1986) [IEEE Buff Book]*, pp. 1–710, Dec. 2001, doi: 10.1109/IEEESTD.2001.93369.

[44] Y. G. Paithankar and S. R. Bhide, *Fundamentals of Power System Protection*. PHI Learning Pvt. Ltd., 2013.

[45] 'Electricity Ten Year Statement 2020', National Grid ESO, 2020. [Online]. Available: https://www.nationalgrideso.com/research-publications/etys/archive

[46] J. L. Blackburn and T. J. Domin, *Protective relaying: principles and applications*. CRC press, 2015.

[47] IEC 61869-2: 2012, 'Instrument Transformers—Part 2: Additional Requirements for Current Transformers'. International Standardization Organization Geneva, Switzerland, 2012.

[48] R. E. Mackiewicz, 'Overview of IEC 61850 and benefits', in *2006 IEEE Power Engineering Society General Meeting*, Jun. 2006, p. 8 pp.-. doi: 10.1109/PES.2006.1709546.

[49] E. O. Schweitzer, K. Behrendt, T. Lee, and D. A. Tziouvaras, 'Digital communications for power system protection: security, availability, and speed', pp. 94–97, Jan. 2001, doi: 10.1049/cp:20010108.

[50] M. Adamiak and M. Redfern, 'Communications systems for protective relaying', *IEEE Computer Applications in Power*, vol. 11, no. 3, pp. 14–18, Jul. 1998, doi: 10.1109/67.694931.

[51] B. Qiu, 'Next generation information communication infrastructure and case studies for future power systems', PhD Thesis, Virginia Polytechnic Institute and State University, 2002.

[52] S. H. Horowitz and A. G. Phadke, *Power system relaying*, vol. 22. John Wiley & Sons, 2008.

[53] ALSTOM (Firm), *Network protection & automation guide: protective relays, measurement & control.* Stafford, England? Alstom Grid, 2011.

[54] S. IEC, 'Measuring relays and protection equipment-Part 151: Functional requirements of over/under current protection', *IEC 60255-151*, 2009.

[55] N. Minh Khoa, N. Hieu, and V. Dinh, ‘A Study of SVC’s Impact Simulation and Analysis for Distance Protection Relay on Transmission Lines’, *International Journal of Electrical and Computer Engineering (IJECE)*, vol. 7, May 2017, doi: 10.11591/ijece.v7i4.pp1686-1695.

[56] G. Ziegler, *Numerical Distance Protection: Principles and Applications*. John Wiley & Sons, 2011.

[57] H. Khorashadi Zadeh and Z. Li, ‘Adaptive load blinder for distance protection’, *International Journal of Electrical Power & Energy Systems*, vol. 33, no. 4, pp. 861–867, May 2011, doi: 10.1016/j.ijepes.2010.11.012.

[58] G. Benmouyal, D. Hou, and D. Tziouvaras, ‘Zero-setting power-swing blocking protection’, in *31st annual western protective relay conference*, Citeseer, 2004, pp. 19–21.

[59] M. A. Aftab, S. M. S. Hussain, I. Ali, and T. S. Ustun, ‘Dynamic protection of power systems with high penetration of renewables: A review of the traveling wave based fault location techniques’, *International Journal of Electrical Power & Energy Systems*, vol. 114, p. 105410, Jan. 2020, doi: 10.1016/j.ijepes.2019.105410.

[60] K. J and K. B, ‘Understanding Fault Characteristics of Inverter-Based Distributed Energy Resources’, National Renewable Energy Laboratory (NREL), NREL/TP-550-46698, 2010.

[61] M. Brucoli, T. C. Green, and J. D. F. McDonald, ‘Modelling and Analysis of Fault Behaviour of Inverter Microgrids to Aid Future Fault Detection’, in *IEEE International Conference on System of Systems Engineering, 2007. SoSE ’07*, Apr. 2007, pp. 1–6. doi: 10.1109/SYSOSE.2007.4304253.

[62] N. Zhou, J. Wu, and Q. Wang, ‘Three-Phase Short-Circuit Current Calculation of Power Systems with High Penetration of VSC-Based Renewable Energy’, *Energies*, vol. 11, no. 3, Art. no. 3, Mar. 2018, doi: 10.3390/en11030537.

[63] R. Aljarrah, H. Marzooghi, J. Yu, and V. Terzija, ‘Monitoring of fault level in future grid scenarios with high penetration of power electronics-based renewable generation’, *IET Generation, Transmission & Distribution*, vol. 15, no. 2, pp. 294–305, 2021, doi: https://doi.org/10.1049/gtd2.12021.

[64] J. Yang, J. E. Fletcher, and J. O’Reilly, ‘Short-Circuit and Ground Fault Analyses and Location in VSC-Based DC Network Cables’, *IEEE Transactions on Industrial Electronics*, vol. 59, no. 10, pp. 3827–3837, Oct. 2012, doi: 10.1109/TIE.2011.2162712.

[65] K. I. Jennett, C. D. Booth, F. Coffele, and A. J. Roscoe, ‘Investigation of the sympathetic tripping problem in power systems with large penetrations of distributed generation’, *IET Generation, Transmission Distribution*, vol. 9, no. 4, pp. 379–385, 2015, doi: 10.1049/iet-gtd.2014.0169.

[66] O. Goksu, R. Teodorescu, C. L. Bak, F. Iov, and P. C. Kjær, ‘Impact of wind power plant reactive current injection during asymmetrical grid faults’, *IET Renewable Power Generation*, vol. 7, no. 5, pp. 484–492, Sep. 2013, doi: 10.1049/iet-rpg.2012.0255.

[67] J. Fortmann *et al.*, 'Fault-ride-through requirements for wind power plants in the ENTSO-E network code on requirements for generators', *IET Renewable Power Generation*, vol. 9, no. 1, pp. 18–24, 2015, doi: 10.1049/iet-rpg.2014.0105.

[68] R. Li, C. Booth, A. Dyśko, A. Roscoe, H. Urdal, and J. Zhu, 'A systematic evaluation of network protection responses in future converter-dominated power systems', in *13th International Conference on Development in Power System Protection 2016 (DPSP)*, Mar. 2016, pp. 1–7. doi: 10.1049/cp.2016.0063.

[69] L. He, C. C. Liu, A. Pitto, and D. Cirio, 'Distance Protection of AC Grid With HVDC-Connected Offshore Wind Generators', *IEEE Transactions on Power Delivery*, vol. 29, no. 2, pp. 493–501, Apr. 2014, doi: 10.1109/TPWRD.2013.2271761.

[70] 'Distance protection for transmission lines of DFIG-based wind power integration system - ScienceDirect'. https://www.sciencedirect.com/science/article/pii/S0142061517327540 (accessed Oct. 31, 2018).

[71] M. M. Alam, H. Leite, J. Liang, and A. da S. Carvalho, 'Effects of VSC based HVDC system on distance protection of transmission lines', *International Journal of Electrical Power & Energy Systems*, vol. 92, pp. 245–260, 2017, doi: https://doi.org/10.1016/j.ijepes.2017.04.012.

[72] M. M. Alam, H. Leite, N. Silva, and A. da Silva Carvalho, 'Performance evaluation of distance protection of transmission lines connected with VSC-HVDC system using closed-loop test in RTDS', *Electric Power Systems Research*, vol. 152, pp. 168–183, Nov. 2017, doi: 10.1016/j.epsr.2017.06.025.

[73] A. Hooshyar, M. A. Azzouz, and E. F. El-Saadany, 'Distance Protection of Lines Emanating From Full-Scale Converter-Interfaced Renewable Energy Power Plants—Part I: Problem Statement', *IEEE Transactions on Power Delivery*, vol. 30, no. 4, pp. 1770–1780, 2015, doi: 10.1109/TPWRD.2014.2369479.

[74] R. Jain, B. K. Johnson, and H. L. Hess, 'Performance of line protection and supervisory elements for doubly fed wind turbines', in *2015 IEEE Power Energy Society General Meeting*, Jul. 2015, pp. 1–5. doi: 10.1109/PESGM.2015.7285711.

[75] Y. M. Alsmadi *et al.*, 'Detailed Investigation and Performance Improvement of the Dynamic Behavior of Grid-Connected DFIG-Based Wind Turbines Under LVRT Conditions', *IEEE Transactions on Industry Applications*, vol. 54, no. 5, pp. 4795–4812, Sep. 2018, doi: 10.1109/TIA.2018.2835401.

[76] J. Jia, G. Yang, A. H. Nielsen, and P. R. Hansen, 'Impact of VSC Control Strategies and Incorporation of Synchronous Condensers on Distance Protection under Unbalanced Faults', *IEEE Transactions on Industrial Electronics*, pp. 1–1, 2018, doi: 10.1109/TIE.2018.2835389.

[77] M. Nagpal and C. Henville, 'Impact of Power-Electronic Sources on Transmission Line Ground Fault Protection', *IEEE Transactions on Power Delivery*, vol. 33, no. 1, pp. 62–70, Feb. 2018, doi: 10.1109/TPWRD.2017.2709279.

[78] A. Haddadi, M. Zhao, I. Kocar, U. Karaagac, K. W. Chan, and E. Farantatos, 'Impact of Inverter-Based Resources on Negative Sequence Quantities-Based Protection Elements', *IEEE Transactions on Power Delivery*, vol. 36, no. 1, pp. 289–298, Feb. 2021, doi: 10.1109/TPWRD.2020.2978075.

[79] A. Hooshyar, M. A. Azzouz and E. F. El-Saadany, ‘Distance Protection of Lines Emanating From Full-Scale Converter-Interfaced Renewable Energy Power Plants—Part II: Solution Description and Evaluation’, *IEEE Transactions on Power Delivery*, vol. 30, no. 4, pp. 1781–1791, 2015, doi: 10.1109/TPWRD.2014.2369480.

[80] S. Paladhi and A. K. Pradhan, ‘Adaptive Distance Protection for Lines Connecting Converter-Interfaced Renewable Plants’, *IEEE Journal of Emerging and Selected Topics in Power Electronics*, pp. 1–1, 2020, doi: 10.1109/JESTPE.2020.3000276.

[81] National Grid, ‘Electricity Ten Year Statement 2016’, National Grid, 2016.

[82] M. Nedd, Q. Hong, K. Bell, C. Booth, and P. Mohapatra, ‘Application of synchronous compensators in the GB transmission network to address protection challenges from increasing renewable generation’, 2017.

[83] A. J. Roscoe, G. Jackson, I. M. Elders, J. McCarthy, and G. M. Burt, ‘Demonstration of sustained and useful converter responses during balanced and unbalanced faults in microgrids’, in *Electrical Systems for Aircraft, Railway and Ship Propulsion (ESARS), 2012*, Oct. 2012, pp. 1–6. doi: 10.1109/ESARS.2012.6387439.

[84] M. A. U. Khan, Q. Hong, A. Egea-Àlvarez, A. Dyśko, and C. Booth, ‘A communication-free active unit protection scheme for inverter dominated islanded microgrids’, *Electrical Power and Energy Systems*, Mar. 2022, Accessed: Apr. 22, 2022. [Online]. Available: https://www.sciencedirect.com/journal/international-journal-of-electrical-power-and-energy-systems

[85] D. Liu *et al.*, ‘Evaluation of HVDC system’s impact and quantification of synchronous compensation for distance protection’, *IET Renewable Power Generation*, Mar. 2022, Accessed: Apr. 22, 2022. [Online]. Available: https://ietresearch.onlinelibrary.wiley.com/journal/17521424

[86] D. Tzelepis *et al.*, ‘Impact of Synchronous Condensers on Transmission Line Protection in Scenarios with High Penetration of Renewable Energy Sources’, p. 5 pp.-5 pp., Jan. 2020, doi: 10.1049/cp.2020.0095.

Appendix A: recorded data from studies concerned with investigating the impact of changing various converter fault response parameters

Table A - 1 Impact of varying converter responses under ABC faults with balanced converter output

No.	Energy source	Initial delay (ms)	Ramp rate (GVA /cycle)	Final fault level (GVA)	Fault location			Fault location		
					1%	50%	99%	1%	50%	99%
					T_{trip1} (ms)	T_{trip1} (ms)	T_{trip1} (ms)	T_{trip2} (ms)	T_{trip2} (ms)	T_{trip2} (ms)
0	SG only	\	\	4.7	18.3	19.2	328.4	20.9	22.4	344.8
1	VSC only	2	1.5	2.4	35.1	29.6	329.0	25.2	25.1	349.9
2	VSC only	25	1.5	2.4	59.7	31.6	329.5	25.4	25.4	365.8
3	VSC only	50	1.5	2.4	58.9	40.2	329.7	25.1	24.8	455.3
4	VSC only	75	1.5	2.4	86.6	32.5	328.6	25.3	24.9	334.8
5	VSC only	100	1.5	2.4	87.3	87.5	329.7	25.8	25.7	339.1
6	VSC only	2	1.15	2.4	37.4	24.6	322.9	25	25.4	335
7	VSC only	2	0.8	2.4	58.5	30.8	328.1	25	25.7	337.6
8	VSC only	2	0.45	2.4	67.2	59.1	356.9	37	37	335.8
9	VSC only	2	0.1	2.4	-	-	-	37.6	36.8	334.7
10	VSC only	2	1.5	2.1	36.1	21.6	327.2	25.5	24.8	346
11	VSC only	2	1.5	1.8	34.0	26.8	327.1	25.2	25.3	339.8
12	VSC only	2	1.5	1.5	-	25.7	327.9	25.5	24.9	343.9
13	VSC only	2	1.5	1.2	-	-	-	37.7	37.2	339.8

Table A - 2 Impact of varying converter responses under AB faults with balanced converter output

No.	Energy source	Initial delay (ms)	Ramp rate (GVA /cycle)	Final fault level (GVA)	Fault location			Fault location		
					1%	50%	99%	1%	50%	99%
					T_{trip1} (ms)	T_{trip1} (ms)	T_{trip1} (ms)	T_{trip2} (ms)	T_{trip2} (ms)	T_{trip2} (ms)
0	SG only	\	\	4.7	19.9	21.2	323.2	20.2	21.9	336.1
1	VSC only	2	1.5	2.4	32.8	30.9	329.9	24.3	26.9	339.8
2	VSC only	25	1.5	2.4	51.3	52.5	351.2	37.7	37.7	334.3
3	VSC only	50	1.5	2.4	81.7	79.9	381.2	37	37.4	-
4	VSC only	75	1.5	2.4	108.9	104.5	402.3	37.8	36.2	471.2
5	VSC only	100	1.5	2.4	119.7	129.3	428.8	36	36.4	489.1
6	VSC only	2	1.15	2.4	31.5	30.8	330.9	25.4	36.3	342.1
7	VSC only	2	0.8	2.4	39.6	30.4	328.8	25.8	26.9	341.1
8	VSC only	2	0.45	2.4	41.5	42.5	340.4	37.8	36.9	339.7
9	VSC only	2	0.1	2.4	-	-	-	36.1	37.6	337.5
10	VSC only	2	1.5	2.1	30.6	29.2	331.3	25.5	27	340.3
11	VSC only	2	1.5	1.8	34.0	29.4	332.1	26.1	25.3	336.7
12	VSC only	2	1.5	1.5	57.1	57.7	353.7	27.4	25.5	339.9
13	VSC only	2	1.5	1.2	-	-	-	36.3	36.4	351.1

Table A - 3 Impact of varying converter responses under AN faults with balanced converter output

No.	Energy source	Initial delay (ms)	Ramp rate (GVA /cycle)	Final fault level (GVA)	Fault location			Fault location		
					1%	50%	99%	1%	50%	99%
					T_{trip1} (ms)	T_{trip1} (ms)	T_{trip1} (ms)	T_{trip2} (ms)	T_{trip2} (ms)	T_{trip2} (ms)
0	SG only	\	\	4.7	18.4	19.2	319.9	20.6	25.8	335.8
1	VSC only	2	1.5	2.4	32.2	30.0	328.8	22	24.9	335.2
2	VSC only	25	1.5	2.4	46.2	50.8	348.8	26	26.3	344.3
3	VSC only	50	1.5	2.4	67.9	60.9	320.2	26.2	26	-
4	VSC only	75	1.5	2.4	141.8	141.9	398.2	25.5	41.6	338
5	VSC only	100	1.5	2.4	122.6	142.8	429.9	25.3	26	342
6	VSC only	2	1.15	2.4	30.9	30.8	330.4	46.4	28.2	340.8
7	VSC only	2	0.8	2.4	32.1	32.6	332.5	27.4	26.1	339.6
8	VSC only	2	0.45	2.4	41.6	41.3	340	25.5	26.2	336.9
9	VSC only	2	0.1	2.4	-	-	-	25.4	25.6	335
10	VSC only	2	1.5	2.1	69.9	70.	368.3	24.3	25.1	343.2
11	VSC only	2	1.5	1.8	28.8	67.9	365.1	22	24.5	341.5
12	VSC only	2	1.5	1.5	-	-	-	22.8	25	347.3
13	VSC only	2	1.5	1.2	-	-	-	22.6	26.1	343.2

Table A - 4 Impact of varying converter responses under AN faults with unbalanced converter output

No.	Energy source	Initial delay (ms)	Ramp rate (GVA /cycle)	Final fault level (GVA)	Fault location			Fault location		
					1%	50%	99%	1%	50%	99%
					T_{trip1} (ms)	T_{trip1} (ms)	T_{trip1} (ms)	T_{trip2} (ms)	T_{trip2} (ms)	T_{trip2} (ms)
0	SG only	\	\	4.7	18.4	19.2	319.9	21.2	26.2	340.5
1	VSC only	2	1.5	2.4	21.7	28.6	328	25.2	25.6	360.2
2	VSC only	25	1.5	2.4	40.5	41.2	341.6	26.2	26.2	336
3	VSC only	50	1.5	2.4	74.5	74.6	367.6	25.5	26.3	341.5
4	VSC only	75	1.5	2.4	121.4	172.3	467.1	25.5	26.2	339.8
5	VSC only	100	1.5	2.4	151.9	155.6	453.2	25.8	26	340
6	VSC only	2	1.15	2.4	21.6	29.8	375.9	25.7	25.8	365
7	VSC only	2	0.8	2.4	22.1	33.2	331.5	25.2	25.6	351.8
8	VSC only	2	0.45	2.4	20.7	37.9	337.4	25.7	25.5	352.6
9	VSC only	2	0.1	2.4	21.0	58.3	357.3	25.9	25.6	342.3
10	VSC only	2	1.5	2.1	25.2	38.1	336.8	28.3	39.7	360
11	VSC only	2	1.5	1.8	25.0	91.6	336.6	27.7	34.8	349.7
12	VSC only	2	1.5	1.5	25.4	104.1	337.1	27.8	35.1	351.9
13	VSC only	2	1.5	1.2	90.5	95.5	400.2	28.1	43.4	346.3

Appendix B: recorded data for the study of impact of changing fault locations for various fault infeed machine/converter configurations .

Table B - 1 Impact of varying fault locations under ABC faults with balanced converter output

Energy source		SG	VSC1	VSC2	SG	VSC1	VSC2
No.	Fault Location	T_{trip1} (ms)	T_{trip1} (ms)	T_{trip1} (ms)	T_{trip2} (ms)	T_{trip2} (ms)	T_{trip2} (ms)
1	50%	18.9	22.1	31.2	22.7	37.6	24.7
2	60%	22.3	23.8	30.4	25.4	37.3	25.2
3	70%	26.8	23	31.9	25.9	56.7	90.2
4	75%	34.3	29	75.2/370	47	46.5	379.7
5	77%	34.8	29.5	75.6/331	70.7	72.3	383.4
6	79%	35.8	59.2	78.5/328.5	109.5	75	387.3
7	81%	38.3	74	78.1/330.8	350.7	93.7	379.9
8	83%	330.6	328.7	77.9/329.8	349.3	349.7	378.9
9	85%	315.2	330.9	78.3/330.3	345.5	354.3	380.1
10	87%	316	329.8	77/328.5	348.4	351.1	387.2
11	89%	319.5	328.6	77/330.6	344.4	356.6	380.7
12	91%	317.1	328.8	329.5	347.1	335.5	387
13	93%	315.6	327.6	330.9	345.4	335.9	380.4
14	95%	316.8	329	331.3	345	353.2	374.8

Table B - 2 Impact of varying fault locations under AB faults with balanced converter output

Energy source		SG	VSC1	VSC2	SG	VSC1	VSC2
No.	Fault Location	T_{trip1} (ms)	T_{trip1} (ms)	T_{trip1} (ms)	T_{trip2} (ms)	T_{trip2} (ms)	T_{trip2} (ms)
1	50%	26.4	29.9	243.3	25	36.6	36.5
2	60%	26.4	29.7	249.1	42.5	26.2	37.7
3	70%	26.7	38.5	261.7	37.6	37.3	36.4
4	75%	27.1	53.1	262.6	37.9	37.3	87.9
5	77%	28	63.8	265.4	42.4	36.3	87.3
6	79%	28.3	64.8	264.6	36.4	37.7	86.8
7	81%	27.4	328.5	264.7	340.9	37.6	90.4
8	83%	325.3	330.9	577.7	339.9	37.1	377.8
9	85%	326.4	330.2	583.7	354.1	37.4	379.4
10	87%	324.9	331.4	574.1	335.6	36.2	374.8
11	89%	324.7	330.3	579.2	341	336.6	386
12	91%	325.4	331.2	580.4	340.8	336.2	381.6
13	93%	324.5	330.3	586.1	339.9	335.5	380.7
14	95%	325.8	331.1	579.8	350.2	341.2	375.7

Table B - 3 Impact of varying fault locations under An faults with balanced converter output

Energy source		SG	VSC1	VSC2	SG	VSC1	VSC2
No.	Fault Location	T_{trip1} (ms)	T_{trip1} (ms)	T_{trip1} (ms)	T_{trip2} (ms)	T_{trip2} (ms)	T_{trip2} (ms)
1	50%	25.6	31.6	143.4	26.3	24.3	26
2	60%	25.5	31.7	141	25.8	40.2	26
3	70%	26.5	32.7	145.7	35.1	39.9	27.7
4	75%	27.7	73.1	145.1	49.6	52.1	35.2
5	77%	28.9	74.1	146.2	64.9	72.1	36
6	79%	29.1	74.1	147.9	75.2	76	36.3
7	81%	28.7	86.5	145.8	350.8	80.6	36.2
8	83%	316.3	330.7	485.5	349.9	351.5	36.8
9	85%	317.2	330.4	519/-	350	347	37.2
10	87%	317.6	330.1	520/-	349.9	340.2	39.7
11	89%	325.1	330.2	510.2/-	346.9	345.2	337
12	91%	324.8	330.0	516.1	350.8	345.2	336.2
13	93%	324.6	330.1	512.8	351	345	340.9
14	95%	326.7	331.9	508.6/-	351	342.2	339.9

Table B - 4 Impact of varying fault locations under AN faults with unbalanced converter output

Energy source		SG	VSC1	VSC2	SG	VSC1	VSC2
No.	Fault Location	T_{trip1} (ms)	T_{trip1} (ms)	T_{trip1} (ms)	T_{trip2} (ms)	T_{trip2} (ms)	T_{trip2} (ms)
1	50%	25.6	28.6	74.1	26.3	25.5	25.6
2	60%	25.5	28.9	76.2	25.8	35.3	26.1
3	70%	26.5	37.1	77.4	35.1	96.5	28.3
4	75%	27.7	101.5	82.9	49.6	95.6	35.2
5	77%	28.9	140.5	70.9	64.9	127.4	36.2
6	79%	29.1	101.8	98.2	76.6	90.7	39.4
7	81%	28.7	106.9	98.2	75.2	130.4	36.4
8	83%	316.3	326.8	368	350.8	360.4	40.9
9	85%	317.2	330	368.2	349.9	359.6	42.8
10	87%	317.6	436.6	368.2	350	360.2	335.7
11	89%	325.1	427.9	370.1	349.9	362.2	337.5
12	91%	324.8	328.9	368.2	346.9	360.2	336.5
13	93%	324.6	329.4	367.7	350.8	360.9	340.4
14	95%	326.7	329.7	368.8	351	356.2	340.1

Appendix C: recorded data for studies investigating the impact of changing converter penetration levels.

Table C - 1 Impact of varying converter penetration level under ABC faults with balanced converter output

No.	Penetration Level	Fault location			Fault location		
		1%	50%	99%	1%	50%	99%
		T_{trip1} (ms)	T_{trip1} (ms)	T_{trip1} (ms)	T_{trip2} (ms)	T_{trip2} (ms)	T_{trip2} (ms)
1	0% - VSC1	22.8	19.3	318.7	20.9	22.4	344.8
2	25% - VSC1	23.6	19.7	319.2	20.8	22	336
3	50%- VSC1	23.7	19.3	318.6	21.8	22.3	339.1
4	75%- VSC1	25	21.6	319.3	22.3	21.3	341
5	100%- VSC1	34.1	28.9	327.2	25.5	25.2	335.5
6	0% - VSC2	22.9	18	317.9	22.5	25	341.4
7	25%- VSC2	23.3	19.1	318.1	22.7	22.4	339.6
8	50%- VSC2	23.5	19.9	317.5	20.3	22.5	335
9	75%- VSC2	24.8	20.8	445.5	21.4	22.7	338.9
10	100%- VSC2	88.6	88.8	329.4	25.1	25.3	393.8

Table C - 2 Impact of varying converter penetration level under AB faults with balanced converter output

No.	Penetration Level	Fault location			Fault location		
		1%	50%	99%	1%	50%	99%
		T_{trip1} (ms)	T_{trip1} (ms)	T_{trip1} (ms)	T_{trip2} (ms)	T_{trip2} (ms)	T_{trip2} (ms)
1	0% - VSC1	20.7	21.1	322.8	20.2	21.9	336.1
2	25% - VSC1	21.7	22.6	323.7	21.6	20.9	339.1
3	50%- VSC1	23.2	23.6	323.9	19	21.8	339.2
4	75%- VSC1	23.2	24.5	324.6	21.7	21.8	339.9
5	100%- VSC1	34.7	31.6	332.5	27	25.8	337.3
6	0% - VSC2	20.7	21.5	322.6	21.6	21.7	344.6
7	25%- VSC2	21.5	22.6	322.7	20.9	21.7	345.4
8	50%- VSC2	22.3	25.8	324.9	20.2	21.1	355.2
9	75%- VSC2	23.3	26.1	324.8	21.8	21.4	349.5
10	100%- VSC2	221.5	250.1	564.3	37.4	37.6	390.7

Table C - 3 Impact of varying converter penetration level under AN faults with balanced converter output

No.	Penetration Level	Fault location			Fault location		
		1%	50%	99%	1%	50%	99%
		T_{trip1} (ms)	T_{trip1} (ms)	T_{trip1} (ms)	T_{trip2} (ms)	T_{trip2} (ms)	T_{trip2} (ms)
1	0% - VSC1	18.7	18.6	319.8	20.6	25.8	335.8
2	25% - VSC1	20	20.5	322.5	21	25.6	345
3	50%- VSC1	19.5	22.5	324.9	20.8	26.3	336.2
4	75%- VSC1	20.8	23	323.9	21	37	340
5	100%- VSC1	32.2	30	32.8	22.7	50	341.2
6	0% - VSC2	18.9	18.6	319.8	21.1	26	342.5
7	25%- VSC2	18.6	20	312.2	21.1	25.7	338
8	50%- VSC2	19.6	21.2	325.2	21.3	26.3	335.3
9	75%- VSC2	19.4	23	325.8	21.2	26.1	336.3
10	100%- VSC2	141.4	141.7	565.1	26.1	26.2	338.2

Table C - 4 Impact of varying converter penetration level under AN faults with unbalanced converter output

No.	Penetration Level	Fault location			Fault location		
		1%	50%	99%	1%	50%	99%
		T_{trip1} (ms)	T_{trip1} (ms)	T_{trip1} (ms)	T_{trip2} (ms)	T_{trip2} (ms)	T_{trip2} (ms)
1	0% - VSC1	18.7	18.6	319.8	21.2	26.2	340.5
2	25% - VSC1	19.1	19.8	322.6	21.6	26.1	342.1
3	50%- VSC1	20.5	21	324.8	20.4	25.8	345.1
4	75%- VSC1	20.9	25.6	326.2	20.7	25.5	350.3
5	100%- VSC1	28.1	30.4	327.6	25.9	25.4	362.7
6	0% - VSC2	18.7	18.6	319.8	20.3	26.1	341.4
7	25%- VSC2	19.5	19.8	320.1	20.3	25.4	341.7
8	50%- VSC2	20	21.3	324.9	20.3	25.7	343
9	75%- VSC2	20	22.4	325.2	20.7	25.7	340.5
10	100%- VSC2	87.4	86.9	378.7	25.6	26	341.1

Appendix D: recorded data for studies concerned with investigating the impact of changing remote end fault infeed level.

Table D - 1 Impact of varying fault level contribution from the grid under ABC faults with balanced converter output

No.	Energy source	Remote end infeed (GVA)	Fault location			Fault location		
			1%	50%	99%	1%	50%	99%
			T_{trip1} (ms)	T_{trip1} (ms)	T_{trip1} (ms)	T_{trip2} (ms)	T_{trip2} (ms)	T_{trip2} (ms)
1	SG only	20	22.4	18.3	318.9	25.2	24.8	335.7
2	SG only	15	24.4	19.1	319.5	25.3	24.8	340.7
3	SG only	10	24.3	18.1	319.1	25.3	25.5	340.5
4	SG only	5	24.1	18.8	317.5	25.1	25.4	356.1
5	SG only	1	33.2	85.6	-	-	46.8	344.5
6	VSC1 only	20	34.5	30.1	328.2	25.8	25.6	435.7
7	VSC1 only	15	35.3	29.2	328.1	25.5	25	434.5
8	VSC1 only	10	56.7	24.2	329.8	25.7	25.5	434.6
9	VSC1 only	5	36	22.9	329.2	25.7	24.9	431.1
10	VSC1 only	1	87.5	90.8	566/-	25.3	25.7	433.7
11	VSC2 only	20	89	30.5	330.2	25.4	24.9	436.3
12	VSC2 only	15	86.1	31.2	329.6	25.6	25	434.8
13	VSC2 only	10	86.2	31.6	329.9	25.6	25.4	433.8
14	VSC2 only	5	86.1	85	330	25.7	25	439.8
15	VSC2 only	1	88.3	85.3	387	25.3	24.8	439.6

Table D - 2 Impact of varying fault level contribution from the grid under AB faults with balanced converter output

No.	Energy source	Remote end infeed (GVA)	Fault location			Fault location		
			1%	50%	99%	1%	50%	99%
			T_{trip1} (ms)	T_{trip1} (ms)	T_{trip1} (ms)	T_{trip2} (ms)	T_{trip2} (ms)	T_{trip2} (ms)
1	SG only	20	19.5	21.7	322.1	36.3	26.2	339.2
2	SG only	15	19.5	21.3	322.2	25.7	25.7	340.6
3	SG only	10	20.4	20.9	322	25.8	25.7	335.1
4	SG only	5	19.5	21.9	323	24.2	25.6	346.5
5	SG only	1	32.5	95.2	-	37.8	42.3	-
6	VSC1 only	20	32.1	32.5	330.1	36.7	36	399.4
7	VSC1 only	15	32.1	31.9	330.3	37.1	37.3	394.2
8	VSC1 only	10	32.3	31.7	330.2	37.4	36.2	403.2
9	VSC1 only	5	34	31.4	330	35.9	37.7	397
10	VSC1 only	1	74.3	-	383.6	37.6	36.1	392.9
11	VSC2 only	20	226.5	242.3	577.1	37.4	36.5	395.3
12	VSC2 only	15	222.3	249.8	579.4	36.1	37	390.4
13	VSC2 only	10	230	260.3	601.2	36.2	36.8	390.4
14	VSC2 only	5	251.7	285.7	617.2	37.1	36.5	389.7
15	VSC2 only	1	54.6	43.7	348.6	36.7	37.3	392.2

Table D - 3 Impact of varying fault level contribution from the grid under AN fault with balanced converter output

No.	Energy source	Remote end infeed (GVA)	Fault location			Fault location		
			1%	50%	99%	1%	50%	99%
			T_{trip1} (ms)	T_{trip1} (ms)	T_{trip1} (ms)	T_{trip2} (ms)	T_{trip2} (ms)	T_{trip2} (ms)
1	SG only	20	18.7	19.5	319.9	24.2	25.4	341.5
2	SG only	15	18.7	20.2	321.2	24.4	24.9	357.7
3	SG only	10	18.9	20.8	319.7	22.8	26.1	355.7
4	SG only	5	18.7	20.4	320.2	22	26	345.2
5	SG only	1	39.3	90.7	-	42.9	25.7	344.9
6	VSC1 only	20	31.4	30.5	330.5	25.5	25.9	336
7	VSC1 only	15	31.2	31	330.3	25.3	25.9	336.5
8	VSC1 only	10	31.4	30.4	330.5	25.4	25.5	340
9	VSC1 only	5	31.1	30.9	330.4	23.1	24.3	339.8
10	VSC1 only	1	75.1	130.7	595.6	21.8	25.6	395.6
11	VSC2 only	20	141.7	141.5	519.1	25.6	26	337.4
12	VSC2 only	15	141.8	142.0	583.2	25.4	25.8	340.5
13	VSC2 only	10	141.2	145.5	581.3	26.1	25.6	336
14	VSC2 only	5	240.5	245.8	622.2	21.9	24.5	336.1
15	VSC2 only	1	308.7	313.8	685.9	24.1	26	401

Table D - 4 Impact of varying fault level contribution from the grid under AN faults with balanced converter output

No.	Energy source	Remote end infeed (GVA)	Fault location			Fault location		
			1%	50%	99%	1%	50%	99%
			T_{trip1} (ms)	T_{trip1} (ms)	T_{trip1} (ms)	T_{trip2} (ms)	T_{trip2} (ms)	T_{trip2} (ms)
1	SG only	20	18.7	19.5	319.9	25	25.7	362.4
2	SG only	15	18.7	20.2	321.2	25.6	25.9	356.1
3	SG only	10	18.9	20.8	319.7	25.6	25.8	464.7
4	SG only	5	18.7	20.4	320.2	25.5	25.3	362.7
5	SG only	1	39.3	90.7	-	21.1	26.7	343.8
6	VSC1 only	20	27.9	28.9	327.5	25.2	26	343.7
7	VSC1 only	15	28.4	28.1	329.5	25.4	26.1	339.6
8	VSC1 only	10	27.3	28.3	329.5	25.8	26.1	341.9
9	VSC1 only	5	26.2	25.4	332.1	25.3	25	340.8
10	VSC1 only	1	-	-	-	21.8	25.4	399.8
11	VSC2 only	20	87.1	86.4	380	25.2	25.8	341.3
12	VSC2 only	15	87.5	86.7	379.8	26.1	26	337.2
13	VSC2 only	10	87.5	80	376.8	25.5	25.5	334.8
14	VSC2 only	5	83.7	79.2	375.9	22.2	25.2	335.7
15	VSC2 only	1	123.3	123.1	610.4	22.3	25.2	400